NISTIR 6535

Critical Issues in the Characterization of Polymers For Medical Applications

Prepared by:

Walter G. McDonough
Eric J. Amis

U.S. DEPARTMENT OF COMMERCE
Technology Administration
National Institute of Standards and Technology
Gaithersburg, MD 20899-0001

And

Joachim Kohn

New Jersey Center for Biomaterials
and
Wright-Rieman Laboratories, Department of Chemistry
Rutgers - The State University of New Jersey
Piscataway, NJ 08854-8087

June 14, 2000

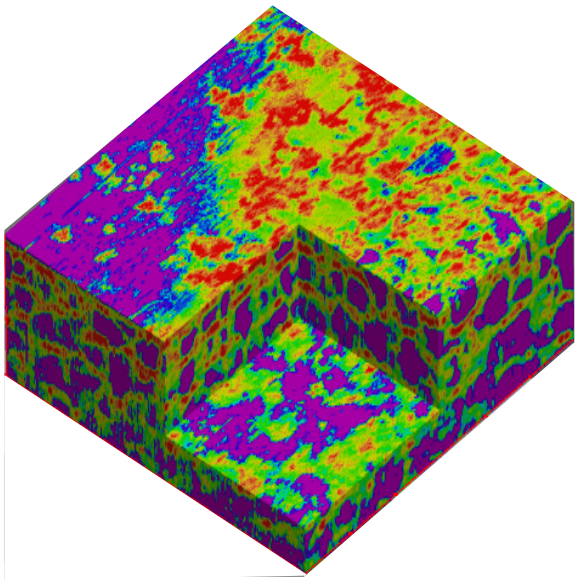

Disclaimer:

Certain commercial materials and equipment are identified in this article to specify the experimental procedure. In no instance does such identification imply recommendation or endorsement by the National Institute of Standards and Technology or that the material or equipment identified is necessarily the best available for the purpose.

This manuscript contains several contributions from non-NIST authors. As such, these sections are exempt from the NIST requirements for SI units and statements of experimental uncertainty.

Cover picture:

Shown is an Optical Coherence Tomography volumetric reconstruction of a hydrophilic polymeric tissue scaffold in water. The scaffold dimensions are 3.0 mm long by 3.0 mm wide by 0.84 mm high. The pores are indicated by the purple regions, and the scaffold itself is colored from red to green. This volumetric representation indicates that the vast majority of the pores are closed, making it a poor candidate for successful cell infiltration. From: " Optical Coherence Tomography (OCT) for Imaging Materials and Tissue Engineering Scaffolds."

Executive Summary

On June 14, 2000, the New Jersey Center for Biomaterials and the Polymers Division of the National Institute of Standards and Technology (NIST) co-sponsored a one-day workshop on **Critical Issues in the Characterization of Polymers for Medical Applications**. The workshop; defined some of the critical issues in the design and characterization of polymers for medical applications and highlighted the expertise and technologies available at both NIST and the New Jersey Center for Biomaterials for developing polymers for medical applications.

The meeting featured presentations from researchers, a poster session, and a facilitated discussion. The presentations were made in three sections. In the Design and Synthesis section, Prof. Jennifer West from Rice University discussed the advances in material design for biomedical polymers. She focused her presentation on bioactive tissue engineering scaffolds and on nitric oxide producing polymers for the prevention of thrombosis and restinosis. Prof. Joachim Kohn from Rutgers University followed this presentation with a talk on a combinatorial approach to biomaterials design. He discussed the rationale for the use of combinatorial approaches in biomaterials design and described how the availability of libraries of biomaterials can greatly facilitate the selection of polymers for specific applications since it is possible to pick and choose polymers from within the library. The final talk in this section was given by Prof. Kathryn Uhrich from Rutgers University. She talked about how micelles are frequently used as drug delivery systems because they have useful properties such as the ability to water-solubilize hydrophobic drugs and the ability to be inserted into or passed through cell membranes. She also talked about their concept of polymers that degrade into bioactive molecules. She identified quantifying new bone formation, monitoring salicylic acid concentration *in vivo* and measuring tissue/polymer interfacial interactions as critical issues.

In the New Imaging Techniques section, Dr. Luis Garfias from Lucent Technologies, Bell Laboratories talked about Near-Field Scanning Optical Microscopy (NSOM) for *in-situ* characterization of biomaterials. He focussed his talk on a home-built tuning fork head that enables optical and topographic imaging concurrently. He showed that by using NSOM, he can study *in-situ* the precipitation kinetics at short times and the changes induced after the bone cement is exposed to simulated body fluid. This method has proven useful for non-invasive investigation of changes in biomedical materials. This presentation was followed by one on optical coherence tomography (OCT) for imaging tissue scaffolds by Dr. Joy Dunkers of NIST. She described how OCT is a very promising technique for non-destructive, volumetric, in-situ characterization of scaffold microstructure. It is anticipated that OCT can also be used to study scaffold degradation as well as cell growth. The section ended with Mr. Roger Blaine of TA Instruments talking about micro-thermal analysis (the combination of atomic force microscopy and thermal analysis). The machine he described combines atomic force microscopy for sample preparation, handling, and visualization, and thermal analysis for characterization.

Prof. Michael Jaffe from the New Jersey Institute of technology then led a facilitated discussion on the critical issues in the characterization of polymers for medical applications. Among the critical issues identified were quantifying the importance of surface energy and surface roughness, 2-D surface conformational imaging, *in-vivo* characterization techniques, and the identification of artifacts.

The final section covered State-of-the-Art Research in Biomaterials. Prof. Prabhas Moghe from Rutgers University talked about switching the functional fates of cells on polymer substrates. His talk focused on his recent findings on the means and mechanisms of manipulating the functional behavior of primary liver cells during culture on ligand treated synthetic polymers. He found that the effects of progressive changes in substrate topology and cell specific biochemistry could be systematically mapped in relation to the properties elicited by untextured and untreated base substrates. Dr. Hoda Elgendy of NIST then presented work on biomimetic membranes as in-vitro models to study cell-cell interactions for tissue engineering. In her work, the growth and phenotype of osteosarcoma cells on cell membrane hybrid surfaces are being compared to their growth and phenotype on other traditional biomaterial surfaces. Her group's in vitro observations suggest that biomimetic membrane surfaces constructed from osteosarcoma cell membranes may be suitable biomaterials to support osteoblasts as part of a matrix for enhanced bone repair. The next presentation was by Dr. Alamgir Karim from NIST on using combinatorial methods for investigations in polymer materials science. His group has developed combinatorial and high throughput methods for rapid measurements of properties of polymer coatings such as phase separation and film dewetting. Their results were validated against traditional one-sample measurements and existing physical models. The final presentation of the meeting was given by Dr. Gary Schumacher of the American Dental Association/Paffenbarger Research Center on a microshear test to measure the bond between dental composites and dental substrates. This presentation described some of the opportunities that the microshear bond test offers in enhancing the understanding of dental adhesion and in designing dental adhesive systems with enhanced strength and durability.

In addition to these talks, a poster session was held. Abstracts from these posters are included in this report.

Table of Contents

Workshop Sponsors

National Institute of Standards and Technology

The National Institute of Standards and Technology (NIST) was established by Congress to assist industry in the development of technology needed to improve product quality, to modernize manufacturing processes, to ensure product reliability and to facilitate rapid commercialization of products based on new scientific discoveries.

An agency of the U. S. department of Commerce's Technology Administration, NIST strengthens the U.S. economy and improves the quality of life by working with industry to develop and apply technology, measurements, and standards. It carries out this mission through a portfolio of four major programs: Measurement and Standards Laboratories that provide technical leadership for vital components of the nation's technology infrastructure needed by U.S. industry to continually improve its products and services; the Advanced Technology Program, accelerating the development of innovative technologies for broad national benefit through R & D partnerships with the private sector; a grassroots Manufacturing Extension Partnership with a network of local centers offering technical and business assistance to smaller manufacturers; and a highly visible quality outreach program associated with the Malcolm Baldridge National Quality Award that recognizes business performance excellence and quality achievement by U.S. manufacturers, service companies, educational organizations, and health care providers.

The Polymers Division of the Materials Science and Engineering Laboratory is the part of the Measurements and Standards Laboratories that provides standards, measurement methods, and fundamental concepts in support of the measurement infrastructure for U.S. industries that produce or use polymers in essential parts of their business. The Division's programs are planned in response to and anticipation of measurement needs that support emerging markets for polymer materials as well as traditional industrial and technical communities. Our current program areas encompass electronic applications, biomaterials, polymer blends, composites, characterization, and processing. Most of the work in the Division involves direct collaborations with industrial and academic partners. We are always pleased to provide more details and invite inquiries to any of our project leaders.

The New Jersey Center for Biomaterials

The New Jersey Center for Biomaterials is a formal consortium of New Jersey's premier institutions of higher education dedicated to improving health care and the quality of life through advanced materials for tissue repair, tissue replacement, and drug delivery. The Center coordinates clinical, technical and academic resources to develop medical materials for the new millennium. Our programs are designed to promote the discovery of new techniques, materials and products through close collaboration with industry.

The New Jersey Center for Biomaterials creates partnerships for research and development of the next generation of biomaterials. All the Center's programs have been designed to promote the discovery and commercialization of new techniques, materials and products.

.

The Center's Vision: build a nationally leading resource in biomaterials and implant science
The Center's Focus: rational design of new biomaterials
The Center's Mechanism: inventive research through blending of material sciences, engineering and the life sciences.

Research

The Center can quickly take on new research challenges by assembling teams that span the traditional academic disciplines from:

More than 35 faculty members from 5 universities
Participating companies
A growing national network of academic and industrial contacts

Services for Industry

Academic-industrial collaborative research partnerships
Medical Device Concept Laboratory
Industrial membership program
Early-stage, pre-competitive initiative
Consultation and referrals

Network of Shared Facilities

The evaluation of new biomaterials and implants requires specialized analytical and imaging tools. The Center's coordinated network of facilities for fabrication, characterization and imaging offers the academic or industrial biomaterials researcher a single but geographically distributed resource.

Atomic Force Microscopy - Rutgers-Piscataway
Cell Biology - Rutgers-Piscataway
Confocal Microscopy - Rutgers-Piscataway
Electron Microscopy - Rutgers-Piscataway, Stevens-Hoboken
ESCA, Electron Spectroscopy for Chemical Analysis - Rutgers-Piscataway
Fiber Prototyping - Medical Device Concept Laboratory/NJIT-Newark
Large-scale Polymer Synthesis - Rutgers-Piscataway
Mass Spectrometry - Rutgers-Piscataway

Polymer Fabrication & Characterization - Medical Device Concept Laboratory/Polymer Processing Institute/NJIT - Newark
Polymer Characterization - Rutgers-Piscataway
Stereolithography - Princeton

Education and Outreach

Biomaterials research spans many disciplines, ranging from clinical sciences to basic biology to engineering and the physical sciences. Progress toward creating the next generation of medical implants requires scientists who have been prepared to operate within this highly multidisciplinary world. Center programs addressing this need are:

- Postdoctoral Education for Scientists and Clinicians in Tissue Engineering
- Summer Biomaterials Research Awards for Predoctoral Students
- Partnership with Business Faculty

Reaching both professionals and the public with information about the next generation of biomaterials extends the Center's educational activities into the wider community. Current and future programs include:

- Annual Symposium or Lecture Series
- Newsletter
- School groups visit research laboratories
- Museum exhibit programs
- Information resources for legislators

Design

and

Synthesis

Advances in Materials Design for Biomedical Polymers

Jennifer L. West

T.N. Law Assistant Professor of Bioengineering
Rice University, Houston, TX

Although the currently available biomaterials have been successful in many clinical applications, there is still a great need for new polymers with properties specifically designed for biological and medical uses. Many applications that should be feasible are in fact not due to complications arising from the currently available materials. A striking example of this is the small diameter vascular graft. Current materials, such as expanded polytetrafluoroethylene and polyethylene terephthalate, perform well in large diameter applications but cannot be used in vessels smaller than 6 mm inner diameter due to rapid occlusion caused by complications at the blood-material and tissue-material interfaces. Thus, synthetic materials are not available for applications such as coronary artery bypass grafting. The limited biocompatibility of materials currently in use is not surprising, given that they generally were not originally developed for use in the biological milieu, but rather were off-the-shelf materials, often from the textiles and commercial materials industries, that could be adapted for use in a medical device. Further advances in medical implants and devices will undoubtedly require the development of new materials where both the materials properties and the biological interactions have been carefully engineered. This will require an improved understanding of aspects of cell biology and biocompatibility, synthesis of new materials, and better techniques to evaluate materials and their interactions with cells and proteins. Below are descriptions of two novel materials that have been developed in our laboratories where the materials have been designed to have precise biological functions.

Bioactive Tissue Engineering Scaffolds

In designing novel materials for use as scaffolds for tissue formation or regeneration, we have chosen to evaluate the design and function of the natural tissue scaffold, the extracellular matrix (ECM). We have used the ECM as a model material and attempted to mimic many of its properties in a completely synthetic polymer system. The ECM has many complex functions that far exceed the simple mechanical support provided by many materials used as tissue engineering scaffolds. The ECM presents ligands that interact with receptors, such as integrins, on the cell surface to control cell adhesion, cytoskeletal morphology, migration, proliferation, and gene expression. The ECM can also sequester and release soluble factors, including many of the growth factors. Additionally, cells are able to degrade and remodel the ECM via enzymatic processes. We have sought to recreate many of these actions in a synthetic material based on photopolymerizable derivatives of polyethylene glycol (PEG). We have selected PEG as our base synthetic material because it is highly water soluble and is one of the most biocompatible synthetic polymers currently known. Photopolymerizable derivatives of PEG, modified at their termini with acrylate groups, were selected because the photopolymerization reaction used to form the hydrogels can be carried out in the presence of cells; this allows one to suspend cells in an aqueous polymer solution, then create a hydrogel with cells homogeneously seeded throughout the structure upon photopolymerization. The biological activities that we have

imparted on these materials include biospecific cell adhesion, degradation via proteases involved in cell migration and ECM remodeling, and presentation of growth factors to regulate tissue formation.

Biospecific cell adhesion, cell adhesion occurring through targeted receptors, has been achieved with this hydrogel system. The base material must be highly resistant to cell adhesion, as is PEG, and then specific receptor ligands can be incorporated into the material to engineer the receptor binding characteristics. For this purpose, peptide ligands have been covalently attached to PEG monoacrylate. When the peptide-PEG-monoacrylate copolymers are combined with a PEG diacrylate derivative and photopolymerized, the peptides become covalently grafted to the hydrogel network via a PEG spacer arm. The spacer arm gives the peptide a great deal of mobility, facilitating interaction with its receptor on the cell surface. We have shown that hydrogels without peptides or with peptides that are not ligands for cell adhesion receptors are not cell adhesive, while cell adhesion is observed on hydrogels with peptide ligands and depends on the concentration of ligand present in the hydrogel structure.

During tissue formation, a number of proteolytic enzymes, such as the matrix metalloproteases, are secreted into the ECM in order to create pathways for cell migration and to allow remodeling of the ECM. These are the processes of biodegradation that occur naturally in the ECM. We have chosen to target biodegradation of the hydrogel scaffolds to these proteases as it should couple biodegradation to tissue formation. We have synthesized PEG diacrylate derivatives that contain in their backbone peptides that are substrates for specific proteolytic enzymes, including collagenase, elastase, and plasmin. These materials will degrade in solutions of the targeted protease, but not in solutions of other enzymes or without enzymes. We have further shown that migrating cells can degrade these materials in a modified Boyden chamber apparatus.

It is also possible to tether growth factors to these hydrogel scaffolds in order to exert additional control over the tissue formation process. For example, we have covalently attached transforming growth factor-beta1 (TGF), a factor that stimulates synthesis of matrix proteins, to PEG monoacrylate in a fashion similar to that used for the peptide cell adhesion ligands. The TGF-PEG-monoacrylate can be combined with a PEG diacrylate derivative; upon photopolymerization, TGF is covalently grafted to the hydrogel structure via a PEG spacer arm. We have shown that attachment of TGF to PEG monoacrylate results in a slight loss of activity relative to unmodified TGF. However, when grafted to the hydrogel network, greater bioactivity was observed with the tethered TGF than with the same amount of unmodified TGF soluble in the media. This is presumably due to the prevention of TGF internalization.

Nitric Oxide Producing Polymers for the Prevention of Thrombosis and Restenosis

Approximately 40 % of all patients treated with percutaneous transluminal coronary angioplasty will experience failure of the procedure to thrombosis (blood clot formation, due largely to platelet adhesion and aggregation) or restenosis (due in part to excessive proliferation of smooth muscle cells in the arterial wall). During the angioplasty procedure, the inflation of the balloon destroys the endothelial cells that line the artery wall. The endothelial cells normally prevent thrombosis and limit smooth muscle cell proliferation. Endothelial cells accomplish these tasks by acting as a mechanical barrier between the blood and the arterial wall; this prevents interaction between platelets and adhesive ligands in the arterial wall and limits the diffusion of circulating factors into the arterial wall. Endothelial cells also prevent platelet

adhesion and smooth muscle cell proliferation by actively secreting a number of anti-platelet and anti-proliferative substances, notable nitric oxide (NO). NO is formed by endothelial cells from the conversion of L-arginine to L-citrulline by the enzyme nitric oxide synthase. In order to reduce the complications associated with balloon angioplasty, we are designing materials to replace some of the functions of the damaged endothelial cells, namely the non-thrombogenic mechanical barrier and the production of NO.

To replace the mechanical barrier function, the goal was to create a very thin layer of a semipermeable polymer on the lumenal surface of the arterial wall over the region of the denuded endothelial cells. To accomplish this, the hydrogel layer needs to be applied via a catheter-based approach. Thus, we wanted to have all components in a liquid state and form a hydrogel coating *in situ.* To do this, we have developed an interfacial photopolymerization process where a non-toxic photoinitiator is adsorbed on the tissue surface, the vessel is then filled with a photopolymerizable PEG diacrylate derivative, and upon exposure to light from a fiber optic threaded through the vessel, the aqueous PEG derivative solution is converted to a hydrogel where it is in contact with the photoinitiator, namely at the lumenal surface of the arterial wall. This process can be used to create hydrogel coatings as thin as 5 μm that adhere and conform to the underlying tissue. These materials prevent platelet adhesion following angioplasty and limit the diffusion of plasma proteins into the vessel wall.

In order to have sustained release of NO from these hydrogel barriers, we have synthesized PEG derivatives that contain groups, such as diaziniumdiolates and S-nitrosothiols that hydrolyze to produce NO. We have developed photopolymerized hydrogels with various covalently grafted NO donor groups and have observed production of NO over periods ranging from hours to months, depending on what NO donor group is utilized. We have further shown that these materials are highly effective in preventing platelet adhesion and aggregation as well as smooth muscle cell proliferation. We believe that these materials will be effective in the prevention of thrombosis and restenosis following vascular injury such as that caused by balloon angioplasty.

A Combinatorial Approach to Biomaterials Design

Elsie Effah-Kaufmann, Debbie Schachter, Stephen Brocchini, Kenneth James, Varawut Tangpasuthadol and Joachim Kohn

New Jersey Center for Biomaterials
Piscataway, NJ

Rationale for the Use of Combinatorial Approaches in Biomaterials Design

Metals and various industrial plastics (e.g., polysiloxanes, polyurethanes, Dacron® , Teflon® , polyethylene) continue to be the most widely used raw materials for the design of medical implants. These biostable, synthetic implant materials lack the molecular sequences and patterns crucial to normal cell function and often trigger aberrant cell responses upon long-term implantation.[1] The choice of synthetic degradable polymers is also very limited. Since 1969, polymers derived from lactic and glycolic acid,[2,3] polydioxanone,[4] and a polyanhydride[5] derived from sebacic acid and bis(p-carboxyphenoxy)propane are the only synthetic *degradable* polymers that have gained an extensive regulatory approval history in the USA.

The systematic study of material-dependent biological responses and the optimization of medical device performance necessitate a collection of materials exhibiting gradations in physicomechanical, chemical, and/or biological properties. For example, one of the central themes in tissue engineering is the use of polymeric scaffolds that can provide a suitable environment for the reconstruction of functional tissue.[6] Initial research results indicate that the development of optimal scaffolds for a wide range of applications will depend on the availability of degradable biomaterials whose physicomechanical and chemical properties closely match a set of predetermined requirements.[7]

To address both the slow rate of materials development and the lack of a wide range of promising degradable polymer candidates for biomedical applications, we explored combinatorial approaches in materials design.[8] Combinatorial approaches have led to dramatic changes in the way lead compounds for the discovery of new drugs are identified.[9] The ability to create thousands of structurally related compounds within a single reaction vessel followed by the identification of potential lead compounds in a selective bioassay has increased the pace of drug discovery.[10] Unfortunately, this approach for creating a large number of compounds within one reaction vessel is not readily applicable to biomaterials design. Starting with a mixture of monomers and creating a mixture of different polymers within the same reaction vessel would result in a blend of polymers that could not be resolved into individual compounds. Thus, we focused our attention on a combinatorial system of monomers that can be polymerized in a *parallel* fashion so that each polymer contained within the library is obtained in pure form in its own reaction vessel. We have used this approach to create the first combinatorial library of 112 degradable polyarylates based on tyrosine.[8] Since then, we have studied the use of these materials in exploring fundamental correlations between systematic changes in the chemical composition of the polymers, their physicomechanical properties, and the proliferation of fibroblasts on these polymer surfaces in vitro.

Summary of Results

The first combinatorial library of degradable polymers consisted of polyarylates (see Figure 1 for general chemical structure). These polymers are A-B type copolymers consisting of an alternating sequence of a diphenol and a diacid. The library was prepared by copolymerizing, in all possible combinations, 14 different tyrosine-derived diphenols and 8 different aliphatic diacids, resulting in 8x14=112 distinct polymers. This library was then used to identify correlations between polymer structure and glass transition temperature, air-water contact angle, mechanical properties, and a variety of cellular responses. The pendent chain and backbone structures of the polymers included in the library were systematically varied by (i) simple homologative variations in the number of methylene groups, (ii) substitution of oxygen for methylene groups, and (iii) introduction of branched and aromatic structures. The polymers contained within the library exhibited incremental variations in Tg (from 2 ^{o}C to 91 ^{o}C) and air-water contact angle (from 64 ^{o}C to 101 ^{o}C). In a selected subgroup of polymers, tensile strength of thin solvent cast films ranged from about 6 MPa to 45 MPa, while Young's modulus (stiffness) ranged from about 0.3 GPa to 1.7 GPa.

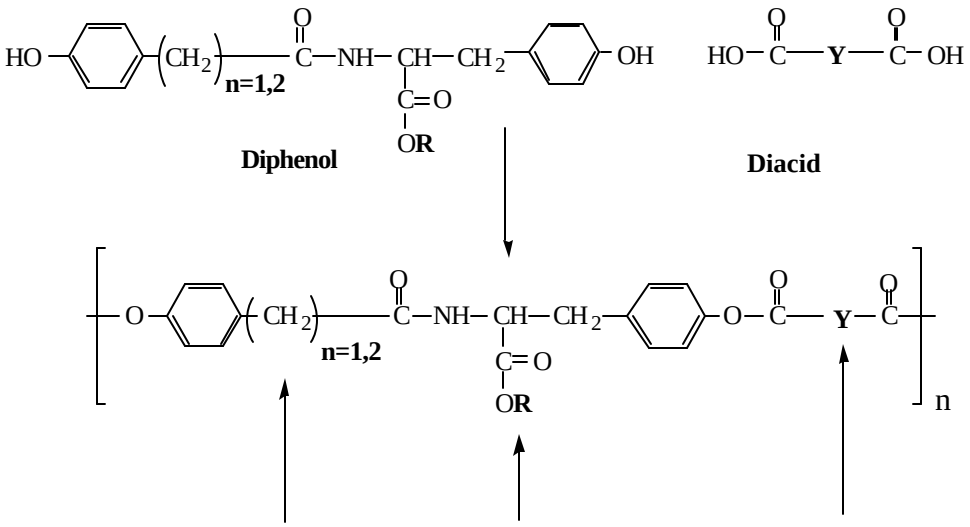

Figure 1: General chemical structure of the library of tyrosine-derived, degradable polyarylates. These materials are alternating A-B type copolymers consisting of diacids and diphenols. The arrows point to those regions within the polymer structure where systematic variations were introduced. See Figure 2 for additional details on the variations in the polymer backbone (Y) and the pendent chain (R).

Spin-coated surfaces were used as substrata and the responses (attachment, migration, proliferation, and differentiation) of several cell lines were studied in vitro in serum containing media. Two specific types of correlations can be obtained. In Fig. 1, the level of alkaline phosphatase in cultures of an osteoblast-like cell line (UMR-106) seeded on 12 different polyarylate surfaces is followed over 14 days. Some of the polymers facilitated the early maturation of UMR-106 cells as evidenced by the prominent peaks in alkaline phosphatase activity at the 7 day time point. Figure 2 represents the result of a typical screening experiment in which one polymer, poly(DTO glutarate) (highest bar), was identified for detailed follow-up studies.

In a different set of experiments, subgroups of polymers can be used to search for more general structure-property correlations. For example, keeping the backbone element "R" constant, the glutaric acid containing polymers having a methyl, ethyl, butyl, hexyl, octyl and dodecyl pendent chain were evaluated as growth substrates for rat lung fibroblasts under identical conditions. A linear correlation between the air-water contact angle of the polymers and their ability to promote cell growth in serum-containing media was observed (Figure 3). This trend was mirrored by the amount of fibronectin adsorbed onto the polymer surfaces (Figure 3). We propose that the adsorption of fibronectin to the polymer surface was controlled by the chemical composition of the surface, which in turn gave rise to the close correlation between polymer structure and cell growth.

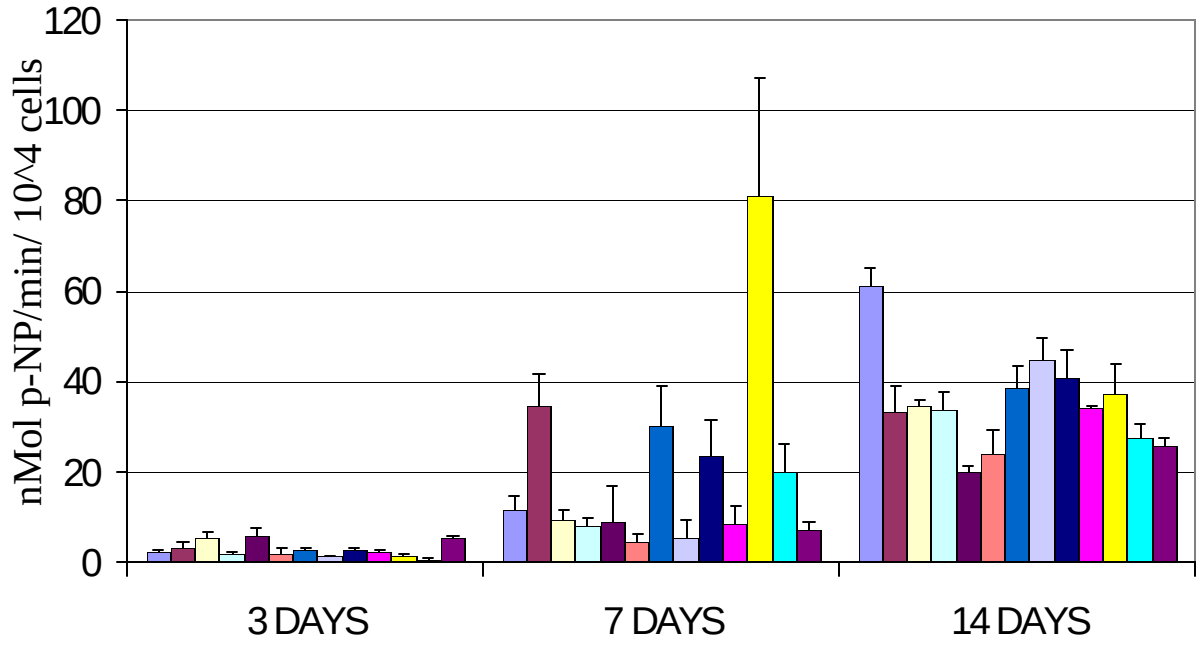

Figure 2: Alkaline Phosphatase levels generated on 13 different polymer surfaces. Each bar represents one specific polymer. The 13th bar represents tissue culture polystyrene as control.

The above studies are two representative examples for a wide range of experiments that can be designed to establish correlations between chemical structure of a polymer, the adsorption of serum proteins on the surface, and the resulting cellular response. Such correlations can be identified more readily when subgroups of structurally related polymers are available for screening, making combinatorial approaches an important new tool in biomaterials design.

From an applied perspective, the availability of libraries of biomaterials can greatly facilitate the selection of polymers for specific applications since it is possible to pick and choose polymers from within the library. For example, if a polymer having a contact angle of $70^o \pm 1^o$ is required for a specific application, 10 different polymers are available that fulfill this requirement while providing a range of cellular interactions, mechanical properties, and processing characteristics (with T_g ranging from 27 ^{o}C to 82 ^{o}C). Likewise, if a specific application would require a polymer with a T_g close to body temperature, 7 polymers would fulfill this requirement (T_g = 34 ^{o}C to 38 ^{o}C), while independently providing a range of air-water contact angles (70 ^{o} to 97 ^{o})

and mechanical properties. Finally, cell proliferation and mechanical properties can be varied independently. For example, poly(DTE succinate) and poly(DTO succinate) have similar tensile properties but fibroblast proliferation was 97 % and 26 % (relative to TCPS) respectively.

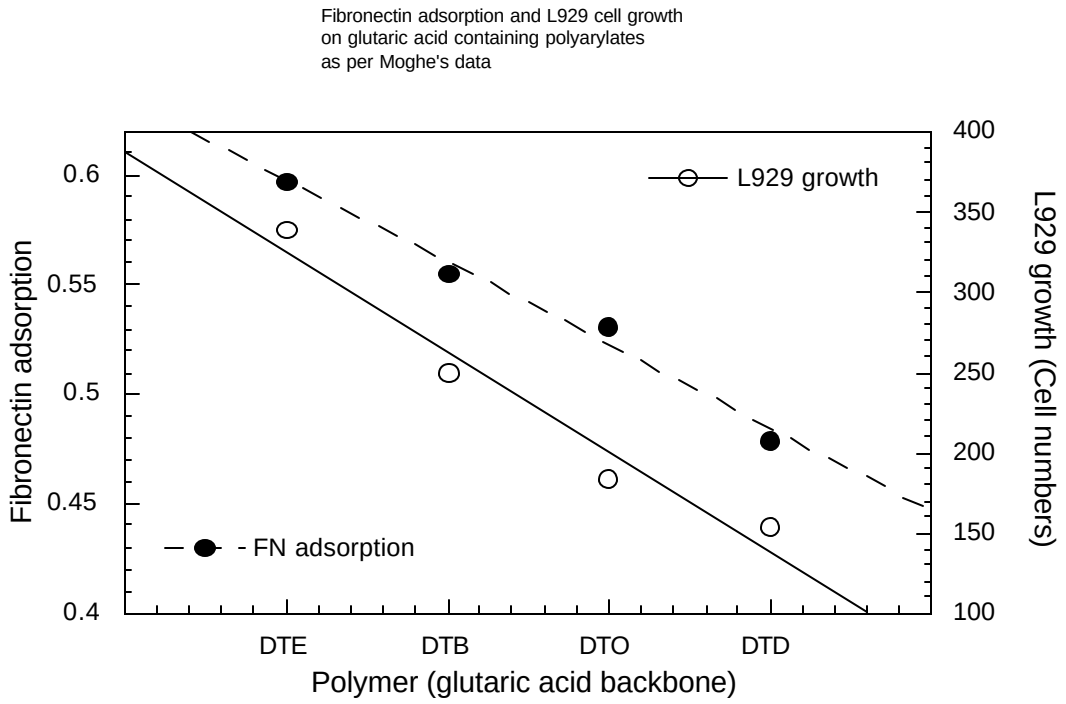

Figure 3: Comparison of fibronectin adsorption and cell growth on a subfamily of polyarylates.

REFERENCES

1 Ratner, B.D., Castner, D.G., Horbett, T.A., Lenk, T.J., Lewis, K.B. and Rapoza, R.J., Biomolecules and surfaces, *Vac. Sci. Technol. A* 1990, **8(3, part 2)**, 2306-2317

2 Kulkarni, R.K., Pani, K.C., Neuman, C. and Leonard, F., Polylactic acid for surgical implants, *Arch. Surg.* 1966, **93**, 839-843

3 Törmälä, P., Vasenius, J., Vainionpää, S., Laiho, J., Pohjonen, T. and Rokkanen, P., Ultra-high strength absorbable self-reinforced polyglycolide (SR-PGA) composite rods for internal fixation of bone fractures: *In vitro* and *in vivo* study, *J. Biomed. Mater. Res.* 1991, **25**, 1-22

4 Ray, J.A., Doddi, N., Regula, D., Williams, J.A. and Melveger, A., Polydioxanone (PDS), a novel monofilament synthetic absorbable suture, *Surg. Gynecol. Obstet.* 1981, **153**, 497-507

5 Chasin, M., Domb, A., Ron, E., Mathiowitz, E., Langer, R., Leong, K., Laurencin, C., Brem, H. and Grossman, S., Polyanhydrides as drug delivery systems, in *Biodegradable Polymers as Drug Delivery Systems* (Eds. M. Chasin and R. Langer), Marcel Dekker, New York, NY, 1990, pp 43-70

6 Langer, R. and Vacanti, J., Tissue engineering, *Science* 1993, **260**, 920-926

7 Hubbell, J., Biomaterials in tissue engineering, *Biotechnology* 1995, **13**, 565-576

8 Brocchini, S., James, K., Tangpasuthadol, V. and Kohn, J., A combinatorial approach for polymer design, *J. Amer. Chem. Soc.* 1997, **119(19)**, 4553-4554

9 Lowe, G., Combinatorial chemistry, *JCS Reviews* 1995, **1995**, 309-317

10 Mitscher, L.A., Some rumin ations on the present and future roles of combinatorial and multiplex syntheses in medicinal chemistry, *ChemTracts-Org. Chem.* 1995, **8(1)**, 19-25

Novel Polymers for Drug Delivery

Kathryn Uhrich

Associate Professor of Chemistry
Rutgers University, New Brunswick, NJ

Unimolecular Micelles

Micelles are colloids frequently used as drug delivery systems because of several useful properties. First, the hydrophobic microenvironment of micelles can water-solubilize hydrophobic drugs, expanding the pharmaceutical potential of otherwise useful compounds. This function has long been investigated as a means of improving solubility for drug delivery, particularly for parenteral or oral administration, as well as for ophthalmic, topical, rectal and nasal delivery. A second important function of micelles is their small size (less than 100 nm) which allows them to evade the reticuloendothelial system (RES) and behave as passive targeting agents. Third, the interplay between the hydrophobic domains of the polymer carriers and hydrophobic lipids of cell membranes enables micelles to be inserted into or passed through cell membranes. Yet, there is no systematic understanding of the factors that govern their ability to interact with cell membranes. Lastly, the major drawback to their extended clinical use is that micelles are thermodynamically unstable; they disorganize upon dilution in the bloodstream, by temperature increases or by interacting with various blood components.

The desirable features of micelles as described above can be used to design a polymer system that models micellar systems yet overcomes their major limitation by covalently binding the "unimers" such that dilution is not possible. In addition to biocompatibility and biodegradability, we designed polymers that encapsulate hydrophobic drugs to make them water-soluble, much as conventional micelles do. These polymeric micelles were designed with a hyperbranched hydrophobic interior (core) and hydrophilic exterior (shell). They are similar to conventional micelles but superior in that the polymeric micelles are thermodynamically stable.

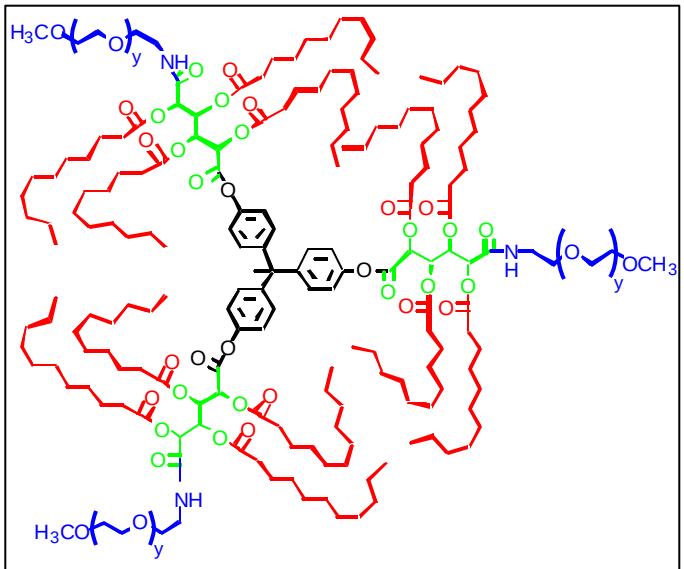

"Hyperbranched polymers deliver drugs steadily", *Chemical & Engineering News* , **77**, 63 (Jan. 18,1999).

Several drugs are being encapsulated within the interior; drug release is likely diffusion-controlled and dictated by the polymers' hydrophobic/hydrophilic ratio.

In preliminary studies, we observed that when lidocaine is encapsulated within the unimolecular micelles, *15 times more drug permeates the skin at a rate nearly 20 times faster* than when lidocaine is not encapsulated. This enhancement effect is unprecedented, and the mechanism is unclear.

Having demonstrated controlled drug release *in vitro* and *in vivo*, our next goal is to elucidate the mechanism of delivery using liposomes as simple

mimics of cell membranes. Transmission electron microscopy, dynamic light scattering analysis, and microcalorimetry studies further demonstrate the thermodynamic stability. Furthermore, cells grown in solutions of these polymers (concentrations from 10^{-8} M to 10^{-2} M) have growth rates similar to controls.

Notably, the micellar polymers designed for drug delivery applications appeal to a wide range of industries other than pharmaceutics including as dry cleaning, cosmetics and beauty aids, waste water treatments, and controlled release of pesticides. The similarity between all these industries is the need to solubilize hydrophobic compounds into aqueous media.

Critical issues are: (i) maximizing drug encapsulation within the polymer, (ii) monitoring polymer degradation *in vivo*, (iii) measuring interaction (e.g., stabilization) of polymer with cell membranes, (iv) quantifying biodegradability (enzymatic vs. hydrolytic) *in vitro* and *in vivo*, and (v) accurately measuring polymer size in aqueous solution (TEM vs. DLS).

Polyanhydrides as Polymeric Prodrugs

Aromatic polyanhydrides are clinically used as drug delivery systems for treatment of brain cancer. However, the slow degradation rate and the relative insolubility of the degradation products, especially in organic solvents, are major drawbacks for most biomedical applications. To improve the degradability and solubility of the aromatic polyanhydrides, the aromatic ring substitution was altered from *para*- to *ortho*-substituted. As expected, the *ortho*-substituted polymers have excellent solubility properties and appear to undergo surface erosion. Our evaluation of the degradation products obtained from polyanhydrides led to the design of an alternate polymer with potentially significant applications. Replacing the ether bond with an ester bond yields a poly(anhydride-ester) that degrades into salicylic acid (SA), an anti-inflammatory, antipyretic and analgesic agent.

The poly(anhydride-esters) are biodegradable (bioresorbable) materials that can be used for short-term dental and medical treatments. This polymer system is the first example in which the polymer itself is a controlled-release system: the polymer membrane degrades into SA, which has analgesic properties. This project focuses on the most significant aspect of this novel degradable polymer - localized reduction of inflammation and restoration of healthy tissues. Our goals are to evaluate the ability of poly(anhydride-esters) to simultaneously reduce inflammation while restoring tissues. Significantly, the polymer's primary use is as a suture material to facilitate healing of soft tissue.

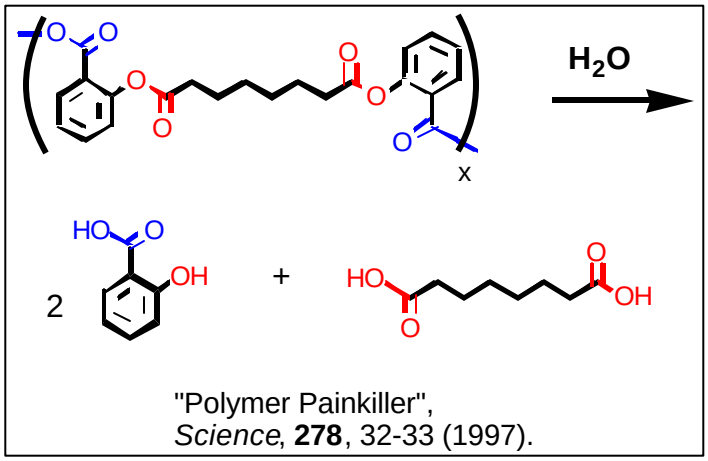

"Polymer Painkiller",
Science, **278**, 32-33 (1997).

In our preliminary animal studies, we observed that membranes of poly(anhydride-esters) locally reduced inflammation when implanted orally. Significantly, we noted *nearly 40 % more new bone growth in the areas surrounding the poly(anhydride-ester) implants* relative to the control polymers. Currently, we are evaluating our degradable polymers for controlling and preventing periodontal disease; future studies will focus

on orthopedic applications because of the unusual ability of the poly(anhydride-esters) to promote bone growth.

Based upon our concept of polymers that degrade into bioactive molecules, we are currently synthesizing other salicylate-containing polymers to treat diseases such as inflammatory bowel disease (e.g., Crohn's disease) and tuberculosis.

Critical issues are: (i) quantifying new bone formation, (ii) monitoring SA concentration *in vivo*, and (iii) measuring tissue/polymer interfacial interactions.

New

Imaging

Techniques

Near-Field Scanning Optical Microscopy (NSOM) for *In-situ* Characterization of Biomaterials

Luis F. Garfias

Lucent Technologies, Bell Laboratories
Materials Reliability and Component Processing Research Department,
600 Mountain Avenue, Murray Hill, NJ 07974-0636, USA

ABSTRACT

The aim of the present talk is to focus on the characterization of biomedical materials *in-situ* by using a modified Near-Field Scanning Optical Microscope (NSOM) with a home-built tuning fork head that enables concurrently optical and topographic imaging. The first example involves micropatterned substrates used for neuronal outgrowth. We have imaged *in-situ* the adsorption of two proteins, Laminin and Bovine Serum Albumin (BSA). Characterization of the orientation of micropatterned proteins is crucial for obtaining cell growth (such as neuron cells) in the desired configuration. The second example is related to the characterization of bone cements prepared with functionalised methacrylates. Bone cements act as fasteners and elastic buffers between a metallic prosthesis and bone. They exhibit improved biocompatibility, which reduces 'aseptic loosening', one of the main reasons for revision surgery after Total Hip Replacement. It is expected that calcium phosphate precipitation occur when these novel bone cements are exposed to simulated body fluid. By using the NSOM we can study *in-situ* the precipitation kinetics at short times and the changes induced after the bone cement is exposed to simulated body fluid.

INTRODUCTION

Characterization of materials using high-resolution *in-situ* techniques has become a very important subject in the past few years. In several areas of science (including electrochemistry, biology, chemistry, physics and medicine), the development of new methodologies and materials relies on the imaging of nanometer size features. More importantly, several preparation methods have to be performed within a liquid, since the solution plays a significant role in the whole process. In the present investigation, we focus on the characterization of biomedical materials *in-situ* by using a modified Near-Field Scanning Optical Microscope (NSOM). The NSOM used in this work has been adapted with a home-built tuning fork head that enables concurrently optical and topographic imaging[1,2]. In this case, all the images had been obtained by using an optical fiber that is used to concurrently obtain the topography and the optical images[3]. Full experimental detail on the setup of these experiments can be found in reference 3; a configuration setup diagram is shown in figure 1.

Characterization of the protein pattern both topographically and chemically is critical to engineering specific cellular responses. In the present study, NSOM was used to obtain simultaneous optical and topographical images of protein-micropatterned glass substrates. This technique allows direct observation in aqueous solutions of surface topography and light reflection without perturbation of the system, yielding images with nanometer resolution. Additionally, because NSOM is a non-contact imaging method, it enables non-destructive imaging of proteins in their natural, hydrated, configuration.

Low modulus bone cements have been suggested to reduce aseptic loosening in implants, one of the main causes of revision surgery after Total Hip Replacement (THR). Bone Cements

act as elastic buffers between the metallic prosthesis and bone. They exhibit improved biocompatibility and provides a softer cushion i.e. avoid stress concentration at some points in the cement. The traditional approach to obtain low modulus bone cements is by the addition of polymer with low glass transition temperature (Tg) like poly (ethyl methacrylate). In the present work, the Tg of the samples has been lowered by using hydrophilic polymers (MAA and DEAEMA) that are able to absorb water; this 'added' water facilitates the plasticisation of the bone cements. In our studies we expect to find evidences of calcium phosphate precipitation (besides fluid adsorption) when bone cements are exposed to simulated body fluid. The traditional way of observing this phenomenon is after several days of conditioning and then analyzing the substrate by SEM or look for Ca or P on the surface.

EXPERIMENTAL

Tip Preparation

All NSOM probes were prepared from type F-AS optical fiber (3.7 μm core diameter with 125 μm ± 2 μm of cladding and 245 μm ± 15 μm of polymer coating), obtained from Newport Corporation. The optical fibers were pulled with a commercial pulling machine (Sutter Instruments). The apex of the fibers was 100 nm or less, as shown in Figure 2 below.

Preparation of Micropatterned Surfaces

Microlithography originally developed by the microelectronics industry, can be used to precisely place protein on a support and to reproducibly control cell placement and orientation in vitro. In the present work, regions or stripes of permissive protein (Laminin) were alternated with regions of non-permissive protein (BSA) deposited on glass substrates. The resultant interface serves as a guide to orient many cell types, particularly neuronal cells. To create the samples, acid-etched no.1 glass coverslips were photolithographically micropatterned with alternating 20 μm Laminin-rich stripes and 10 μm bovine serum albumin (BSA) stripes. Samples were stored at 4 ºC in Hanks Balanced Salt Solution until imaged at various times ranging from 0 h to 30 d[4].

Bone Cement Preparation

Bone cements were prepared by mixing a solid component (containing a preformed polymer and benzyl peroxide) and a liquid component (containing methyl methacrylate or a mixture of monomers MMA-MAA or MMA-DEAEMA, and a tertiary amine like N, N-dimethyl-p-toluidine as activator)[5]. The main reason for using functionalised methacrylates is to improve cell attachment (osteoblast), to lower its glass transition temperature (Tg) by water absorption in hydrophilic polymers, and to induce the precipitation of calcium phosphate. In the present work, the following three types of samples were studied:

1. MMA (Base), which contains only methyl methacrylate.
2. MMA0.7-MAA0.3 which contains 0.7 (molar fraction) of methyl methacrylate and 0.3 (molar fraction) of methacrylic acid and,
3. MMA0.92-DEAEMA0.08 which contains 0.92 (molar fraction) of methyl methacrylate and 0.08 (molar fraction) of diethyl amino ethyl methacrylate.

RESULTS AND MAIN FINDINGS

Micropatterned Surfaces

Topographical and optical images were obtained on the NSOM, first of the micropatterned photoresist (see Figure 3) and then of the micropatterned proteins after deposition (see Figure 4). The surface features were measured from the topographical images while the optical images were examined to confirm the observed height changes in the topographical images. Multiple regions were imaged on several coverslips at each time to determine characteristic surface features of protein-patterned surfaces in a stereotypical aqueous environment. Additionally, *in-situ* images were taken of the micropatterned surface at each stage of protein deposition to determine how each stage/step contributes to topological surface features. We have found that, after 8 days in storage, the micropattern does not degrade. We are currently investigating the effect of aging and the effect of using alternative substrates (e.g., polymers). Additionally, we hope to examine the patterned features resulting from other patterning methods, such as microcontact printing. Finally, we will correlate these findings with results obtained by using different analysis methods (XPS, ATR-FTIR).

Bone Cements

We followed the precipitation kinetics at short times by using the *in-situ* NSOM. Figure 5 to 7 show images of the three different samples after exposure to deionized water for 5 days at 50 ^{o}C. None of the three samples were affected by continuous immersion in pure water at room temperature. However, exposure to pure water at 50 ^{o}C shows some marked differences. The base material did not degrade whereas the sample MMA0.7-MAA0.3 showed some cracks after the long-term exposure. The sample MMA0.92-DEAEMA0.08 showed swelling in certain regions. We are currently investigating the effects of exposure to Simulated Body Fluid (SBF) and Hank's solution (with added glucose) at room temperature. We plan to examine the surface *in-situ* during exposure to both solutions and to correlate these results with those obtained by other methods (XRD, DMTA, DSC).

MAIN CONCLUSIONS AND FUTURE WORK

We have developed a novel method to investigate surface topography *in-situ* in liquids, based on the NSOM. This new method can be used to investigate *in-situ* electrochemical reactions in liquids. Fluorescence and optical microscopy can be achieved both *in-situ* and *ex-situ.* This method has proven useful for non-invasive investigation of changes in biomedical materials. At the present time the lateral resolution is around 100 nm.

Future work will focus on continued development of these techniques and the exploration of new problems that can be solved by *in-situ* monitoring of surface reactions in liquids. We are currently investigating techniques for the preparation of smaller size nanoprobes (10 nm) that can increase the lateral resolution.

ACKNOWLEDGMENTS

I would like to thank the contributors to the present work, K. E. Schmalenberg and K. E. Uhrich from Rutgers University, Department of Chemistry and D. M. Thompson and H. M. Buettner from Rutgers University, Chemical and Biochemical Engineering for their studies of Micropatterned Substrates used for Neuronal Outgrowth. I also thank J. V. Cauich from CICY-Merida in Mexico for the studies on bone cement.

REFERENCES

1. P. I. James, L. F. Garfias-Mesias, P. J. Moyer and W. H. Smyrl J. Electrochem Soc. 145, L64 (1998).
2. L. F. Garfias-Mesias and W. H. Smyrl, J. Electrochem Soc. 146, 2495, (1999).
3. L. F. Garfias-Mesias and D. J. Siconolfi, J. Electrochem. Soc. 147, July, (2000).
4. Y. Travaly. K. Schmalenberg, R. Parikh, H. Buettner and K. Uhrich, Langmuir, in press, (2000).
5. E. Islas-Blancas, M. Cervantes-Uc and J. V. Cauich-Rodriguez, Il Latinoamerican Congress on Biomaterials, La Habana, Cuba, Nov. 1-5, (1999).

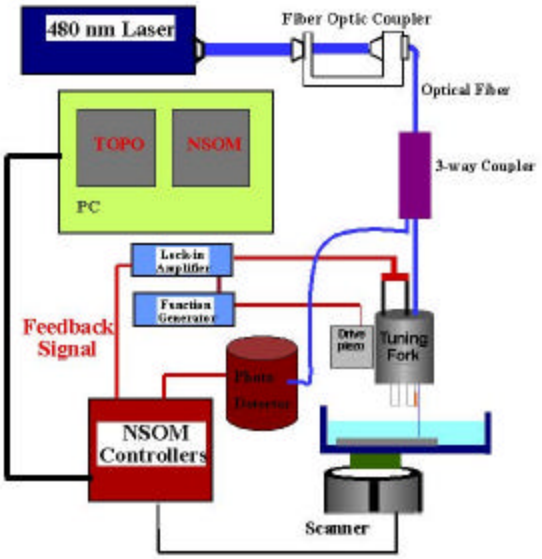

Figure 1. Setup to obtain High Resolution Topography and Optical Imaging

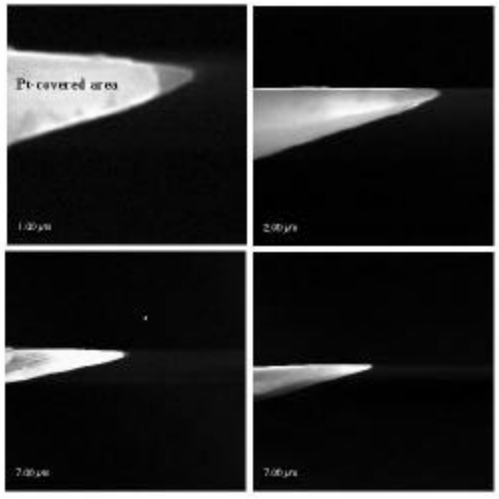

Figure 2. High Resolution SEM of Pt coated Optical Fibers Nanoprobes

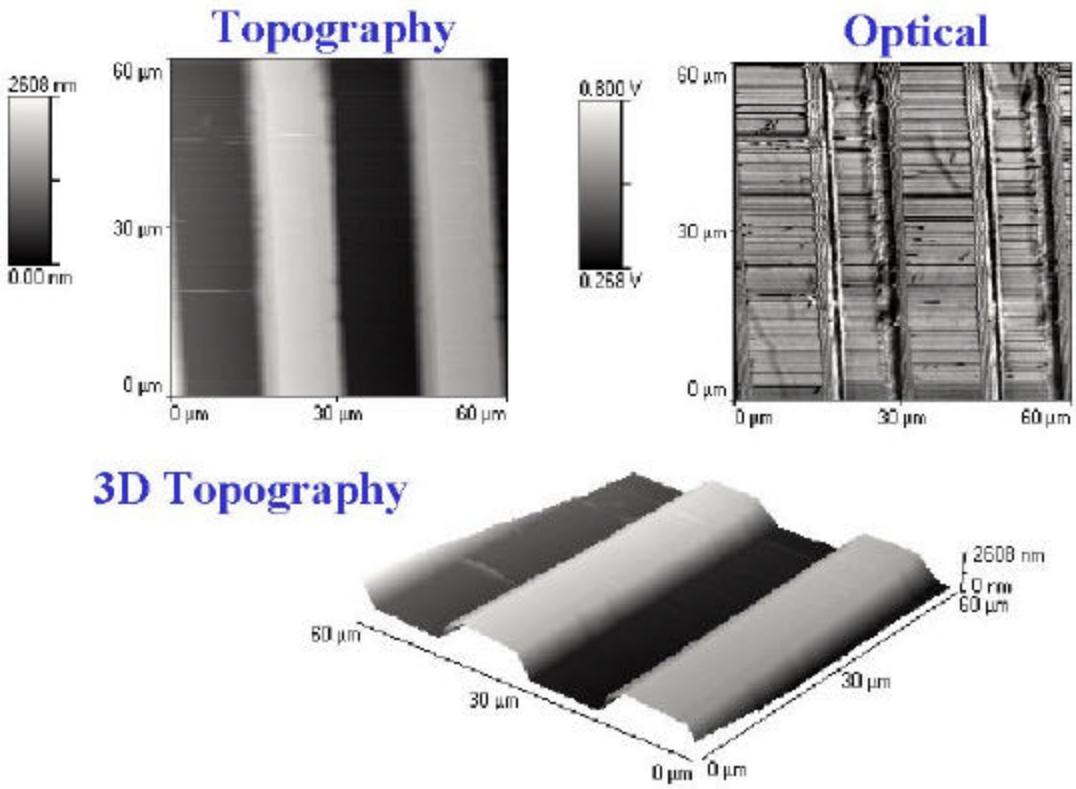

Figure 3. *In-situ* Imaging of Micropattern

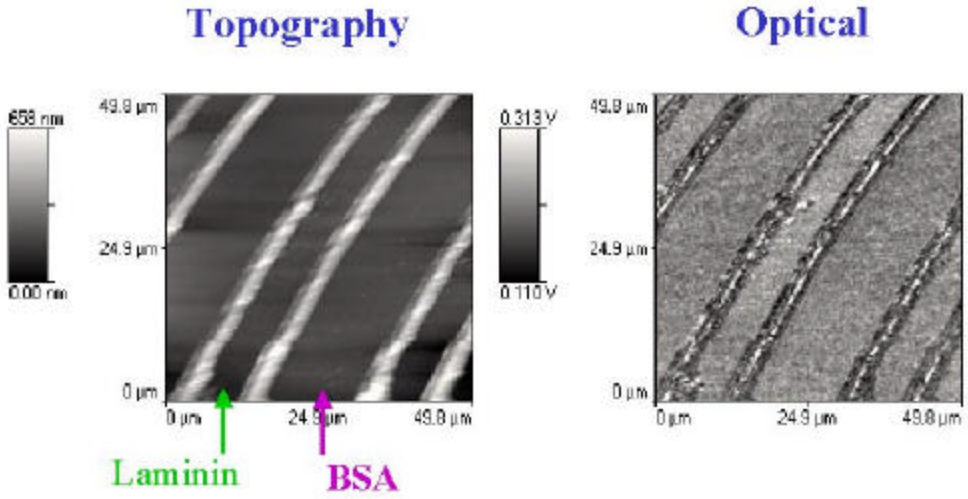

Figure 4. *In-situ* Imaging of Protein Micropattern

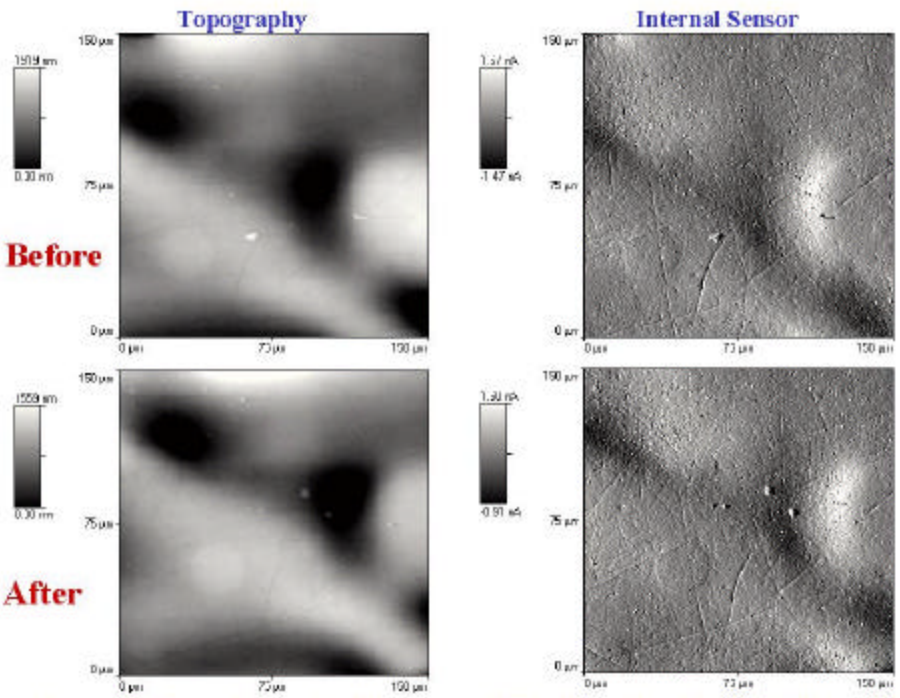

Figure 5. Bone Cements Prepared With Functionalised Methacrylates Base Before & After Exposure to H_2O at 50°C 5 days

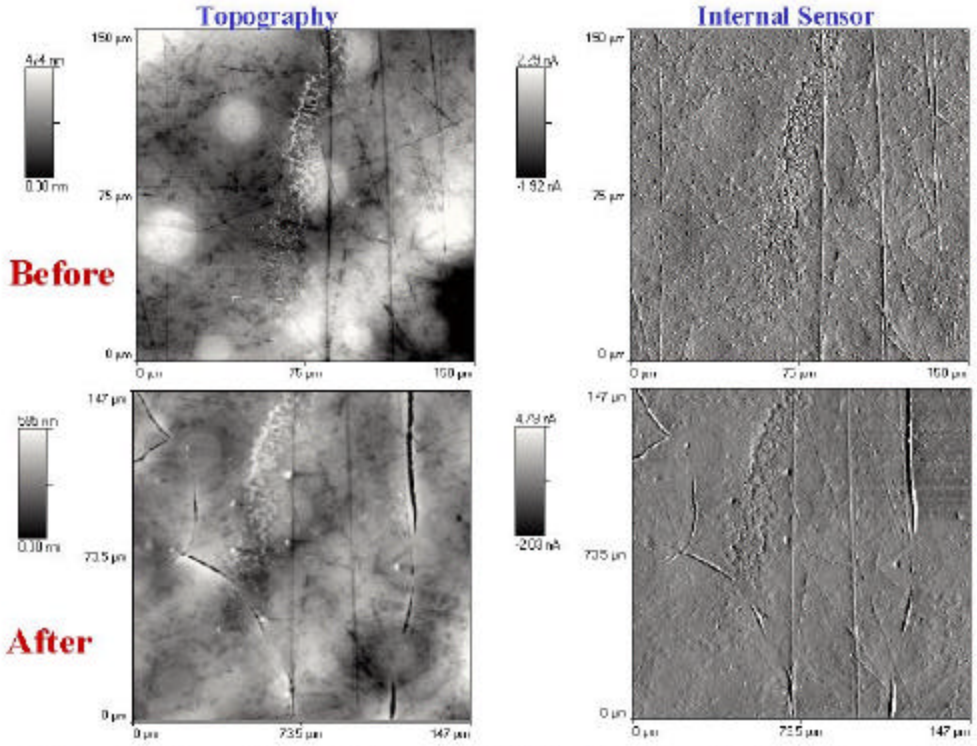

Figure 6. Bone Cements Prepared With Functionalised Methacrylates 0.7-0.3 Before & After Exposure to H_2O at 50°C 5 days

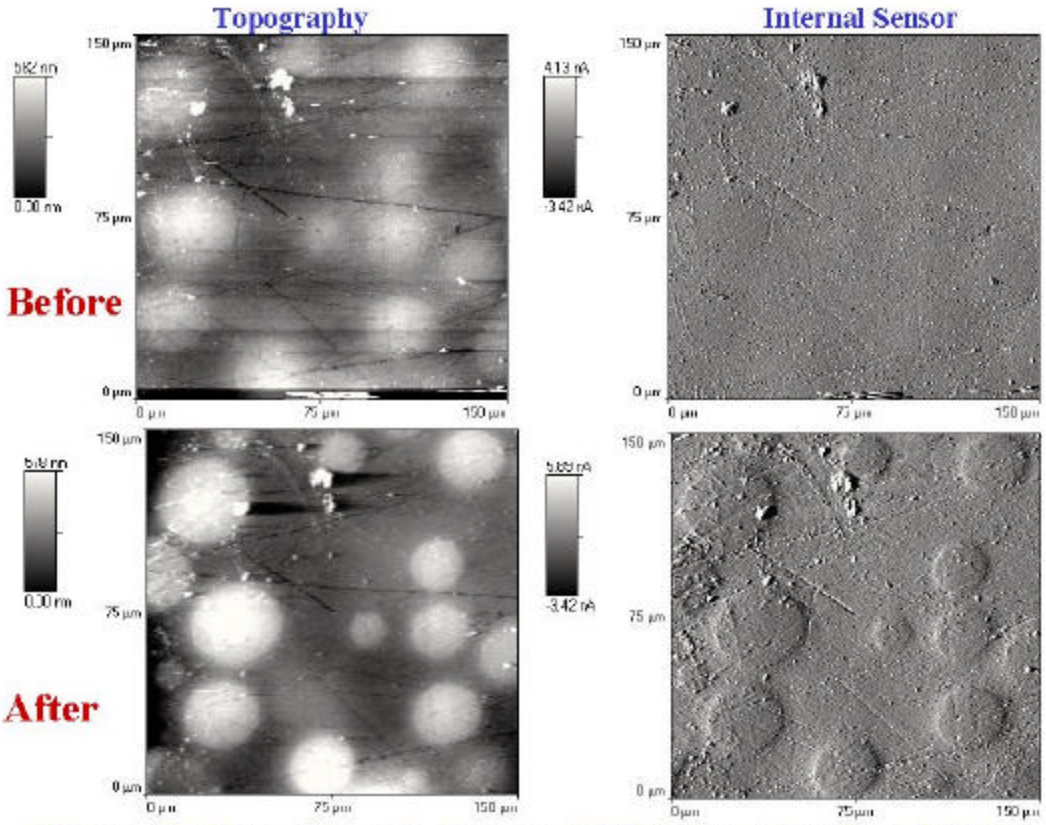

Figure 7. Bone Cements Prepared With Functionalised Methacrylates 0.92-0.08 Before & After Exposure to H_2O at 50°C 5 days

Optical Coherence Tomography for Imaging Tissue Scaffolds

Joy P. Dunkers[1], Kristen Sakala Labazzo[2], and Joachim Kohn[2], Richard S. Parnas[1]

[1]Polymers Division
National Institute of Standards and Technology
Gaithersburg, MD

[2]Wright-Rieman Laboratories
Department of Chemistry
Rutgers University
Piscataway, NJ

Introduction

It is generally understood that a complex interaction of many variables influence the success of cell infiltration, proliferation, and differentiation within a tissue scaffold [1]. One parameter that has a large influence on the development of functioning tissue is the microstructure of the scaffold itself. Characterization of the size and connectivity of pores inside the scaffold is necessary for evaluating the potential of any candidate scaffold.

Traditionally, destructive techniques have been used to characterize the scaffold such as scanning electron microscopy (SEM). With SEM, the scaffold must be freeze-dried, sectioned, and mounted for analysis. This procedure substantially alters the size and shape of the pores when compared to their in-situ state. These effects are more pronounced in materials such as hydrogels, whose intended structures are best observed in an aqueous environment. Hydrogels swell considerably when placed in aqueous solutions. Therefore, observation of dried samples utilizing SEM does not provide an accurate picture of the internal structure. With environmental SEM (ESEM), the scaffold can remain wet. When using ESEM, the sample remains hydrated by balancing the vacuum applied to the sample chamber with the introduction of water vapor. However, it is doubtful whether the scaffold remains fully hydrated. Ideally, the microstructure should be non-destructively evaluated for scaffolds fully swollen in biological media.

Most recently, x-ray computed tomography of scaffolds with synchrotron sources has been used to characterize scaffold microstructure and tissue growth with resolutions to a few microns and with no degradation of the tissue from the soft x-ray source [2]. However, this characterization approach is not practical because of extremely limited access to this costly technique. New methods to rapidly and accurately analyze scaffolds in a timely manner at a reasonable cost are desired. One promising non-destructive evaluation technique is optical coherence tomography (OCT).

Optical coherence tomography is a non-invasive, non-contact optical imaging technique that allows the visualization of microstructure within scattering media [3,4,5,6]. OCT uses light in a manner analogous to the way ultrasound imaging uses sound, providing significantly higher spatial resolution (10 μm to 20 μm) albeit with shallower penetration depth. OCT is based upon low-coherence optical ranging techniques where the optical distance to individual sites within the sample is determined by the difference in time, relative to a reference light beam, for an incident light beam to penetrate and backscatter within the sample (Figure 1). This temporal delay is probed using a fiber optic interferometer and a broadband laser light source. The fiber optic

interferometer consists of single-mode optical fiber coupled with a 50/50 fiber optic splitter that illuminates both the sample and a linearly translating reference mirror (Figure 1). Light reflected from the reference mirror recombines with light back-scattered and reflected from the sample at the 50/50 splitter to create a temporal interference pattern that is measured with a photodiode detector. The depth within the sample is determined by dividing the distance traversed by the reference mirror by the group refractive index of the sample. The resulting interference patterns are present only when the optical path difference of the reference arm matches that of the sample arm to within the coherence length of the source. The axial, or z, spatial resolution that can be obtained with OCT is determined by the coherence length, or inverse spectral width, of the source and is typically 10 μm to 20 μm. The transverse, or x, spatial resolution of OCT is determined by the focal spot size on the sample, which is typically 10 μm to 30 μm. The practical limitation on the depth of penetration within the sample is the attenuation of light caused by out-of-plane scattering. Three-dimensional images of the sample are obtained by rastering the sample in x between successive OCT measurements along the y-axis.

This work focuses on exploring OCT as a way to characterize the microstructure of tissue scaffolds. First, the microstructure of the closed cell scaffold is presented using a traditional, destructive characterization technique: scanning electron microscopy (SEM). Second, measurement of the group refractive index of the scaffold in distilled water is presented. Then, one strength of OCT is highlighted: a cross-sectional slice inside the scaffold is presented with several pore size and wall thickness measurements. Lastly, the advantages and limitations of OCT are presented.

Experimental

Preparation of Crosslinked Scaffolds for SEM

The scaffolds were first equilibrated in distilled water for 24 h to swell the hydrogel. Samples were then frozen in liquid nitrogen, and immediately freeze-fractured. The fractured samples were dried under vacuum for 24 h before SEM analysis. The dried samples were mounted on aluminum studs and sputter coated with gold/palladium for 120 s. Samples were then analyzed on an Amray 1830I scanning electron microscope at 20 kV [7].

Optical Coherence Tomography

To prepare the scaffold for OCT, the sample was placed in a test tube and evacuated for 10 min to remove air. Then, the distilled water was introduced while the sample was still under vacuum. Using this method, no entrapped air was detected using visual inspection. The scaffold was then placed on a glass petri dish and immersed in distilled water for imaging.

The sensitivity of the OCT system was measured to be 108 dB. The resolution in the axial, or z, direction was 14 μm. The scaffold was imaged using the 26X objective having a resolution of 21 μm in the x direction. The sampling volume was 3.00 mm along x, 3.00 mm along y, and 5.00 mm along z. The pixel size along the x axis was 7 μm, along the y axis was 10 μm, and along the z axis was 5 μm.

Results and Discussion

SEM was used to gather the representative scaffold cross-section in Figure 2. From this micrograph, the closed pore nature of the scaffold is easily identified. However, since the scaffold was dried during preparation for SEM, microstructural details of the scaffold swollen in the aqueous medium are lost. The pore size and connectivity of the swollen scaffold is expected to be substantially different than a dehydrated specimen prepared for SEM. Also, it is unknown to what degree microtoming the sample for SEM alters the microstructure. Using OCT, a scaffold can be volumetrically imaged in its swollen state and examined anywhere within the volumetric image for quantitative information at a resolution of 10 μm to 20 μm.

Before quantitative information about features within a scaffold can be analyzed, a refractive index for the scaffold must be determined. Because the scaffold is a heterogeneous material consisting of swollen polymer and an undetermined volume fraction of pores, the average or group refractive index must be measured for proper image scaling. When performing refractive index measurements, it is important that the sample be thin enough to image the entire thickness. Figure 3 shows a low resolution image of the scaffold on a glass petri dish. The group refractive index is calculated by dividing the thickness of the scaffold in the image (z' + z), by the actual thickness, z. These thicknesses are taken from the pixel heights in the image. For this scaffold, the group refractive index is 1.382. Of course, some positional error in scaling will be introduced because the local refractive index in an image will be different than the group refractive index since the scaffold is highly heterogeneous.

The ability to gather quantitative information from OCT images is shown in Figure 4. Here, an x-y cross-section of the scaffold 280 μm from the surface is shown with pore size and wall thickness measurements. The closed pore nature of this scaffold is also revealed, indicating that it is a poor candidate for cell infiltration and growth.

In order to make the most of this powerful technique, the images must be analyzed keeping the limitations of OCT in mind. There are a number of mechanisms through which image quality degrades. First and foremost, contrast is lost as a function of depth because photons scatter out of the sampling volume. Second, a highly reflecting feature can cause features below it to appear invisible. Third, noise in the form of speckle can be generated by multiple forward scattering of photons that constructively interfere. The magnitude of the aforementioned effects depends upon the differences of refractive index as well as size and shape of the scatterers. Fourth, resolution is degraded by refraction. And finally, sample birefringence can cause feature drop-out. In an OCT system that has polarization compensation, this last limitation is not an issue. The OCT images of the scaffold need to be critically evaluated to determine at what depth information is no longer reliable, meaning that significant feature drop-out or resolution degradation occurs. This will be done in the near future.

Conclusions

Optical coherence tomography is a very promising technique for non-destructive, volumetric, in-situ characterization of scaffold microstructure. OCT can used to probe pore size and connectivity for evaluation of scaffold viability. It is anticipated that OCT can also be used to study scaffold degradation as well as cell growth. For tissue scaffolds and material systems in general, representative images must be evaluated to determine the maximum depth from which data can be reliably used.

References

1 . Speidel, M. and Uggowitzer, P. eds., **Materials in Medicine**, Hochschulverlag AG an der ETH Zurich, 1998.

2 . Mayer, J., Swiss Federal Institute, Zurich, personal communication.

3 . Huang, D., Swanson, E., Lin, C., Schuman, J., Stinson, W., Chang, W., Hee, M., Flotte, T., Gregory, K., Puliafito, C., and Fujimoto, J.G., *Science,* **254**, 1178, (1991).

4 . Fujimoto, J., Brezinski, M., Tearney, G. Boppart, S., Bouma, B., Hee, M. , Southern, J. and Swanson, E., *Nature Medicine,* **1**, 970, (1995).

5 . Bashkansky, M., Duncan, M., Kahn, M., Lewis, D., Reintjes, J., *Opt. Lett.*,. **22**, 61(1997).

6. Dunkers, J. P., Parnas, R. S., Zimba, C. G., Peterson, R. S., Flynn, K. M., Fujimoto, J. G. and Bouma, B. E., *Composites, Part A*, **30**, 139(1999).

7. Identification of a commercial product is made only to facilitate experimental reproducibility and to adequately describe experimental procedure. In no case does it imply endorsement by NIST or imply that it is necessarily the best product for the experimental procedure.

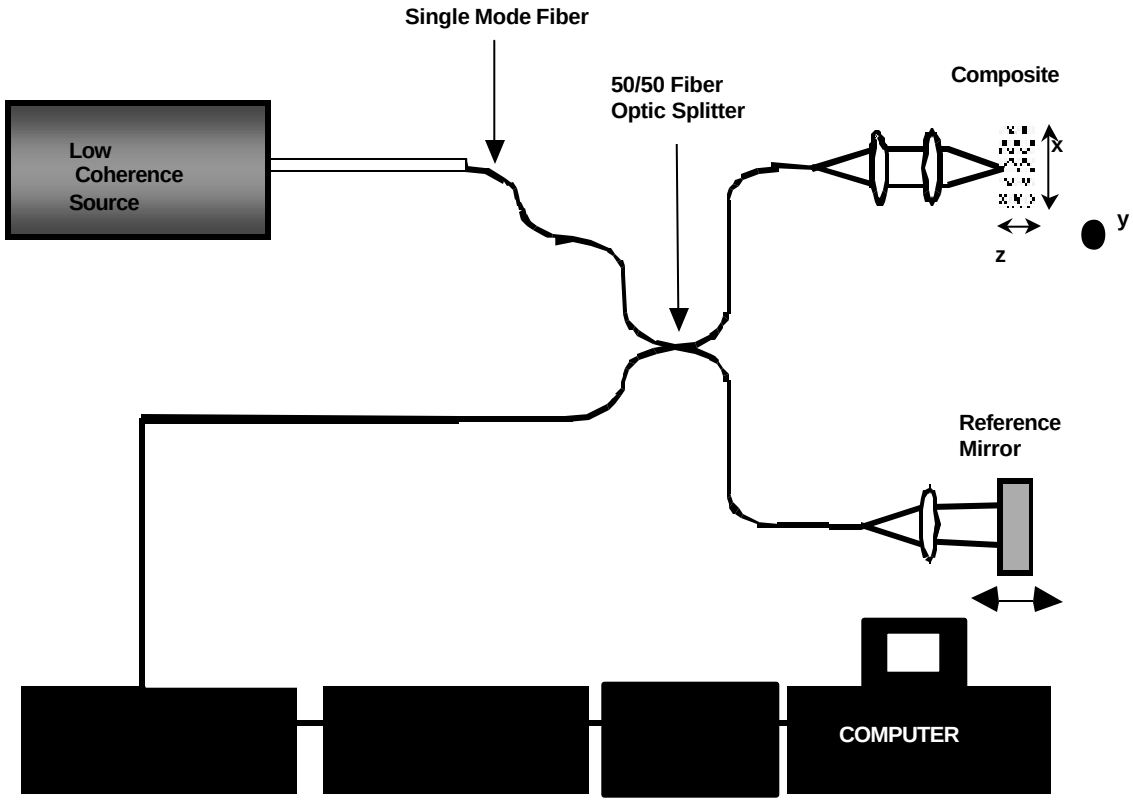

Figure 1: Schematic representation of the OCT system.

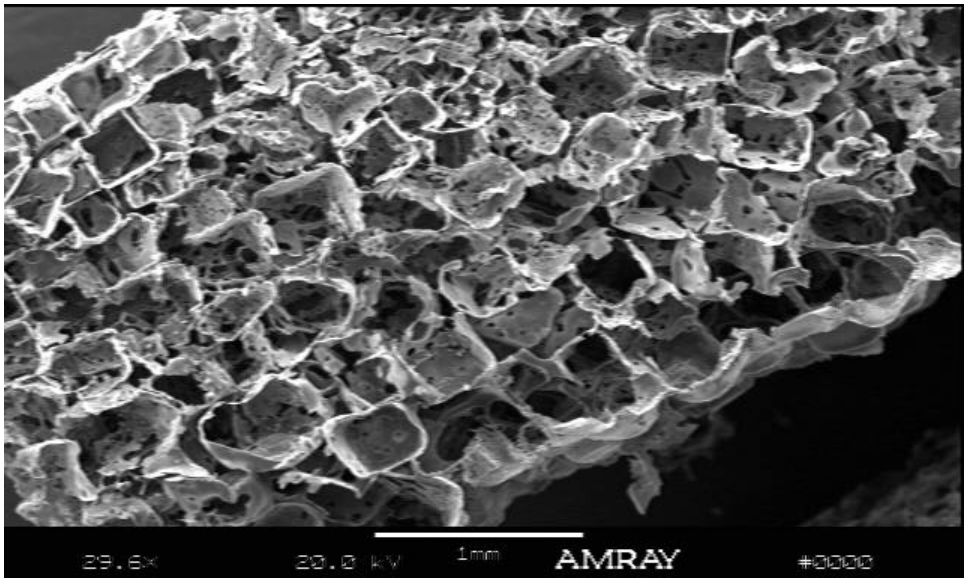

Figure 2: SEM micrograph of hydrogel scaffold.

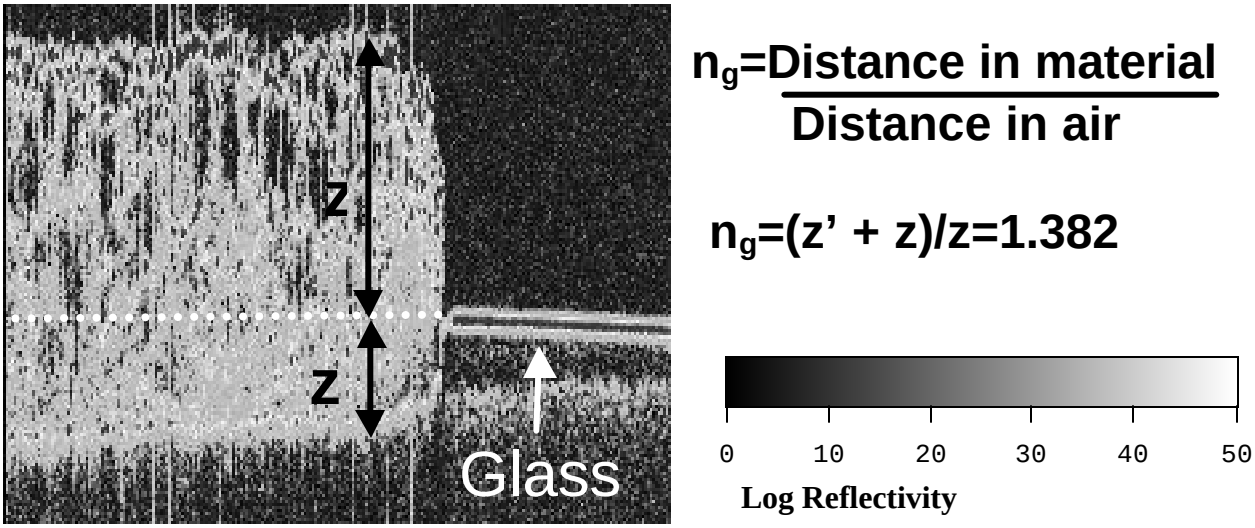

Figure 3: OCT image of hydrogel scaffold in water on glass petri dish.

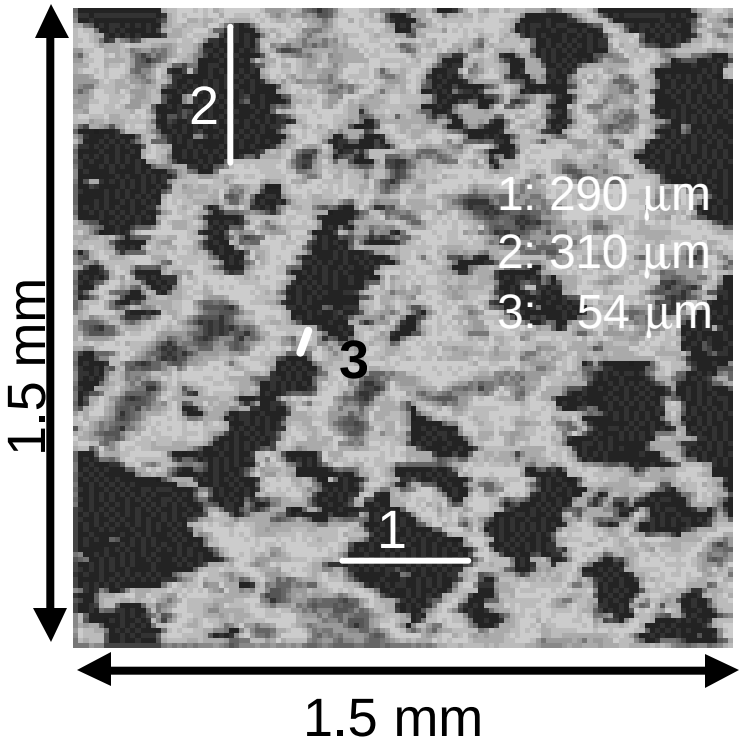

Figure 4: x-y cross-section of volumetric OCT image of hydrogel scaffold in water, 280 μm from the surface

Micro-Thermal Analysis : A Marriage of Atomic Force Microscopy and Thermal Analysis

Roger Blaine

TA Instruments
109 Lukens Drive, New Castle, DE 19720

Scientific intuition holds that resolution and temperature equilibrium in a thermal analysis specimen is enhanced with smaller test specimen size. And if very small test specimens could be used, increased heating rates and shorter experimental times would result. Conventional thermal analysis is limited in sample handling by tweezer, razor blade and eye to test specimens that are on the order of 0.5 mg. Test specimens of this size can be heated at rates up to about 20 °C/min and still achieve uniform temperature across the specimen. Specimens smaller than this size requires rarely used microscopic techniques.

Atomic Force Microscopy (AFM) provides a microscopic tool useful in micro sample handling. In AFM, a needle is rastered across a small surface (typically 10 μm x 10 μm). Atomic forces acting on the probe provide topological images of the surface. These images may then be used to select a small section of the sample for characterization. In Micro-TA, the normal mechanical needle of AFM is replaced with a "V" shaped microscopically thin platinum wire. The wire serves as a micro platinum resistance thermometer. If power is supplied to the wire it serves as a micro heater. The heater power may be controlled to provide a constant temperature, or linear or modulated heating (or cooling). Thus the heated thermal probe simultaneously serves as a micro differential thermal analyzer (μDTA™) and a micro thermomechanical analyzer (μTMA™) characterizing specimens on the order of 2 x 2 μm (10 pg) in size. Micro-thermal analysis (μTA™) may be thought of as a marriage between atomic force microscopy for sample preparation, handling and visualization and thermal analysis for characterization.

The use of very small specimen sizes means that very high heating rates may be used. Typical heating and cooling rates in μTA are 2 °C/s to 25 °C/s (i.e., 12 °C/min to 1500 °C/min).

Facilitated

Discussion

Critical Issues in the Characterizations of Polymers for Medical Applications

Michael Jaffe

Research Professor, New Jersey Institute in Technology
Director, Medical Device Concept Laboratory
Newark, NJ

1. The Issue is the Surface

- ***Defining the interface chemistry between biological systems and synthetic materials***
  surface - protein - cell
  - How do single conformation proteins bind to conformationally degenerate synthetic polymers?
    - ***Mean field versus site specific***

      Global versus local surface free energy sites

    - ***Effects of "roughness" - patterns and walls***
  - Does the cell "read" protein coated surfaces or protein conformations mitigated by original surface features?

2. Critical Surface Tension In-vivo Device Polymers

" Teflon"	***19 dynes/cm***
"Dacron"	***45 dynes/cm***
PE	***35 dynes/cm***

Does the Polymer Matter?
Issues:
- Effect of molecular orientation, crystallinity, tie molecules
- In-vivo relevant testing

3. Surface Characterization

- ***Mechanical testing of the adhesive bond***
- ***Contact angle and other mean field techniques***
- ***Direct imaging - OM , SEM, TEM, STM, AFM***
  - Confocal microscopy
  - AFM based thermal analysis
  - AFM with receptor molecule tips
- ***Optical or stylus based profilemtry***
- ***High vacuum techniques - ESCA, SIMS***
- ***Glancing angle spectroscopies***
- ***Penetration based mechanical testing***
- ***Surface sensitive molecular relaxation spectroscopies***
- ***2D imaging of specific conformations***

4. The Bulk Can't Be Ignored!

All characterization relevant to polymer behavior is relevant to polymers for medical devices

When appropriate, properties should be monitored under bio-relevant conditions

- Mechanical properties, fatigue, transition temperatures, shrinkage

- ***Molecular relaxation spectroscopies may yield insight into both bulk and surface properties***
  - Dynamic Mechanical, Dielectric Loss, Thermally Stimulated Current techniques
  - Measure changes as f(time) at 37 ^{o}C in biorelevant environment (water, saline, serum)

5. Critical Issues

- ***Quantifying the importance of surface energy and surface roughness***
  - ***Developing site specific conformational spectroscopies for:***
  - Scaffold surface
  - Proteins at surface
  - Deterministic cell receptor sites
- ***2D surface conformational imaging***
- ***In-vivo characterization techniques***
- ***Identification of artifacts!***

6. Backup data

Synthetic versus biological polymers
Medical Polymers
Adhesion and Binding
Origin of Surface Chemistry and Physics

Changing the surface chemistry
Patterning the surface
Characterization of polymer structure in the solid state
Porosity characterization
Creating the optimum scaffold for tissue engineering
Designing the starting chemistry
Typical scaffold architecture
Key scaffold properties
Control of bulk scaffold properties
The artificial extracellular matrix

State-of-the-Art

Research

In

Biomaterials

Switching Cell Functional Fates on Polymer Substrates

Prabhas V. Moghe

Department of Chemical and Biochemical Engineering
Rutgers University, Piscataway, NJ 08854, U.S.A

We have been investigating approaches to control cell morphogenesis and motility on polymer substrates that are differentially adhesive. Engineering selective changes in cell functional activity may be essential to the design of polymer substrates in order to allow controlled turn-over of cells at the biomaterials interface upon implantation. The degree of control over cellular responsiveness required is inevitably attuned to the needs of the implant pathology. This talk focuses on our recent findings on the means and mechanisms of manipulating the functional behavior of primary liver cells called *hepatocytes* during culture on ligand treated synthetic polymers.

In our studies, we have compared the consequence of variation in two important biomaterial properties on the alteration in cell functional differentiation. The key properties considered here are the *substrate microtopography* and *substrate bioactivity* (*or* concentration of the cell adhesion ligand). In the first segment of our work, we focused on an amorphous synthetic polymer, 50/50 poly(D,L glycolic-co-lactic acid) (PGLA), whose foams were differentially textured (at subcellular, cellular, and supercellular scales). This material was deliberately chosen because PGLA intrinsically lacks biological binding sites that may activate cell functions. Thus, the effects of progressive changes in substrate topology and cell-specific biochemistry could be systematically mapped in relation to the properties elicited by untextured and untreated base substrates.

In subsequent reports, we studied hepatocyte morphogenesis and functional induction on differentially textured substrates presenting the cell adhesion ligand, collagen. A comparison of our findings from these two systems yields interesting conclusions. If substrate-exerted regulation on cell functions were plotted on the same graph (see below), we would see that the regimes for maximizing cell function on surfaces with variable adhesivity can be significantly distinct. Mechanisms leading to this disparity of cell responsiveness on substrates with or without an adhesion ligand are being examined.

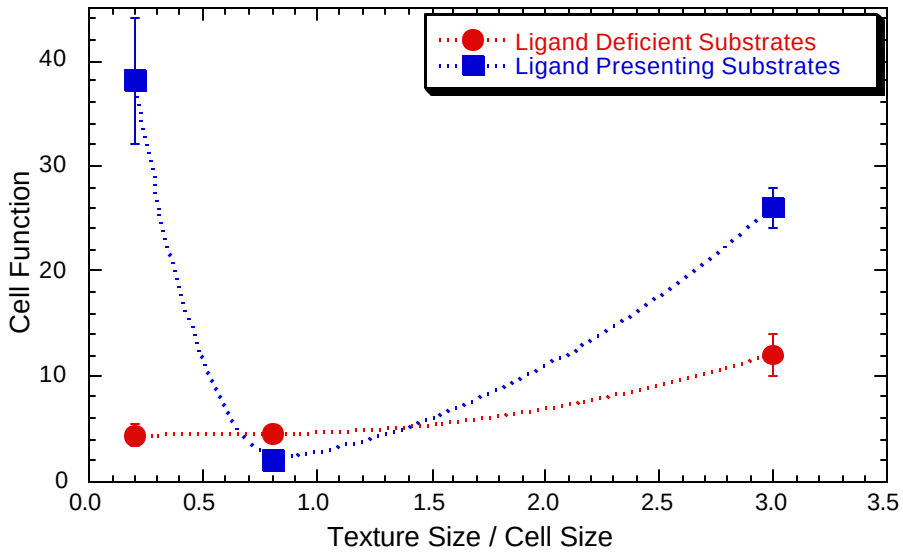

Foremost among the mechanisms, is the role of cell morphogenesis underlying cell-substrate interactions, which will be elaborated during the talk. It is also necessary to consider how cell responsiveness to substrate texture and chemistry may be additionally amplified or repressed in a controlled fashion, for example, in response to biochemical growth factors (whose presence can be a pivotal signal for organ regeneration or wound healing at the implant site). It is believed that variations in cell morphogenesis can "switch" cellular commitment to function versus growth. Based on this premise, we have employed a simple two-dimensional model polymer substrate, to further examine how the morphology of cells can "prime" swings in cell function or growth, following changes in activating growth factors in the cellular microenvironment. We report that the *same* growth factors can be used to either *maximize* cell function, or *minimize* cell function, depending on the corresponding morphogenetic events, which in turn can be controlled at the substrate level (e.g. by microtopography, or stiffness).

In the final segment of the talk, I will report on our finding that for motile cells, the microtopography of ligand-adsorbed polymer substrates can elicit enhanced rate of cell migration at lower levels of ligand concentration than those required on untextured substrates. This observation highlights the intriguing possibility of designing micro and nanoscale substrates with enhanced "sensitivity" to the biological ligand, and perhaps of defining the right biological ligand for more efficiently "gating" the attachment of desired cell types.

Biomimetic Membrane Surfaces for Tissue Regeneration

Hoda M. Elgendy, Curtis W. Meuse, Vitalii Silin, John Woodward, Anne L. Plant

Biotechnology Division, National Institute of Standards and Technology, Gaithersburg, MD 20899-8313

Biomimetic materials based on alkanethiol self-assembled monolayers and cell membranes are under investigation in our laboratory. The use of alkylthiols for modification of metal surfaces is an important approach to controlling surface chemistry in studies of cell adherence and growth[1] and recently as implantation materials for tissue engineering.[2] Phospholipid vesicles spontaneously reorganize at a hydrophobic alkanethiol monolayer on a gold surface to form a hybrid bilayer membrane consisting of a layer of alkanethiol plus a layer of phospholipid.[3] Crude cell membranes can be used in place of phospholipid vesicles to form a cell membrane hybrid bilayer. We have compared the kinetics of formation of cell membrane/alkanethiol hybrid bilayers with that of phospholipid/alkanethiol bilayers and determined that the apparent mechanism of formation of the bilayer is the same.[4] We are examining the potential of these biomimetic materials as a means for modifying surfaces for cell-specific recognition and binding. Cell membrane hybrids have been prepared from membrane preparations of red blood cells[5], COS cellIs[6], 293T cells[6], and rat osteosarcoma cells (CRL-1663)[7]. A number of techniques including ellipsometry, atomic force microscopy, electrochemistry, surface plasmon resonance, and environmental scanning electron microscopy have been applied to characterize cell membrane hybrids[4-7]. Data indicate that some membrane proteins are reconstituted in an active conformation at cell membrane hybrid surfaces. For example, cyclic voltammetry measurements of $K_3Fe(CN)_6$ with red blood cell membrane hybrids indicated that more current can pass through the cell membrane hybrid than can pass through the decanethiol monolayer before adding the cell membrane preparation to it. This current was blocked by DIDS (4,4'-diisothiocyanate stilbene-2,2'-disulfonic acid) suggesting that Band 3 channel protein was responsible for the observed anion conduction.[4] Recently, we have used antibodies to CCR5 chemokine receptor to identify the presence of CCR5 receptor expression in transfected COS cells.[6] In this work osteosarcoma crude membranes were prepared from rat osteosarcoma cells (ATCC:CRL-1663) by osmotic lysis.[7] The protein concentration in the osteosarcoma crude membranes preparation was estimated to be 0.437 mg/mL using Sigma Diagnostic micro protein reagents. Cell membrane hybrid bilayers were prepared from the osteosarcoma crude membrane and octadecanethiol self-assembled monolayers on gold surfaces. Contact angle, ellipsometry and atomic force microscopy have been used to characterize the surfaces of these crude membrane hybrid bilayers. Osteosarcoma cells were seeded on these hybrid membrane bilayer surfaces for 7 d in culture. Cell attachment and growth on crude membrane hybrid bilayers and TCPS surfaces were studied and were found to be comparable. Expression of osteosarcoma markers such as osteocalcin, and alkaline phosphatase are used to confirm that the osteosarcoma cells growing on these biomimetic surfaces are retaining their normal phenotype. The growth and phenotype of osteosarcoma cells on cell membrane hybrid surfaces are being compared to their growth and phenotype on other traditional biomaterial surfaces. Our in vitro observations suggest that biomimetic membrane surfaces constructed from osteosarcoma cell membranes may be suitable biomaterials to support osteoblasts as part of a matrix for enhanced bone repair.

[1] Chen, C. S. et al. Science, 276, 1425 (1997).
[2] Valentini, R. et al. private communication.
[3] Plant, A. L. Langmuir, 15, 5128 (1999).
[4] Hubbard, J. et al. Biophys. Chem. 1998
[5] Rao, N. M. et al. Biophys. J. 73, 3066 (1997).
[6] Roa, N. M. et al. in preparation
[7] Elgendy, H. M. et al. in preparation.

Using Combinatorial Methods for Investigations in Polymer Materials Science

Alamgir Karim, J. Carson Meredith, Amit Sehgal, Eric J. Amis

Polymers Division, NIST, Gaithersburg, MD 20899

Abstract Combinatorial methods of drug discovery in pharmaceuticals research are well known and more recent applications have led to the discovery and synthesis of new inorganic materials, catalysts, and organic polymers. Polymeric coatings play an important role in many industrial applications, such as automotive, electrical, aerospace industries where their stability and integrity is of fundamental importance. Recently, we have developed combinatorial and high throughput methods for rapid measurements of properties of polymer coatings, such as phase separation and film dewetting. The results are validated against traditional one-sample measurements and existing physical models. We have also recently extended our combinatorial methods for characterizing biocompatibility of polymeric biomaterials, such as controlling cell growth on patterned polymer substrates or scaffolds prepared by polymer blend extrusion methods.

I) Combinatorial Phase Separation and Dewetting of Polymer Films

Introduction The material properties of polymeric coatings are sensitive to a variety of factors, including composition, temperature, and thickness. We present combinatorial methods for measuring two important fundamental properties of polymer thin films: dewetting and phase behavior of blends and examine preliminary biocompatibility aspects on similarly modified substrates. In each case library creation, high-throughput measurements, and informatics are used to generate combinatorial maps of wettability and phase behavior. The temperature and film thickness dependence of the dewetting behavior of polystyrene on silicon is evaluated in combinatorial libraries in which thickness and temperature are varied systematically. Automated scanning optical microscopy is used to determine the time-temperature-thickness superposition of dewetting kinetics and to observe transitions between film stability regimes. By a similar methodology, the phase boundary for a polystyrene / poly(vinylmethyl ether) blend film is observed with composition-temperature libraries. The combinatorial method is validated by comparison to previous results. The results show that high-throughput experimentation is useful not only for the discovery of new materials, but also for observation of fundamental materials properties.

Library Creation To investigate polymer thin film dewetting phenomena, we used sample libraries with orthogonal gradients in thickness (h) and temperature (T) to create a large database of dewetting information in a few hours of experiments.[1] Thickness gradients were prepared on "Piranha-etched" silicon wafers (Polishing Corporation of America[2]) with a velocity-gradient, knife-edge coating apparatus. In this procedure, the wafers are cleaned in a Piranha solution to grow a thin (≈10 Å) layer consisting primarily of SiO_x. A drop of polymer solution was spread over the substrate under an angled steel blade (5^o relative to substrate) at constant acceleration. The solvent dried within seconds of spreading, and resulted in a polymer film with a gradient in thickness. The initial and final thickness and the slope of the gradient were controlled with

solution concentration, blade-substrate gap width, and substrate velocity and acceleration. The thickness profiles, measured with 0.5 mm diameter spot-ellipsometry, had power law or polynomial dependence on position on the wafer, depending on the flow conditions. Solutions with mass fractions of 2 % and 5 % polystyrene (Goodyear, M_r = 1900 g/mol, M_r/M_n = 1.19, where M_r and M_n are the mass and number average relative molecular masses) in toluene were used to prepare 25 mm wide sample wafers.

Our high-throughput method for studying polymer blend phase separation involves the creation of libraries with orthogonal gradients in blend composition and temperature.[3] Three steps are involved in preparing composition gradient films: gradient mixing, deposition, and film spreading. Two syringe pumps (Harvard PHD2000), introduce and withdraw polymer solutions of polystyrene (PS, M_r = 96.4 kg/mol, M_r / M_n = 1.01, Tosoh) [4] in toluene, and poly(vinylmethyl ether) (PVME, M_r = 119 kg/mol, M_r/M_n = 2.5) in toluene, to and from a mixing vial at controlled rates. The infusion and withdrawal syringe pumps were started simultaneously while vigorously stirring the vial solution, and a third syringe, was used to manually extract solution from the vial. Because the sample syringe contains a gradient in the PS and PVME composition along the length of the syringe, molecular diffusion will lead to uniform composition over time. However, the timescale for molecular diffusion is many orders of magnitude larger than the sampling time, since the PS and PVME diffusivities are on the order of 10^{-8} cm^2/s.

Next the gradient solution from the sample syringe is deposited as a thin 31 mm long stripe on the silicon substrate. The gradient stripe was quickly placed under a stationary knife edge of equal length. The gradient stripe was spread as a film, orthogonal to the composition gradient direction, for a distance of 40 mm with the flow coating procedure described above. After a few seconds most of the solvent evaporated, leaving behind a thin film with a gradient of polymer composition. The remaining solvent was removed during the annealing step. The film thickness, measured with ellipsometry, varied monotonically from 345 nm to 510 nm between the low and high PS composition ends, due to viscosity variation in the composition gradient solution. We demonstrated previously that the thickness change due to flow induced by the small thickness gradient (≈ 5 nm/mm) is within the standard uncertainty of ± 3 nm.

High Throughput Screening Both the thickness (dewetting) and composition (phase behavior) gradient samples were annealed on a linear *T* gradient heating stage, described elsewhere, [1] over a large range of *T* values, 90 °C < *T* < 160 °C. A CCD camera (Kodak ES1.0) coupled to an optical microscope (Nikon Optiphot 2) sent (1024 x 1024) pixel, 8 bit digitized images to a computer that also synchronized sample stage movement over a grid of *T* and *h* conditions using a robotic *x*,*y* translation stage. For quantitative analysis of images, we averaged the library *T* and *h* values over the image area. At the beginning of each time cycle, the translation stage returned to a home position to within ± 0.5 μm. In a typical experiment, the *T*-*h*-*t* dependence of dewetting structures was followed by collecting a 5 by 5 array of images every 5 min over a period of 2 h, for a total of 600 images. Optical microscope images and photographs capture the phase separation process as a function of *T* and N_{PS} with average standard uncertainties of *T* = ± 1.5 °C and N_{PS} = ± 0.006.

Results and Discussion Figure 1 presents a photograph of a typical temperature-composition library after 2 h of annealing, in which the LCST phase boundary can be seen with the unaided eye as a diffuse curve. Cloud points measured with conventional light scattering are shown as discrete data points and agree well with the phase boundary observed on the library. The diffuse nature of the phase boundary reflects the natural dependence of the microstructure evolution rate

on temperature and composition. Near the LCST boundary the microstructure size gradually approaches optical resolution limits (1 μm), giving the curve its diffuse appearance.

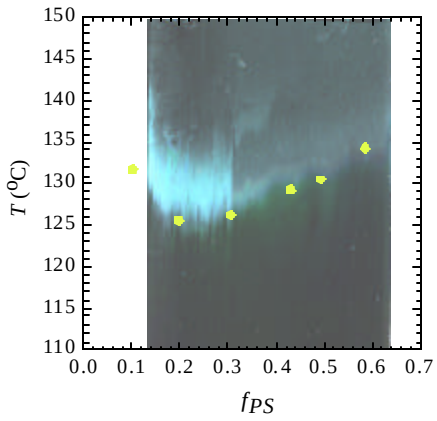

Figure 1. Photograph of a combinatorial library indicating the known LCST phase boundary for PS-PVME. For validation, the discrete points are conventional light scattering cloud points for known compositions of the PS and PVME used in the combinatorial library.

The quantitative agreement of the asymmetric shape and values of the LCST boundary with bulk cloud point values validates the library deposition method and high-throughput approach for mapping polymer blend phase behavior presented here.
By using a combinatorial technique to prepare libraries in which the temperature and thickness are varied systematically and continuously, we have also measured the temperature-thickness-time dependence of dewetting structures, stability, and kinetics in a small number of experiments. Figure 2 presents a composite optical image of a typical *T-h* library that indicates different dewetted structures and growth rates as a function of *T* and *h*. The libraries are able to reproduce a wide range of dewetted structures observed with our own uniform control samples

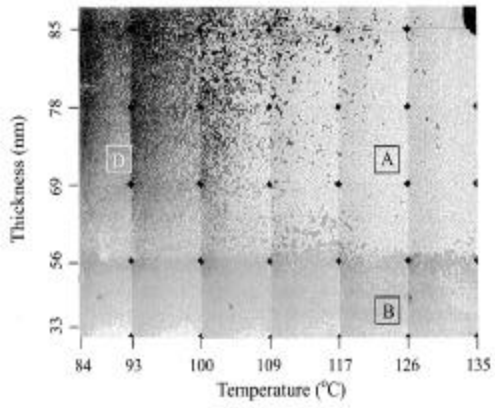

Figure 2. Composite image of overlapping optical micrographs (one square image is 6 mm on a side) of a temperature-thickness library used to study thin film dewetting. Bright regions are more dewet than dark regions. A wide range of structures (holes and polygons) and both metastable and unstable (capillary nucleated) film regions are observed in this image.

and in previous work of others for similar systems, validating our methodology. The method presented here is unique in its ability to rapidly identify fundamental trends in film stability,

nucleation mechanisms, and dewetting kinetics over a wide range of parameter space. Delineating these effects early in a scientific study can lead to observations of novel regions of phase space for thin film phenomena and can be extremely useful in guiding detailed analysis with conventional one-sample for one-measurement approaches.

II) Confined Dewetting and Preliminary Cell Growth Assay on Patterned SAM surfaces

Introduction Surface topography and surface functionality (as can be obtained from the previous section) are a few of the key parameters that determine cell adhesion, expression, growth and function on patterned substrates. Our previous studies on phase separation of polymer blend films on patterned self-assembled monolayer (SAM) substrates have also shown that the phase segregation behavior was well correlated to the underlying chemical pattern. In this study, the topography and morphology of dewetting thin homopolymer films on chemically heterogeneous SAM patterns are investigated by AFM. Thin film dewetting on a patterned substrate was utilized to let polymer physics efficaciously define different topographies for cell growth. Additionally, preliminary results on cell growth assay on the chemically patterned substrates is presented.

Materials The polystyrene (PS) (M_w = 760 g/mol, T_g below ambient temperature) was purchased from the Aldrich Chemical Company and used as received. Toluene and chloroform solutions were prepared from ACS reagent grade solvents from J.T. Baker Inc. Hexadecanethiol (tech. 90 %) and 16-mercaptohexadecanoic acid (90 %) were purchased from Aldrich for generating the SAM patterns. Saturated solutions of 16-mercaptohexadecanoic acid in n-hexadecane (Aldrich, 99+ % anhydrous) and ethanolic (volume fraction 1.0, 200 proof) solutions of hexadecanethiol were used as inks for the stamping procedure. Gold substrates were prepared by vapor deposition [(100 to 300) Å Au over 10 Å Cr] on Si Wafers [4" dia., N type, 100, Polishing Corp. of America].

Substrate preparation The chemical patterns were created by the soft lithographic technique, developed by Whitesides et al. on vapor deposited gold substrates. It consists of transfer of alkane-thiols on to the gold surface by conformal contact of a poly (dimethylsiloxane) stamp previously "inked" with the thiol. The surfaces are then filled with an equivalent chain-length thiol, with a different ω-terminal functional group, to give stable smooth self-assembled mixed monolayer (SAM) with the pattern in surface functionality as defined by the stamp. In this study the gold wafer was stamped with methyl (-CH_3) terminated hexadecanethiol and filled with carboxylic acid (-COOH) terminated mercaptohexadecanoic acid. A unique feature of the stamp is a gradient of pattern widths. The pattern as defined by the stamp consists of linear and parallel bands of –COOH terminal groups of widths ranging from 15 μm to 1μm across the surface separated by –CH_3 terminal thiols of 3 μm width. Ultra-thin films of low molecular mass poly(styrene) from a dilute solution spontaneously dewets and subsequently coalesces into droplet arrays. Initial film thicknesses were estimated to be of the order of (10 to 20) nm.

Instrumentation The AFM measurements were conducted on a Digital Instruments Dimension 3100 Nanoscope III in the Tapping mode™. Cantilevers with a spring constant of 30 Nm^{-1} with silicon tips (radius of curvature of 10 nm) were used to study the surface morphologies. The optical images were acquired on a Nikon Optiphot-2 microscope with a Kodak Megaplus CCD Model ES 1.0 camera mounted on the trinocular head.

Results The late stage of the dewetting process results in droplet arrays giving a highly structured surface (Figure 3). It shows a relatively monodisperse array of droplets on the 6 μm strips. The droplets are in complete registry with the underlying chemical pattern. Droplet

profiles (inset) are used to estimate droplet dimensions and contact angles on different bandwidths. Contact angles are determined to be 4° for the 6 μm band shown and the film thickness is determined to be 12 nm.

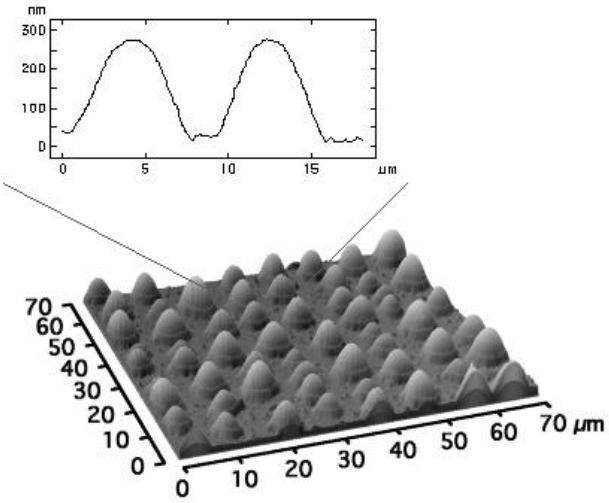

Figure 3. AFM height image of late stage dewetting on a chemical pattern. The droplet size is governed by the confining bandwidth (6μm above, separated by 3 μm non-wetting stripes).

Variation of the bandwidths across the surface shows multiple droplets per band for the 15 μm and the 12 μm widths that coalescence into single droplets for the 9μm stripes. Further confinement results in a crowding effect (6μm band), that changes to disordered bridging for the narrowest 1μm band. Lenz et al. in their theoretical treatment have defined a "channel state", for simple liquids dewetting on a chemically patterned surface, where the dimensions and the contact angle of the fluid are dictated by the confining geometry. It is important to note that Young's law is no longer valid in this confining regime. Extension of the above results to thicker films results in parallel ridge structures, the size and the spacing of which may be controlled explicitly by the underlying pattern. A whole range of surface topologies for cell growth may be addressed in this fashion.

The influence of surface functionality for focal adhesion of cells is explored by extending the soft-lithographic technique to pattern RGDC (arginine-glycine-aspartine-cystine) peptide sequences. The distribution of the peptides on a surface is thus spatially controlled to the step gradient period, with the spacing between the RGDC stripes varying from 15 μm to 1μm. Preliminary experiments on the step-gradient SAM patterned surfaces were performed by exposing them to osteoblast-like cells in-vitro. Fig. 4 shows the attachment of osteoblast cells on the SAM patterns of different pattern widths. Closer inspection of the cells validates that the focal adhesion of the cells is specific to the RGDC stripes. Significantly, changing the spacing between the RGDC bands results in extension of the cells by the focal points to alter cell shape. Control of cell shape and metabolic state by surface immobilized RGDC patterns may thus be achieved.

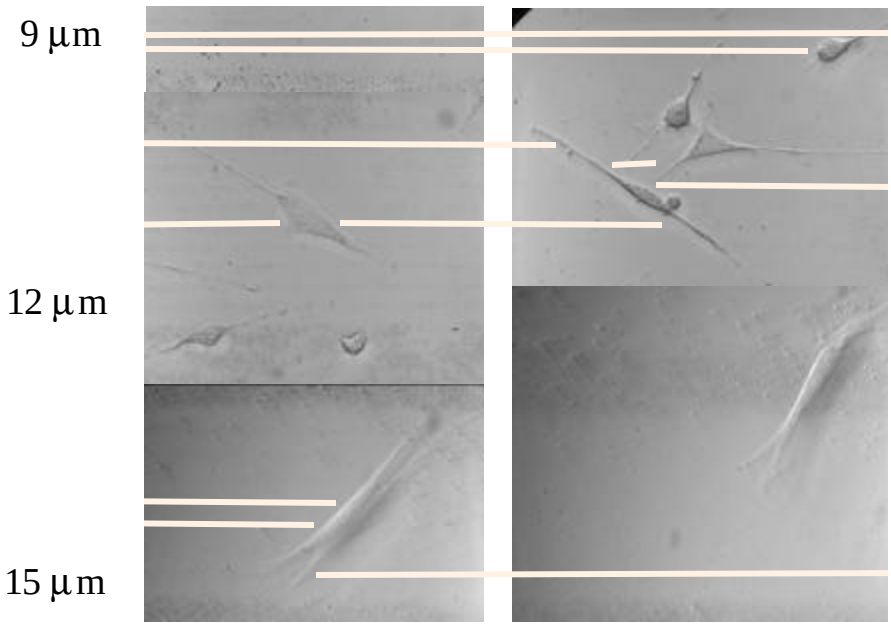

Fig. 4 Cell growth on an RGDC patterned substrate (4 microscope images). The horizontal bands are the stripes of RGDC localization. The cells appear stretched out on the 15 µm RGDC separation. The shape becomes increasingly globular as the spacing is reduced to 12 µm and 9 µm (top right corner).

Acknowledgement. We thank Barry Bauer for supplying the PVME used in this study.

References

(1) Meredith, J. C.; Karim, A.; Amis, E. J. *In Prep*.
(2) Certain equipment and instruments or materials are identified in the paper in order to adequately specify the experimental details. Such identification does not imply recommendation by the National Institute of Standards and Technology, nor does it imply the materials are necessarily the best available for the purpose.
(3) Meredith, J. C.; Karim, A.; Amis, E. J. *Macromolecules*, In Press.
(4) According to ISO 31-8, the term "molecular weight" has been replaced by "relative molecular mass," M_r. The number average molecular mass is given by M_n.

A Microshear Test to Measure the Bond Between Dental Composites and Dental Substrates

Walter G. McDonough[1], Joseph M. Antonucci[1], Gary Schumacher[2], and Yasushi Shimada[3]

National Institute of Standards and Technology, Gaithersburg, MD 20899 U.S.A.
[2]ADAHF/PRC Gaithersburg, MD 20899 USA
[3]Tokyo Medical and Dental University, Tokyo Japan

Introduction: In order to determine the real efficacy and durability of polymeric dental adhesives, thorough clinical testing is necessary. However, in practice, long-term clinical testing is expensive and commercial adhesive materials are constantly undergoing change so that the clinical testing necessary to evaluate their long-term properties and success rates (typically four years) becomes impractical. Thus, there is the need for reliable laboratory tests to serve as screening tools to identify promising new dental adhesive systems and improvements to existing systems. Adding to the challenge is the very complex conditions that a tooth cavity presents to achieving effective adhesion of the restorative material to this heterogeneous mineralized substrate. The mineralized tissues of the tooth, enamel with its prismatic rod-like apatitic structure and dentin with its array of dentin tubules, are both anisotropic materials that present variable substrates for adhesive systems. Depending upon the orientation of the rods and tubules with respect to the adhesive interface, variations in bond strength would be expected. The polymeric adhesive restorative, a viscoelastic material, is constantly exposed to a hostile, multi-challenging milieu comprising masticatory stresses, aqueous fluids that can initiate chemical attack, and cyclic exposure to heat and cold. This list of factors that can affect adhesion to tooth structure is not meant to be exhaustive but rather illustrates the complex nature of properly assessing the bond between the restorative and the mineralized tissue, and illustrates the challenge involved in designing a reliable screening test.

Shear bond testing to assess the bond strength between polymeric adhesives and mineralized tissue is widely used due to the ease of specimen preparation and testing. We have designed and developed a new shear test protocol that minimizes the tensile forces at the interface and maximizes the shear forces. Because our bonded surfaces are very small ($\approx 0.4\ mm^2$), we are able to test many specimens on a single surface of enamel or dentin, thereby aiding in the conservation of teeth. Additionally, we can perform regional mapping of the tooth structure and can reach temperature equilibrium conditions rapidly, which permits accelerated durability studies.

In the case of enamel, adhesion occurs primarily by micro-mechanical interlocking resulting from the penetration of the unpolymerized resin into a superficial porous zone created by chemical etching (acid or through chelation), forming upon on polymerization polymeric tags into the conditioned apatitic structure. Because of the structural anisotropy of enamel, it is thought that variation in enamel bonding sites might influence the bonding strength of direct composite restorative systems to this substrate. The purpose of this study was to study how regional variation in enamel tooth structure and the effect of enamel rod orientation affects the bonding ability of a non-priming adhesive system that employs aqueous phosphoric acid as the

etchant. This paper presents some of the opportunities that the microshear bond strength test offers in enhancing our understanding of dental adhesion and in designing dental adhesive systems with enhanced strength and durability.

Materials and Methods*: The most important elements of the microshear test come with the design of the test. As seen in the figure, cylinders of cured composite resin are bonded onto a prepared substrate, shear tested at a specified rate, and the interfacial properties calculated. Tooth slices were taken from extracted human molars with the selected enamel region sectioned transversely, obliquely, and parallel (longitudinal) to the enamel prism. Each slice was approximately 1.0 mm thick. The enamel slices were bonded to aluminum tabs by first air abrading the aluminum with 50 μm aluminum oxide powder followed by application of a cyanoacrylate adhesive. The exposed tooth surface was then resurfaced under water with 320 grit SiC paper. A phosphoric acid gel (K-etchant gel, Kuraray) was then applied to the resurfaced enamel for 30 s and then the surface was rinsed with water and dried but not desiccated, then the Photo-Bond adhesive resin was applied. Subsequently, an iris was cut from a micro-bore Tygon tube that had an internal diameter of approximately 0.7 mm and affixed to the enamel surface, and then the resin composite was injected into the iris. The resin was photo-irradiated with visible light (maximum absorbance peak 470 nm) for 60 s. After curing, the iris was removed and the specimens were stored in distilled water at 37 ^{o}C for 24 h. The cylindrical specimens were tested in shear at a rate of 0.5 mm/min. The change in load as a function of time was recorded and the shear strength was calculated from the equation $\tau = F/(\pi r^2)$, where τ is the estimated interfacial shear strength, F is the load at failure, and r is the radius of the resin cylinder.

Results and Discussion: Seven specimens were tested for the specimens with rods that were sectioned transversely; the mean shear strength and standard deviation was (31.12 ± 3.38) MPa. The result for five specimens that were sectioned obliquely was (27.78 ± 2.17) MPa. The result for eight specimens that were cut parallel to or longitudinally along the prisms was (13.90 ± 3.11) MPa. The results of this particular study showed that the surface parallel to the enamel prism rods was significantly weaker than were the surfaces cut transversely or obliquely. (One-way analysis of variance, $F = 60.8$; $df = 5, 34$; $p < 0.05$).

Conclusions: A microshear test has been developed that allows one to study adhesion of very small areas (0.4 mm^2 to 1.0 mm^2) that are not accessible to conventional macroshear testing. Thus, the researcher can now horizontally and vertically map interfacial adhesion of different areas and depths of tooth structure, respectively. Furthermore, this method requires significantly fewer extracted teeth for adhesion studies compared to the typical macro adhesion studies.

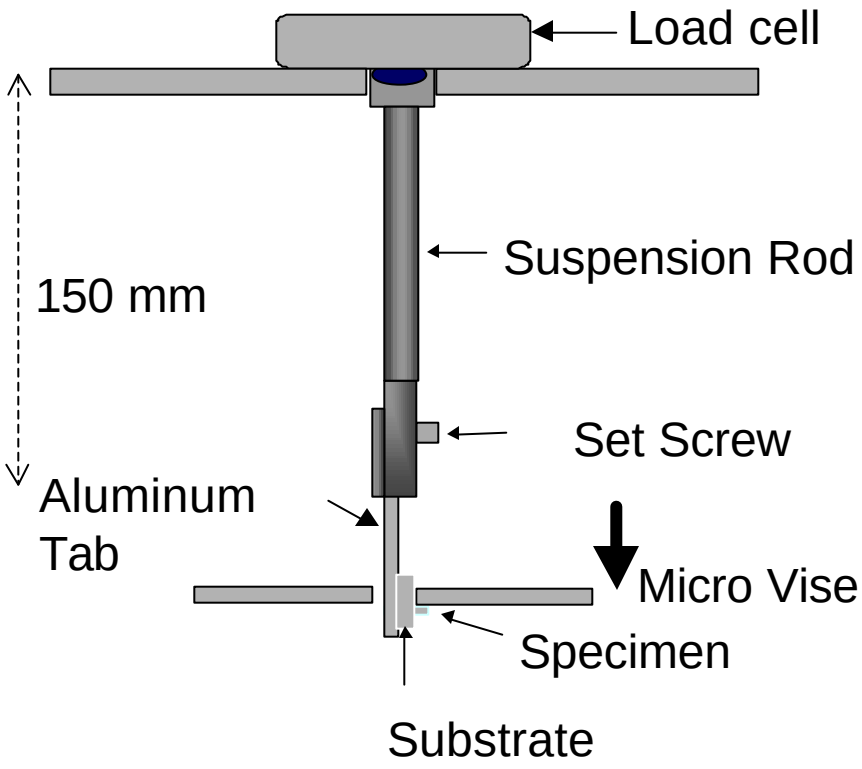

Figure 1: Schematic of the microshear test.

*Materials and equipment are identified only for describing experimental procedure and do not imply recommendation or endorsement.

This work was supported by NIDCR IA Y1-DE-7006-0.

POSTERS

Effect of Resin Composition on the Remineralizing Ability of Amorphous Calcium Phosphate-based Polymeric Composites

J.M. Antonucci[1], D.Skrtic[2] and E.D. Eanes[1]

[1]Polymers Division, [2]American Dental Association Health Foundation-Paffenbarger Research Center, NIST, Gaithersburg, MD 20899-8545

Introduction

Calcium phosphates are finding increasing use as biomaterials, e.g. in the treatment of defective mineralized tissues. Crystalline hydroxyapatite (HAP) is considered to be the final stable product in the precipitation of calcium and phosphate ions from neutral or basic solutions and it is also the structural prototype of the major mineral component of bones and teeth. Over the broad range of solution conditions when precipitation occurs spontaneously, amorphous calcium phosphate (ACP) precedes the formation of HAP. ACP, a plausible key precursor in the biological formation of HAP, is characterized by a high degree of aqueous solubility and facile conversion to HAP, particularly at low pHs (1). These properties, undesirable for applications where structural, mechanical and chemical stabilities are desired, make ACP suitable as a remineralizing agent.

We have recently shown (2) that a new class of polymeric composite materials can be formulated that utilize ACP as a filler with dental monomers such as 2,2-bis[p-(2'-hydroxy-3'-methacryloxypropoxy)phenyl]propane (Bis-GMA), triethylene glycol dimethacrylate (TEGDMA), and 2-hydroxyethyl methacrylate (HEMA). Previous studies have shown that certain variations in methacrylate resin chemical structure and composition may affect the rate and extent of the ion release from ACP-filled composites, the internal conversion of ACP into HAP and the mechanical properties of the composites (4, 5).

The objective of this study was to further explore the effects of the chemical structure and compositional variations of the resins on the release of mineral ions (Ca^{2+} and phosphate). The resins included those previously examined and other types of resin matrices that include urethane dimethacrylate (UDMA), and a carboxylic acid-containing monomer, pyromellitic glycerol dimethacrylate (PMGDMA). The effect of adding a potential coupling agent such as zirconyl methacrylate (ZrMA) was also investigated.

Experimental*

Six photoactivated resins, designated BT, BTHZ, TP, U0H, U66H and U132H were formulated as shown in Table 1. The photoinitiator system comprised camphorquinone (CQ) and ethyl-4-N,N-dimethylaminobenzoate (EDMAB) for BT, BTHZ, U0H, U66H and U132H composites. However, for the TP composites a mixture of 2-benzyl-2-(dimethylamino)-1-(4-(4-morpholinyl)phenyl)-1-butanone (IRGACURE® 369), and 2-hydroxy-2-methyl-1-phenyl-1-propanone plus diphenyl(2,4,6-trimethylbenzoyl) phosphine oxide (DAROCUR® 4265) was combined with CQ to enhance photopolymerization and storage stability. Three types of ACPs were prepared and evaluated as fillers: unhybridized, P_2O_7-stabilized ACP (Pyro-ACP), silica-(TEOS-ACP) or zirconia-hybridized ACP (Zr-ACP) (6).

Table 1. Composition of Resins (mass fraction, %).

Component	BT	BTHZ	TP	U0H	U66H	U132H
BisGMA	49.5	35.1	-	-	-	-
TEGDMA	49.5	35.1	48.65	-	-	-
HEMA	-	28.0	-	-	6.6	13.2
PMGDMA	-	-	48.65	-	-	-
UDMA	-	-	-	99.0	92.4	85.8
ZrMA	-	0.8	-	-	-	-
CQ	0.2	0.2	0.40	0.2	0.2	0.2
EDMAB	0.8	0.8	-	0.8	0.8	0.8
IRGACURE	-	-	0.8	-	-	-
DAROCUR	-	-	1.5	-	-	-

Composite pastes were made up of mass fraction of 40 % filler and a mass fraction of 60 % resin. Uncured pastes were examined by x-ray diffractometry (XRD) and Fourier-transform infrared spectroscopy (FTIR) to discern that no conversion of the ACP filler to HAP occurred at this stage. Composite disks were prepared in Teflon molds (15.8 mm to 19.6 mm in diameter and 1.55 mm to 1.81 mm thick) by visible light photocuring for 2 min/side (TRIAD 2000, Dentsply).
The remineralizing ability of the composites was tested in triplicate by immersing individual disk specimens in buffered saline solutions with conditions: pH = 7.40, ionic strength = 0.13 mol/L, 37 ^{o}C, continuous magnetic stirring and time up to 300 h. Aliquots were taken at predetermined time intervals, filtered, and the filtrates analyzed for their $[Ca]_{tot}$ and $[PO_4]_{tot}$ contents using atomic absorption spectroscopy and UV/VIS spectrophotometry, respectively.
The thermodynamic stability of immersion solutions was calculated as their supersaturation relative to stoichiometric HAP and expressed as the Gibbs free energy, ΔG^{o}:

$$\Delta G^{o} = - 2.303\ (RT/n)\ln(IAP/K_{sp}) \qquad (1)$$

where IAP is the ion activity product for HAP, K_{sp} is the corresponding thermodynamic solubility product, R is the ideal gas constant, T is the absolute temperature (K) and n is the number of ions in the IAP (n =18). IAP and ΔG^{o} were calculated by the solution equilibrium calculation program EQUIL (MicroMath Scientific Software, Salt Lake City, UT).

Upon completion of the immersion tests, the disks were removed, dried at 37 ^{o}C and evaluated for the extent of ACP to HAP conversion that occurred during soaking by XRD and FTIR analysis. Experimental data were analyzed by multifactorial ANOVA (α=0.05). To determine significant differences between specific groups, appropriate multiple comparison tests were performed .

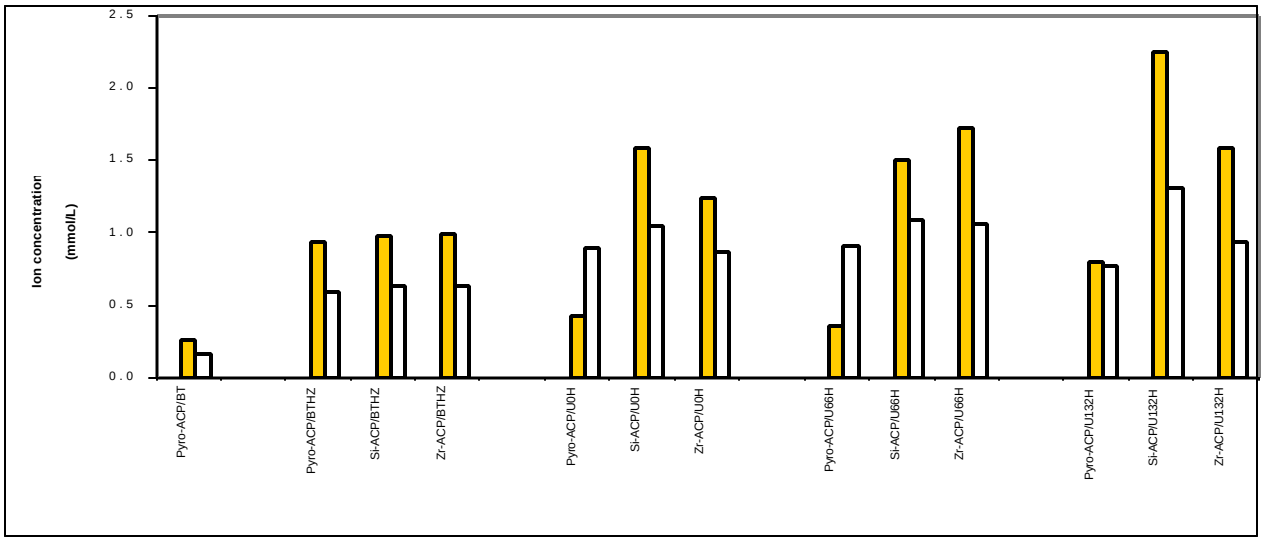

Figure 1. Maximum concentrations Ca (filled bars) and PO_4 (unfilled bars) released from different resins. Number of runs ≥ 3 in each experimental group. Standard deviations of values were < 0.127 mmol/L for $[Ca]_{tot}$ and < 0.057 mmol/L for $[PO_4]_{tot}$.

Results and Discussion

All the composites were capable of releasing mineral ions at levels above the minimum necessary for remineralization as derived from data in Fig. 1.

Mean ΔG^o values ± standard deviation of the mean (SD) of the immersion solutions containing maximum concentrations of Ca and PO_4 released from different ACP composites are given in Table 2. A more negative ΔG^o value represents a solution more supersaturated with respect to stoichiometric HAP.

Table 2. Remineralization Potential of ACP Composites Expressed as ΔG^o (kJ/mol).

	Pyro-ACP	TEOS-ACP	Zr-ACP
BT	-3.33±0.22	-	-
BTHZ	-4.88±0.22	-5.00±0.20	-5.02±0.18
TP	-4.42±0.11	-4.28±0.10	-4.33±0.13
U0H	-4.17±0.11	-6.01±0.18	-5.53±0.19
U66H	-3.95±0.11	-5.96±0.18	-6.12±0.10
U132H	-4.90±0.17	-6.62±0.19	-5.92±0.14

Elevated Ca and PO_4 concentrations were sustained by BTHZ and UH resins (data not shown). However, with increased time TP composites failed to maintain a favorable remineralization potential due to matrix uptake of released Ca via ion binding by the carboxylic acid groups of PMGDMA (Figures 2 a,b).

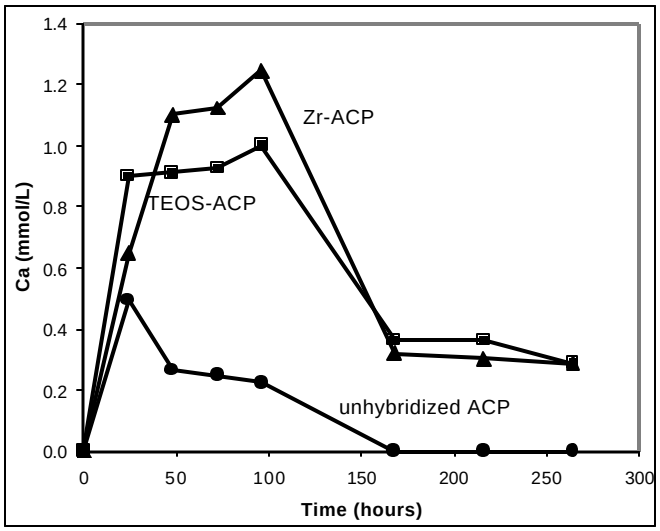

Figure 2a. Ca release from TP composites. Values are averages of triplicate runs. Standard deviations were < 0.028 mmol/L (unhybridized ACP), < 0.030 mmol/L (TEOS-ACP) and < 0.044 mmol/L (Zr-ACP).

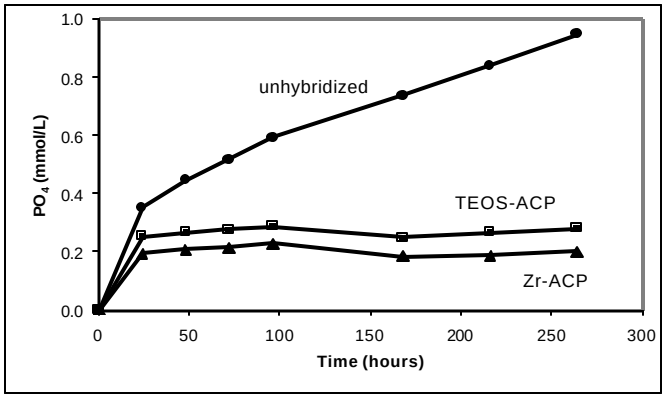

Figure 2b. PO_4 release from TP composites. Values are averages of triplicate runs. Standard deviations were < 0.015 mmol/L (unhybridized ACP), < 0.014 mmol/L (TEOS-ACP) and < 0.010 mmol/L (Zr-ACP).

The ranking of the maximal remineralizing ability of Pyro-ACP composites was: (BTHZ, U132H) >TP> (U0H, U66H)>> BT. Composites based on the TEOS- or Zr-ACP, and U0H, U66H or U132H had significantly higher ($p \leq 0.0013$; Student-Newman-Keuls test) remineralization potential compared to the similarly prepared Pyro-ACP UH composites. Hybridization of the fillers had no effect on Ca or PO_4 ion releases from BTHZ composites. However, internal conversion of ACP to HAP was significantly reduced or almost completely inhibited in the case of BTHZ and UH/ hybridized ACP composites. On the other hand, Ca and PO_4 ion releases from TEOS-ACP and Zr-ACP based UDMA composites were significantly higher than that from Pyro-ACP based UDMA composites.

The most probable mechanism by which the hydrophilic HEMA-enriched matrix composites increased internal mineral saturation was by allowing the uptake of more water and/or better accessibility of the ACP to the water already entrained. In addition to the hydrophilicity of the matrix, cross-link density may effect ion release. The elevated Ca and PO_4 ion releases observed with hybridized ACP-U0H, U66H, or U132H composites was probably due to the enhanced area of contact between the hybrid ACP particulates and UDMA-based resins.

Acknowledgement. This work was supported by NIST and a grant 1R01 DE13169 from NIDCR. We are grateful for a gift of IRGACURE® 369 and DAROCUR® 4265 from Ciba, Hawthorne, NY, and TEGDMA, HEMA and UDMA from Esstech, Essington, PA.

*Disclaimer. Certain commercial materials and equipment are identified in this article to specify the experimental procedure. In no instance does such identification imply recommendation or endorsement by the National Institute of Standards and Technology or the ADA Health Foundation or that the material or equipment identified is necessarily the best available for the purpose.

References

Eanes, E.D.: Amorphous Calcium Phosphate: Thermodynamic and Kinetic Considerations. In: Calcium Phosphates in Biological and Industrial Systems, Amjad, Z. (ed.), Kluwer Academic Publ., Boston, MA, 1998, pp. 21-40.

Skrtic, D.; Eanes, E.D.; Antonucci, J.M.: Polymeric Calcium Phosphates with Remineralization Potential. In: Industrial Biotechnological Polymers, Gebelein, C.G.; Carraher, C.E. (eds.), Technomic Publishing Co., Lancaster, PA, 1995, pp.393-408.

Antonucci, J.M.; Skrtic, D.; Eanes, E.D.: Bioactive Polymeric Dental Materials Based on Amorphous Calcium Phosphate. Effect of Coupling Agents. In: Hydrogels and Biodegradable Polymers for Bioapplications, Ottenbrite, R.M.; Huang, S.J.; Park, K. (eds.), ACS Symposium Series 627, American Chemical Society, Washington DC, 1996, pp. 243-254.

Skrtic, D.; Antonucci, J.M.; Eanes, E.D. *Dent Mater* 1996, *12*, 295.

Park, M.S.; Eanes, E.D.; Antonucci, J.M.; Skrtic, D. *Dent Mater* 1998, *14*, 137.

Skrtic, D.; Antonucci, J.M.; Eanes, E.D.; Eichmiller, F.C.; Schumacher, G.E., *J Biomed Mat Res, Applied Biomaterials*, 2000, accepted.

Methods for Determining the Distribution of Antibiotics in Bone Cement

D.A. Cole*, S. Li**

*Evans East, 104 Windsor Center, Suite 101, East Windsor, NJ 08520
**Hospital for Special Surgery, Biomechanics & Biomolecular Design, 535 East 70th Street, New York, NY 10021

The mixing of antibiotics into bone cement to prevent infection has been used since the 1970's and is still a common practice in total joint replacement surgery. There have been many studies on the elution rate of the antibiotics and the effects of the antibiotics on the properties of bone cement. Differences in diffusion rates have been attributed to differences in porosity of the cement. Further, it has been reported that there can be substantial amounts of antibiotic within the bone cement even after years of implantation. A direct determination of the actual distribution of antibiotic within bone cement is needed to aid in developing methods for optimizing the distribution of bone cement to provide the maximum patient benefit and the lowest cost treatment. This study presents two analytical methods, X-ray Photoelectron Spectroscopy (XPS) and Time of Flight Secondary Ion Mass Spectrometry (TOF-SIMS), for directly determining the distribution and concentration of antibiotics in bone cement.

Antibiotic-containing samples of bone cement were obtained from remnants of actual hip replacement surgeries prepared by vacuum mixing 3 g of the antibiotic Tobramycin Sulfate with 80 g of Simplex P bone cement. Simplex P is a mixture of powdered polymer spheres, liquid monomer, and a barium sulfate opacifier. In the XPS spectra the most convenient tags for Tobramycin were the sulfate peak at 167.6 eV, and the nitrogen peaks at 401.2 eV ($C\text{-}NH_3^+$) and 399.1 eV ($C\text{-}NH_2$). Sulfate from $BaSO_4$ was readily resolved as a separate peak at 170.6 eV. Examination of cross-sectioned bone cement showed that on the scale of the XPS examination (0.8 mm), the concentration of Tobramycin appeared to be nearly evenly distributed as a function of depth into the sample. In the TOF-SIMS data HSO_4^- was the best ion for imaging Tobramycin as it was quite intense. The TOF-SIMS data indicated that on a smaller scale, Tobramycin was found in 'clumps' ranging from < 1 μm to 35 μm with a mean size of 1 μm. Furthermore, TOF-SIMS images of Ba^+ and SO_3^- indicated that the $BaSO_4$ was homogeneously distributed between the powdered polymer spheres and that dark spherical regions in the Ba^+ and SO_3^- images were the polymer powder component of Simples P cement. These results suggest that the majority of the antibiotic is located in the bulk of the cement and might not be released from the bone cement. These methods may now be used to determine the effects of different cement types and mixing methods on the distribution of antibiotic. They also make it possible to image and quantify antibiotics in samples from elution experiments to determine the exact depth from which antibiotic can be released. In this manner, these methods will help improve patient care and potentially reduce the total amount of antibiotic used.

Correlations of Osteoblast Activity and Chemical Structure in the First Combinatorial Library of Degradable Polymers♦

E.A.B. Effah Kaufmann and J. Kohn

Department of Chemistry, Rutgers University, Piscataway, NJ 08854, U.S.A.

Introduction: To address the slow rate of materials development and the lack of a wide range of degradable polymer candidates for biomedical applications, we have explored combinatorial approaches to materials design. Our approach has been to use derivatives of the naturally occurring amino acid, L-tyrosine, to synthesize a novel family of polyarylates.[1] This family is composed of alternating copolymers of a diphenol and diacid linked by ester bonds (Figure 1). The diphenols (ethyl, butyl, hexyl and octyl esters of desaminotyrosyl-tyrosine) provide a means to modify the length of the pendent chain attached to the polymer backbone while the selection of diacids of increasing length (succinic, glutaric, adipic, suberic and sebacic acid) makes it possible to independently change the backbone structure. By copolymerizing each of the diphenols with each of the diacids in a parallel reaction setup, a combinatorially designed library of polymers was obtained.

When synthesizing large numbers of polymers as part of a combinatorial library, it is necessary to also develop efficient techniques for the rapid screening of important material properties. In this preliminary study, we focus on osteoblast proliferation and maturation as a model system for the exploration of cellular response when screening large arrays of structurally related polymers. Herein, we evaluate the ability of selected members of the family of polyarylates to support osteoblast proliferation and maturation by determining total DNA concentration, alkaline phosphatase (AP) activity and metabolic activity of UMR-106 osteoblast-like cells cultured for periods up to 14 days. The use of this family of structurally related polymers allows for the evaluation of cell activity as a function of small changes in substrate structure.

Materials and Methods: All polymers were synthesized and characterized as previously described.[1] Polymer films were fabricated by compression molding. Six mm diameter disks were cut out of the films and used to line the wells of standard 96-well plates. The use of these culture plates allowed for the simultaneous evaluation of up to 24 different polymers. Polymer films were characterized by X-ray Photoelectron Spectroscopy (XPS, Kratos XSAM 800 using unmonochromatized MgKα radiation, 80 eV pass energy for survey spectra and 20 eV for high resolution studies) to determine the surface composition prior to cell seeding.

Rat osteosarcoma cells (UMR-106, ATCC, Manassas, VA) were used. Polymer-lined plates were sterilized (UV light) and seeded at a density of 10^4 cells/cm^2. Cultures were fed with 100 µl / well of Dulbecco's Modified Eagle's minimum essential medium supplemented with 10% fetal bovine serum, 2 mM L-glutamine and 50 U/ml of penicillin/streptomycin (TCM). After 2 days, TCM was replaced with medium supplemented with 50 µg/ml ascorbic acid. This exchange was repeated every other day until day 7 when the high level of cell activity made it necessary to perform daily media replacements. Starting on day 6, the culture medium was supplemented with 3 mM β-glycerophosphate. The cultures were harvested after 3, 7 and

♦ Presented at the Sixth World Biomaterials Congress, Hawaii, May 2000.

14 days. AP activity, total DNA and metabolic activity were measured. Controls for this study were cells on tissue culture polystyrene (TCPS) and polymer substrates without cells. Pair-wise comparisons of all data were done using Student's t-test (statistical significance at $p<0.05$).

Results and Discussion: Polyarylates used in this study had molecular weights of about 100,000 and exhibited the expected surface chemistry as analyzed by XPS. Our results show that the polymers supported the proliferation and growth of cells and did not elicit any noticeable cytotoxic effect. In addition, the cells on all polymers had high levels of AP activity, and metabolic activities were comparable to cells grown on TCPS.

Whereas the flexibility of the polymer backbone did not significantly affect cell proliferation, the results suggest that cell proliferation is modulated by the length of the pendent chain. Thus, polymers having a short ethyl ester pendent chain were more stimulating substrates for proliferation than the more hydrophobic polymers with long alkyl pendent chains. No systematic correlations between polymer structure and AP activity were observed. However, the highest AP activity levels were measured predominantly for those polymers having an ethyl ester pendent chain.

As with all rapid screening techniques, the reproducibility of the results needs to be confirmed. We therefore repeated our biochemical assays in 96-well plates containing no polyarylate inserts and calculated the statistical probability of assessing a false significant difference to be 21 % and 23 % for total DNA and AP activity respectively, based on the experimental variability of these two assays. Thus, approximately 1 of 5 polymers identified to be statistically different may be a "false positive". We regarded this to be an acceptable margin of error for an initial screening test.

Another important aspect of rapid screening relates to the relevance of the observed data. In our model system, 8 of 18 polymers were found to promote the expression of particularly high AP activity. Presumably, high AP activity *in vitro* may indicate a favorable hard tissue response when the material is implanted. While this hypothesis has not yet been validated, it is interesting to note that 5 of the 8 polymers that promoted high AP expression carried an ethyl ester pendent chain. As reported elsewhere, in an independent study, a tyrosine-derived polycarbonate carrying the same ethyl ester pendent chain was shown to have the most favorable bone response in a long-term *in vivo* tissue compatibility study.[2]

Future experiments will focus on more detailed analyses of the expression of the osteoblastic phenotype by cells grown on these polymers, the identification of specific polymer characteristics that stimulate osteoblast activity, and the relevance of the *in vitro* data for predicting the *in vivo* performance of specific polymers.

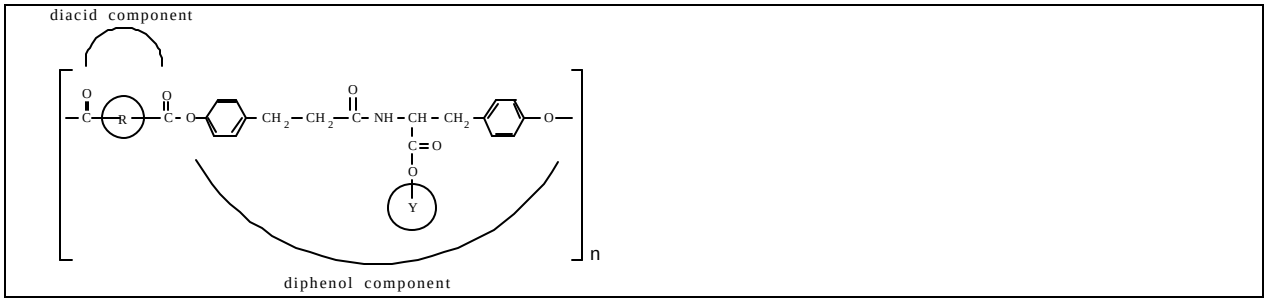

Figure 1: Tyrosine–derived polyarylates. Polymer properties were varied by changes in the pendent chain (Y) and the length of the flexible backbone spacer (R).

References: 1. Brocchini S. et al., *J. Biomed. Mater. Res.*, **42**, 1: 66-75 (1998). 2. James K. et al., *Biomaterials* (1999), in press.
Acknowledgments: Support from NIH grant HL60416, from the New Jersey Center for Biomaterials, and from Advanced Materials Design, LLC is acknowledged. The authors thank Ms. Maura Crowe and Ms. Tonye Briggs for help with polymer processing and cell culture.

Mechanical Properties of Bone Cements Prepared with Functionalized Methacrylates and Bioactive Ceramics

Islas-Blancas E., Cervantes-Uc M., Vargas-Coronado R. and Cauich-Rodríguez J.V.

Centro de Investigación Científica de Yucatán
Apdo. Postal 87, Cordemex, Mérida, Yucatán, México

INTRODUCTION

Bone cements have been in the market for almost 40 years since their introduction by Sir John Charnley. Traditional bone cements, primarily made of MMA and PMMA, exhibit high exotherm of reaction, shrinkage, residual monomer, unsuitable mechanical properties and cement loosening [1]. Improved formulations made use of low toxicity activators, low heat of reaction monomers and bioactive ceramics to improve biocompatibility [2]. In this work, we report the synthesis of bone cements bearing ionisable moieties as a mean of improving biocompatibility. The effect of increasing amounts of ionisable monomer on their mechanical properties and the effect of hydroxyapatite and α-TCP is reported .

MATERIALS AND METHODS

Experimental bone cements were prepared with MMA as base monomer and either methacrylic acid (MAA) or diethylamino ethyl methacrylate (DEAEMA) as comonomer. The acid comonomer was incorporated at 0.1, 0.2 and 0.3 (molar fraction) while the alkaline comonomer was added at 0.04, 0.06 and 0.08 (molar fraction). N,N-dimethyl-p-toluidine was added to the monomer mixture at 2.5 % v/v and 1% w/w BPO to a polymer base Nictone (average diameter=60.6 μm, Mn=150,300, Tg =78.9 °C). The ratio polymer to liquid used was 2. Those formulations containing either HA($D_{0.5}$ = 9.3 μm) or α-TCP ($D_{0.5}$ = 7.6 μm) were prepared with various ceramic concentrations up to 20% w/w and keeping the powder to liquid ratio of 2. Mechanical test were conducted in tension (ISO 527 dumbell), compression and four-point bending according to ISO 5833 using an Instron 1125. Samples were tested after 1 week of preparation. CMW-3 was used for comparison purposes. Fracture surface were observed by SEM.

RESULTS AND DISCUSSION

Tensile strength (σ_T), compressive strength (σ_C) and flexural strength (σ_F) of bone cements prepared with functionalised methacrylates are presented in Table I.

Table I Mechanical properties of PMMA based bone cements

Monomer Composition (mole fraction)	σ_T **(MPa)**	σ_C **(MPa)**	σ_F **(MPa)**
MMA	44.32±4.70	104.60±6.1	35.40±3.80
MAA 0.1 MMA 0.9	34.5±2.8	118.5±5.6	41.6±2.6
MAA 0.2 MMA 0.8	32.5±6.1	126.4±7.3	50.3±7.9
MAA 0.3 MMA 0.7	33.0±3.6	131.8±4.8	42.9±7.7
DEAEMA 0.04 MMA 0.96	41.4±6.9	108.4±1.5	59.4±8.7
DEAEMA 0.06 MMA 0.94	43.4±3.1	97.7±1.9	46.6±3.9
DEAEMA 0.08 MMA 0.92	33.3±4.4	86.3±2.8	35.6±7.8
CMW-3	35.3±9.5	117.0±3.7	44.3±10.4

Bone cements prepared with either methacrylic acid or diethylamino ethyl methacrylate as comonomer exhibited, in general, lower tensile strength than bone cements without comonomer. However, by adding increasing amounts of MAA the compressive strength of these novel bone cements was improved. On the other hand, the addition of DEAEMA tended to diminish their compressive strength. CMW-3 bone cements exhibited higher compressive and flexural strength but lower tensile strength than bone cements without comonomer. However, on selected formulations containing comonomers, the mechanical properties of the proposed bone cements were better than CMW-3.

The addition of bioactive ceramics to selected formulations containing functionalised methacrylates rendered in general bone cements with inferior mechanical properties. It is thought that the presence of ceramic rich areas led to premature failure. Furthermore, the addition of ceramics led to an increase in viscosity, which in turn increased porosity and residual monomer.

Table II Mechanical properties of hydroxyapatite/α-TCP filled bone cements.

Bone Cement Composition	σ_T **(MPa)**	σ_C **(MPa)**	σ_F **(MPa)**
MMA 20% HA	29.4±4.5	86.3±4.7	39.0±3.7
MAA 0.3 MMA 0.7 20% HA	34.4± 2.9	120.1±3.6	39.5±3.6
DEAEMA 0.08 MMA 0.92 20% HA	20.0±3.3	72.7±4.2	34.0±3.5
MMA 20% α-TCP	34.8±4.2	116.6±2.6	43.9±3.4
MAA 0.3 MMA 0.7 20% α-TCP	32.9±4.6	141.1±5.2	37.3±4.7
DEAEMA 0.08 MMA 0.92 20% α-TCP	20.4±4.4	27.6±2.2	45.1±4.6

CONCLUSIONS

Bone cements synthesized through functionalised methacrylates exhibited interesting mechanical properties when tested one week after preparation. High concentrations of MAA and low concentrations of DEAEMA exhibited the best mechanical properties. The addition of either HA or α-TCP although may improve biocompatibility has a deleterious effect on their mechanical behavior.

REFERENCES

1.Hench L.L. and Ethridge E.C., "Orthopedic Implants" in Biomaterials: An Interfacial Approach (Academic Press, New York, 1982) 225-252.
2.Lewis G., J. Biomed. Mater. Res. (Appl. Biomater.) 1997; 38: 155-182.

ACKNOWLEDGEMENTS

We want to thank CONACYT (México) for their financial support.

Development of Biodegradable Polymer Scaffolds Using Co-Extrusion Techniques

Newell Washburn and Alamgir Karim

National Institute of Standards and Technology
Polymers Division, Gaithersburg, MD 20899

The preparation of biodegradable polymeric scaffolds using co-extrusion techniques is presented. Blends of poly(,-caprolactone) (PCL, $M_n \cong 80{,}000$) and poly(ethylene oxide) (PEO, $M_n \cong 100{,}000$) were prepared in a twin screw extruder by mixing at 100 °C for 10 min. Compositions with volume fraction ranging from (0. 30 to 0.70) PCL were investigated and the blends were then soaked in water to dissolve the PEO, resulting in a porous structure. The as-mixed blends had pore sizes on the order of 1 μm, too small to be of use in tissue engineering. Therefore, following extrusion the blends were annealed at 80 °C for times ranging from (10 to 150) min to drive coalescence and produce larger domains. Systematic variations in the morphology of the blends were observed as a function of composition and annealing time.

After annealing for 20 min and dissolving the PEO, the 70 % PCL blend consists of spherical inclusions in the PCL matrix. A scanning electron micrograph of the blend is shown below. These inclusions range from (1 to 10) μm and appear to form a droplet structure.

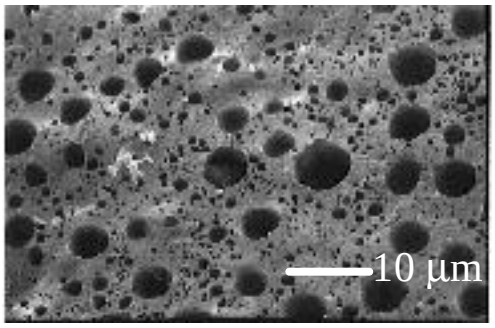

After annealing the 50 % PCL blend for 20 min and dissolving the PEO, the pores in the structure appear to have developed into a continuous domain with a characteristic length of roughly 20 μm.

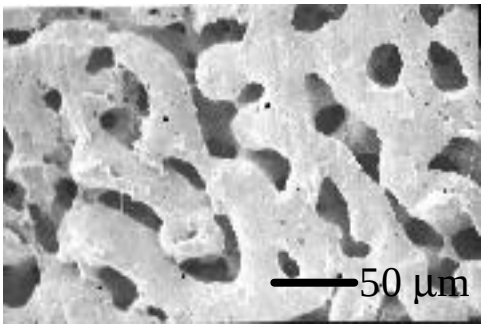

At 30 % PCL and 20 min annealing, the structure has become more open and the void space in the material is approaching a characteristic length of around 50 μm.

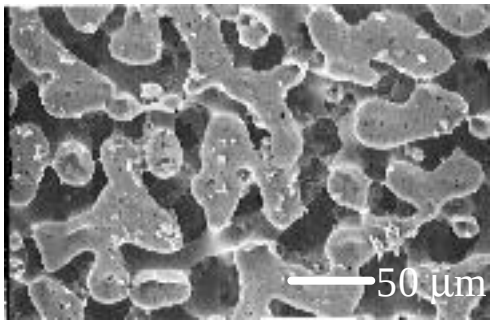

This porous structure is approaching the size scale thought to be optimal for tissue engineering (≅ 100 μm). However, it is not possible to extend the size scales of the structure indefinitely using longer annealing times or smaller volume PCL volume fractions. With longer annealing times, the 30 % PCL sample crumbles into particulate matter after dissolution of the PEO. The 50 % PEO sample does develop larger domain structures but a PCL-rich skin forms on the surface of the material, which would inhibit penetration of the cells into the interior. With these low molecular weight polymers it has not been possible to observe the interior of the material while keeping the morphology intact. At less than 30% PCL, the blend loses its shape with even short periods of annealing, indicating this composition is roughly at the percolation threshold. However, it should be possible to create materials with 100 μm void space.

Amorphous Alloys Containing Cobalt for Orthopaedic Applications

John A. Tesk,[1] Christian E. Johnson,[2] Drago Skrtic,[3] Ming S.Tung,[3] and Stephen Hsu[4]

[1] Polymers Division, National Institute of Standards and Technology (NIST), Gaithersburg, MD
[2] Metallurgy Division, NIST
[3] American Dental Association Health Foundation Paffenbarger Research Center, NIST
[4] Ceramics Division, NIST

Abstract: Numerous approaches are currently being employed in attempts to develop orthopaedic biomaterials that offer improved performance over existing materials. For example, many approaches for applying calcium-phosphate coatings to orthopaedic implants have been used for the purpose of more rapidly and firmly anchoring them to bone. Also, because wear debris from orthopaedic implants has been implicated as a major cause for the end-of-effective-service of orthopaedic implants [*1,2*], there is a strong interest in exploring new bearing designs, including new material couples, that may reduce wear debris effects and, hence, help to prolong effective implant service. In this regard, various methods to produce harder, more wear-resistant surfaces on orthopaedic hip implants are being investigated. While modifications of existing materials and mechanical designs must surely be investigated, the potential of new technologies should also be explored for what they may have to offer and for what may be learned toward solving the problem.

Amorphous metal alloys have unique properties and structures, unlike those of their crystalline counterparts that may lend themselves toward orthopaedic implant applications. For example, a multiphase crystalline structure may exhibit poor corrosion resistance while the amorphous structure is corrosion resistant. The high hardnesses of some amorphous alloys may make them useful for wear resistant applications. Cobalt-based, electrodeposited alloys may be particularly compatible for producing desirable surfaces on orthopaedic Co-Cr-Mo alloys.

One way to produce metallic glasses is by electrodeposition, which is a facile method for applying coatings. By this method metallic glasses can be produced that have a variety of structures and properties. They may be produced as alloys of single phase structures or as mixed-phase, layered, structures of which one or all of the layers may be glassy, each with differing, predominate, elemental composition. By control of the electrodeposition times, voltages, voltage waveforms, solutions and other characteristics of processing, the compositions and thicknesses of the layers can be controlled.

This report on work-in-progress provides 1) results of some tests on the corrosion resistance of amorphous A-Co-20P, and 2) hardness of some electrodeposited amorphous Co-Cr-C alloys, Co (0 to 42) %, Cr (88 to 14) %, C (12 to 8) %, respectively {mass fractions, Co (0 to 50) %, Cr (97 to 50) %, C (2 to 3) %}.

Cobalt-Phosphorus Alloys

Amorphous Co-20P alloy (A-Co-20P {atomic fractions are used throughout the paper when specifying particular compositions within an alloy system}) has an as-deposited Knoop hardness number (HK) of *ca* 620. The surface of anodized A-Co-20P has been described elsewhere as predominately phosphorus oxide that may react with water to form an adsorbed hypophosphite layer. Others reported corrosion resistance without pitting. Hence, the potential

of A-Co-20P for use as an implant coating to induce bony apposition was evaluated. This evaluation consisted of tests of corrosion resistance and solution chemistry.

The tests showed a continuous dissolution of cobalt from previously anodically polarized amorphous Co-20P alloy, with no apparent cessation of that behavior. This is proof that surfaces of that alloy are not passive (this occurred in acids, water, or acidified calcium phosphate solutions). The evidence presented in the literature of a phosphorus enriched surface cannot be discounted, but because the surface does not passivate, amorphous Co-20P is not suitable for use as an implant material.

However, amorphous Ni-Cr-P alloys can be passivated and the presence of phosphorus in their surface layers contributes to this passive behavior. By analogy with the nickel alloys, it is reasonable to expect that similar behavior could be obtained if an amorphous Co-Cr-P alloy could be obtained by adding chromium to the Co-P system to make it more corrosion resistant, with both Cr and P contributing to a corrosion resistant surface. If this analogy carries forth, then there remains the possibility of fabricating implantable amorphous Co-Cr-P alloys that would also have the property of osseous integration by direct bonding to bone, through calcium linkages to phosphorus in the passive layer on the surface of the alloy.

Cobalt-Chromium-Carbon Alloys

Co-Cr-C, was found to have an as-deposited HK of *ca* 690. Heat treatment produced Knoop hardness numbers (HKs) of *ca* 1350, between the HKs of zirconia and alumina. Wear and corrosion resistance are expected to be good, but adherence needs to be assessed.

The potential advantages of these alloys for use as coatings for orthopaedic bearing surfaces and instruments lie in: 1) heat treated condition hardnesses that, based on the hardnesses attainable from heat treated amorphous chromium-carbon, are expected to lie between those of high purity zirconia and high purity alumina and which should, therefore, provide highly wear resistant surfaces, 2) chemical compositions that should impart good corrosion resistance, 3) electrochemical deposition processing that should be a facile method for producing uniform coatings on simple geometry bearing surfaces. Therefore, the objective of this research was to investigate whether, in fact, high hardnesses, similar to those attainable from heat treated amorphous chromium-carbon, could be attained, 2) and whether the electrodeposited coatings had adherence and wear resistance sufficient to render them potentially useful for service as wear-resistant coatings for orthopaedic implant surfaces and instruments.

While the data obtained thus far have been limited to structure and hardness determinations, there are a number of conclusions that may be drawn from the results.
These are:

1) X-ray diffraction reveals the as-deposited layers of Cr and Co as both being amorphous.

2) Heat treated deposits develop HKs that exceed those of zirconia and significantly approach those of alumina. These high HKs indicate potential usefulness for increasing the wear resistance of orthopaedic joints and instruments.

3) The cobalt layer is not corrosion resistant, indicating that chromium is not present in sufficient quantity in the as-deposited Co layer and that the layered deposits used for the current research are too thick to have allowed sufficient diffusion of chromium into the cobalt to impart corrosion resistance.

4) The cobalt and chromium layers appear to interdiffuse at their interfaces to the extent of ca 0.2 μm.

5) Other experience in this laboratory is that electrodeposition can deposit alternating layers of Co-C and Cr-C, with layer thicknesses controllable from 2 μm to 10 nm (40 atoms). Therefore, it is likely that thin, layered structures of cobalt-chromium-carbon can interdiffuse sufficiently to provide good corrosion resistance throughout heat treated deposits.

6) Layers are bonded together well enough to resist delamination under indentation.

7) Adherence and wear tests are needed to confirm whether or not useful properties can be attained with deposits on orthopaedic bearing alloys.

Small Changes in Polymer Structure Can Dramatically Increase Degradation Rates: The Effect of Free Carboxylate Groups on the Properties of Tyrosine-Derived Polycarbonates

Sascha Abramson, Durgadas Bolikal, Howard Levene, Joshua Simon, and Joachim Kohn

Department of Chemistry, Rutgers University, Piscataway, New Jersey, 08854

Introduction

Variations in the degree of pendant chain esterification in poly(γ-ethyl glutamate) were used previously to control the rate of dissolution of this polymer.[1] In an extension of this principle, we synthesized a series of degradable tyrosine-derived polycarbonates in which we varied the proportion of ester versus free carboxylate pendant chains. We observed that with increasing fraction of free carboxylate pendant chains many of the general polymer properties remained constant while the rate of polymer degradation and bioresorption could be dramatically increased.

This relatively small change in the chemical structure of the polymer solved a limitation in the utility of this polymer system: while tyrosine-derived polycarbonates exhibit excellent bone apposition, good biocompatibility and processibility, their rate of bioresorption (1-4 years) is too slow for many applications.[2,3]

Here we report on the synthesis and characterization, as well as initial *in vitro* degradation and *in vivo* biocompatibility studies of tyrosine-derived polycarbonates containing both ethyl ester and free carboxylate pendant chains. In this polymer system, the degradation time can be varied from hours to years, while keeping many other material properties constant.

Methods

The synthesis of the monomer, desaminotyrosyl-tyrosine ethyl ester (DTE), has been described previously.[4] Desaminotyrosyl tyrosine benzyl ester (DTBn) was synthesized in an analogous fashion. DTE and DTBn were copolymerized as described.[4] The benzyl ester pendent chains were then removed by catalytic hydrogenation to produce a polymer containing a predetermined fraction of free carboxylate pendent groups, designated as DT (Figure 1).

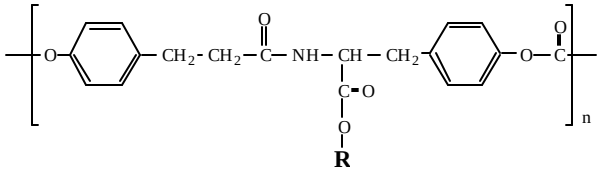

Fig 1. Repeat unit of poly(DTE-co-X%DT carbonate). When R=ethyl the repeat unit is designated as "DTE". When R=H (free carboxylate), the repeat unit is designated as "DT". "X" represents the molar fraction (in %) of carboxylate containing repeat units in the polymer.

Polymer purity and material properties were evaluated as detailed previously.[4] Solvent cast films and porous scaffolds were fabricated using published procedures.[4,5] Scaffolds fabricated from poly(DTE-co-0%DT carbonate) and poly(DTE-co-25%DT carbonate) were implanted in a rabbit calvaria defect. Polymers were heat extruded into rods at 170 °C and compression molded into films at ~130 °C. *In vitro* degradation studies were conducted at 37 °C, using either simulated body fluid (SBF) or phosphate buffer solution (PBS).

Results and Discussion

Polymers with free carboxylate content ranging from 0 % – 100 % were synthesized with similar molecular weights around 100,000. Specific polymers of this family were selected for further studies. Tg (midpoint) increased linearly from 95 °C to 125 °C, a difference of only 30 °C, as free carboxylate content increased from 0 % to 50 %. All polymers in this range of free carboxylate groups could be compression molded to form films and solvent cast to form films and porous scaffolds. While it was readily possible to extrude polymers with 0 % and 5 % free carboxylate content to form rods, the thermal processibility of polymers with higher free carboxylate content still needs to be explored. Solvent cast films had tensile moduli between 1.6 GPa - 2.0 GPa with no significant differences related to free carboxylate content. Porous scaffolds had similar biomodal distribution of large pores in the range of 200 µm to 400 µm and small pores of 20µm, irrespective of free carboxylate content.

While many material properties remained similar, there was a marked difference in the degradation of the polymers. The polymer containing *no ethyl ester* pendent groups, poly(100% DT carbonate), completely dissolved in PBS at 37 °C within 7 hours. The polymer containing *no free carboxylate* pendent groups, poly(DTE-co-0%DT carbonate) showed no mass loss even when incubated for over 18 months under identical conditions. Polymers with intermediate levels of free carboxylate pendent groups had intermediate rates of backbone degradation (as measured by the residual molecular weight as function of incubation time) and intermediate rates of mass loss. For example, poly(DTE-co-50%DT carbonate) retained only about 20% of its initial mass after 100 h of incubation. There was a non-linear correlation between the molar fraction of free carboxylate pendent chains and the rates of degradation and mass loss. At low DT contents (< 25 %), the main effect of the incorporation of free carboxylate groups into the polymer structure was an acceleration of the rate of degradation, without commensurate mass loss. Rapid mass loss was observed *in vitro* only at rather high DT contents (>35 %).

Initial biocompatibility and degradation studies were conducted *in vivo* over a period of 16 weeks. Scaffolds made of poly(DTE-co-0%DT carbonate) and poly(DTE-co-25% DT carbonate) were used to fill a 8 mm diameter defect in the rabbit calvaria defect model. Our results indicated that both polymers facilitated the same degree of bone ingrowth into the scaffold and defect healing. Inflammation and/or encapsulation of the implant by fibrous tissue (foreign body response) were not observed. While poly(DTE-co-0%DT carbonate) did not resorb to any measurable extent during the course of the study, scaffolds prepared of poly(DTE-co-25%DT carbonate) resorbed completely during the 16 week study. This observation indicates that there may be a difference in the rate of mass loss/resorption under *in vitro* or *in vivo* conditions.

Conclusions

The DTE/DT copolymers represent a new series of tyrosine-derived polycarbonates. At relatively low DT content, the presence of free carboxylate pendent chains has a minor effect on the materials properties while significantly increasing the rates of polymer degradation and mass loss. This allows one to match the degradation rate of these polymers to specific applications.

References

1. Anderson J. M. et al., **1985**, *Biocompatibility of Tissue Analogs*, (D.F. Williams, ed.), 1, 67.
2. Levene H. et al,, **1999**, 25th *Annual Meeting of the Society for Biomaterials, p. 13*
3. James K., et al, *Biomaterials*, **1999**, in press
4. Pulapura S and Kohn J, *Biopolymers*, **1992**, 32, 411.
5. Lhommeau, C. et al, **1998**, *Second Bi-Annual Meeting of the Tissue Engineering Society*, p. 468.

Acknowledgement: This work was supported by NIH grant GM39455 and by NIST-ATP grant 70NANB7H3066 awarded to Integra Lifesciences Corporation.
Adapted from abstract accepted for Sixth World Biomaterials Congress, Kamuela, Hawaii, U.S.A.

Surface Modification and Characterization in Blends of Linear and Hyperbranched Polymers

Michael Mackay, Ye Hong, Glenda Carmezini, Matthew Libera

Department of Chemical, Biochemical and Materials Engineering
Stevens Institute of Technology
Castle Point on the Hudson
Hoboken, NJ, 07030

Bryan Sauer

DuPont Central Research & Development
Experimental Station
Wilmington, DE, 19880

Blends of a hyperbranched polyester (HBP) having alkane end groups tend to phase separate to a fiber surface when melt blended with a linear polymer such as polyethylene. The resultant fiber has a surface that is significantly different to the virgin polymer and was developed through normal melt extrusion.

The pure polyethylene fiber has a water contact angle of ca. 84-degrees while the pure HBP has a water contact angle of 108-degrees, a 0.5wt % blend of the HBP with polyethylene has a water contact angle of 90-degrees. So, the surface has been chemically modified with very little of the additive. We will also show how the surface can be physically modified through development of roughness on various length scales. Thus, it is possible to develop tissue scaffolds with different chemical and physical properties. This poster will show some of the techniques we have used to characterize the surface.

A Novel Multiaxial Wear Tester for Accelerated Testing of Materials

*Shen, M., **,+Hsu, S., **Tesk, J., *Christou, A.,

*Department of .Materials and Nuclear Engineering, University of Maryland, College Park, MD
**National Institute of Standards and Technology, Gaithersburg, MD

Relevance to Musculoskeletal Conditions: Development of an accelerated wear tester that is clinically relevant will allow rapid evaluation of potential materials to be used in the artificial joint replacement.

Introduction: There is a need for an accelerated wear tester that can evaluate different material pairs in a short time. Current pin-on-disc tester and ASTM F732 test methods produce results that often contradict long term simulator tests. Recent papers [1,2] suggest that multiaxial motions are important in reproducing the surface textures and wear debris morphology. The objective was to design and build a universal wear tester that is capable of multiaxial motion, programmable load history, and able to evaluate various material combinations, including hard on hard bearing material pairs.

Method: Two moving stages, driven by separate motors, are placed orthogonal to each other. For this evaluation, the contact surfaces consist of an ultra-high molecular weight polyethylene (UHMWPE) pin and a Co-Cr alloy disc. One stage holds the pin, which glides on an inclined plane. Loading is achieved by geometric interference only with the disc on the second stage. There are actuators placed underneath the stages so that the inclined angles can be adjusted and programmed. Both the stroke lengths and frequencies (velocities) of motions of the two stages are independently controlled. In theory, virtually any pattern of motion can be achieved by adjusting the stroke length and frequency of the two stages. The machine is designed to be rigid and stiff with minimal vibration. The test is controlled by a PC using LabVIEW TM software (National Instruments)[a] . Three known wear-level UHMWPE samples were used. These were samples subjected to three different gamma irradiation conditions: 40 kGy in air, 40 kGy in vacuum, and 80 kGy in vacuum. Wear results of the two 40 kGy materials had been published by Schmidt et al.[3] . These samples were used to calibrate the tester and to develop the test protocol. The UHMWPE pins were cylindrical in shape and had dimensions of 6.35 mm in diameter and 19.05 mm in length. The Co-Cr alloy discs had dimensions of 50.8 mm in diameter and 5.8 mm in thickness. The discs were polished to have a typical centerline surface roughness Ra=0.0 mm. The wear tests, in bovine serum, were conducted by using the following procedure. The UHMWPE pins were presoaked in bovine serum for a minimum of 14 d prior to testing. They were cleaned and weighed periodically during the test. A minimum of 3 soak control pins were used in each test. For motion control, one stage was set to oscillate at a frequency of 1.8 Hz and a stroke length of 9.5 mm, while the second stage was set at 0.9 Hz and a stroke length of 19.1 mm. By setting the phase difference between the two oscillation directions, the pin traced a figure-8-shaped path on the Co-Cr disc (0.9 Hz, mean linear velocity, ca. 49 mm/s). The load was controlled by the geometric interference. The Co-Cr disc was set at an incline of 2^{o} with the horizontal and the upper stage (UHMWPE pin) has a 0.6^{o} incline angle. This setup resulted in a load history similar to a Paul type loading curve. The peak load attained from the geometric interference was approximately 400 N with a mean contact pressure of

≈13 MPa. The peak load was monitored and adjusted to be nearly constant throughout the test to compensate for the wear and creep deformation. A spike load was provided by a set of two actuators underneath the sample holder to provide a computer program driven increase of load by10 % during 20 % of the cycles. The pin position was adjusted with respect to the inclined plane so that a 0.2 s relaxation time (no contact) was included in each cycle (20 % of the cycle time). During the test, the normal force and the tangential force were continuously measured by a force transducer mounted on the top stage.

Results: Wear (mass loss) of UHMWPE was obtained in 5 d or less. The mass loss data were corrected for fluid uptake by using the average mass gains in the soak control pins. Results are shown in Fig. 1. The ranking of materials is consistent with previously published results for 40 kGy, air and vacuum specimens [3] . Surface texture, as observed by using a scanning electron microscope (SEM), is shown in Fig. 2. It can be seen that 1) separation among the three samples was achieved; 2) the worn surface texture is similar to the *in vivo* case 4 . The wear debris in the serum were also collected and examined by using SEM. The wear debris morphology was similar to those observed in retrieval studies [4,5] .

Discussions: A versatile wear tester has been designed and built. The initial study showed that with this tester, test procedures can be developed to achieve clinically relevant simulations in a short time. With the continuously monitored force traces, this tester can be used to study the wear mechanisms of different material pairs. Understanding of the wear mechanisms will aid the rapid development of improved artificial joint materials development.

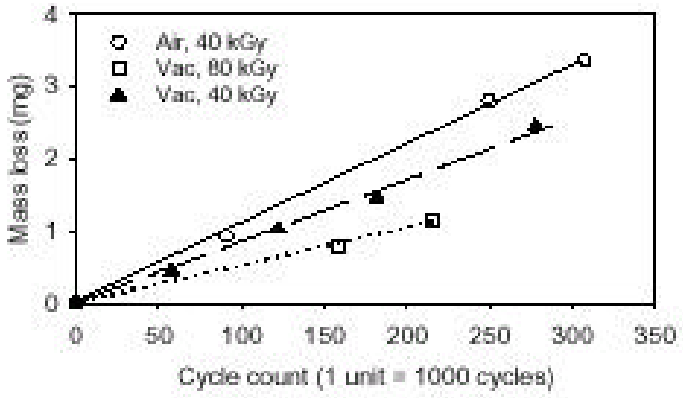

Figure 1: Wear results of the three UHMWPE materials
(Standard deviations < 0.05 mg; not a complete statement of uncertainty)

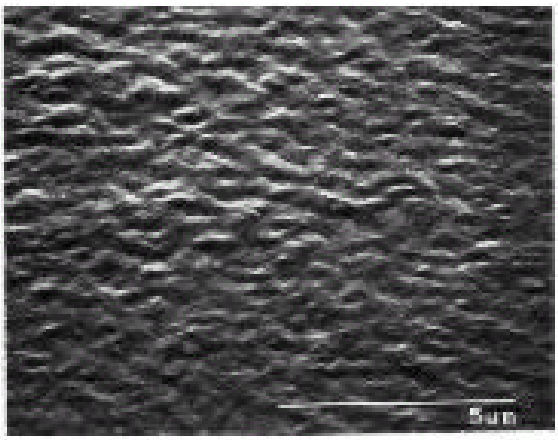

Figure 2: Worn surface of air, 40 kGy pin

Acknowledgment: The authors acknowledge support and guidance from the NIST Orthopaedic Consortium (Biomet, Johnson & Johnson Professional, Osteonics, Zimmer).

[a] Materials and equipment are identified only for describing experimental procedure and do not imply recommendation or endorsement by NIST.

References: 1) Bragdon et al., Proc. Instn. Mech. Engrs., **21**0:157, 1996. 2) Bragdon et al., Trans. 5 th World Biomat. Cong., 788, 1995. 3) Schmidt et al., Trans. Soc. for Biomaterials, **2**1:415, 1998. 4) McKellop et al., CORR, No. 311, 3, 1995. 5) Schmalzried et al., J Biomed. Mater. Res. (Appl. Biomater),**3**8:203, 1997.

Properties of Calcium Phosphate Cement with Chondroitin Sulfate

Satoshi Hirayama[1,2], Francis W. Wang[1], Shozo Takagi[3], Takuji Ikemi[2]

[1] Polymers Division, National Institute of Standards and Technology, Gaithersburg, MD 20899
[2] School of Dentistry at Matsudo, Nihon University, Matsudo, Chiba, Japan 271-8587
[3] American Dental Association Health Foundation, Paffenbarger Research Center, Polymers Division, National Institute of Standards and Technology, Gaithersburg, MD 20899

Introduction

A self-setting calcium phosphate cement (CPC) consisting of tetracalcium phosphate (TTCP) and dicalcium phosphate anhydrous (DCPA) that forms hydroxyapatite (HA) as the final product has been the subject of considerable interest in biomaterials research. As originally formulated CPC (powder/liquid mass ratio = 4) hardens in about 30 min using water as the liquid. Aqueous polymer solutions also have been used with CPC powder to form polymeric calcium phosphate cements. Proteoglycans (PGs) are widely distributed in connective tissues and their glycosaminoglycan (GAG) component regulates the character of PGs. GAGs have an essential role in tissue differentiation, cell migration and adhesion. GAGs have been implicated in binding to calcium ions and HA crystals, playing a role in the regulation of mineralization. Chondroitin sulfate is a mucopolysaccharide with a high affinity for HA that has been observed in osteoblast-like cells in culture, and is a major structural component of cartilage, bone and other connective tissue structures. The objectives of this study were to evaluate the setting times, mechanical strengths and HA conversion of chondroitin sulfate-modified CPCs that were prepared from various of aqueous chondroitin sulfate solutions rather than water as the liquid component of the self-setting CPCs.

Materials and Methods

Preparation of CPC: TTCP was prepared by heating an equimole mixture of DCPA ($CaHPO_4$) and $CaCO_3$ at 1500 °C for 6 h followed by quenching at room temperature. The TTCP and DCPA were ground in a planetary ball mill to obtain powders with mean particle sizes of 17.8 μm and 1.0 μm, respectively. The CPC powder was prepared by mixing in a micro-mill ground TTCP and DCPA at the mole ratio of 1: 1. The powder consisted of mass fractions of 72.3 of TTCP and 27.7 of DCPA. **CPC liquid:** Aqueous solutions of chondroitin sulfate A (CSA, Sigma) at mass fractions (5, 15, 25, and 50) % were used as the cement liquids. Distilled water was used as the control. **Measurement of setting time:** Hardening times of CPC-CSA specimens were measured by using the Gilmore needle method. CPC powder (0.3 g) and liquid were mixed at the powder/liquid (P/L) mass ratio of 4.0 to form the cement paste. The paste was packed into a stainless steel mold (6.0 mm diameter (D) × 3.0 mm high (H)), and both the top and bottom surfaces of the mold were then covered with glass plates held by a C-clamp. The mold was then kept at 37 °C in a 100 % relative humidity box. A specimen was considered set when the 400 g mass loaded on the Gilmore needle with a tip diameter of 1 mm failed to make a perceptible circular indentation on the surface of the specimen. **Sample preparation:** The amounts of CPC powder used for preparing diametral tensile strength (DTS) and compressive strength (CS) samples were 0.18 g and 0.65 g, respectively at P/L mass ratio of 4.0. After mixing for 30 s for DTS specimens or 45 s for CS specimens, the cement pastes were packed into stainless steel molds (6.0 mm D × 25.4 mm H), and placed in a constant-pressure loading device. The top and bottom plungers of the constant-pressure device were placed in contact with the top and bottom surfaces of the cement paste, and pressures of 0.7 MPa and 2.8 MPa were applied in the fabrication of the DTS and CS specimens, respectively. The cement pastes, under pressure in the molds, were kept for 4 h in a 100 % relative humidity box at 37 °C. Then, the hardened specimens were removed from the molds and stored in distilled water at 37 °C for 20 h. **DTS and CS measurements:** The diameter and height of each specimen were measured with a

micrometer before the DTS and CS measurements. The DTS and CS were measured using a Universal Testing Machine at displacement rates of (10 and 1) mm/min, respectively. For each material, five specimens were measured for each strength test. **Extent of HA formation:** After the CS measurement, a crushed specimen was dried in an oven at 70 °C and then ground to a fine powder. The fine powder was characterized by X-ray diffraction analysis (XRD) to determine the extent of HA formation. **Scanning electron microscopy (SEM):** Several fractured and dried pieces from tested DTS specimens were mounted on aluminum stubs and coated with gold-palladium. Both the exterior and interior surfaces of these specimens were analyzed by SEM in order to determine the type of calcium phosphates present in the hardened CPC.

Results and Discussion

The setting times of all in the CSA-CPC group were significantly longer ($p < 0.05$) than that of the control. However, the setting times of the various CSA-CPCs were not significantly different form each other, even though the HA conversion of the CSA-CPC group decreased with the increasing mass fraction of the CSA in solution (Table 1). These results appeared to indicate that CSA, especially at high concentrations, may have an inhibiting effect on HA formation, perhaps because of its ability to bind calcium ions derived from the CPC powder. The results of the XRD and SEM observations showed that unconverted TTCP and DCPA remained in the specimens made from solutions with CSA mass fractions of (15, 25, or 50) %. Thus, it seems that aqueous CSA solutions, especially with high concentration of CSA, delayed or interfered with the HA-setting reaction of CPC.

Table 1 The setting time and HA conversion of CPC with several concentrations of CSA. (Number of specimens = 5)

Concentration of CSA	Setting time (min)	HA conversion (%)
Mass fraction (%)	Mean ± s.d.	Mean ± s.d.
0 (control)	30.0 ± 1.0	87.2 ± 2.5
5	35.3 ± 2.5	82.1 ± 1.7
15	35.0 ± 2.7	74.5 ± 3.2
25	35.3 ± 1.5	70.5 ± 8.8
50	36.7 ± 2.9	65.1 ± 6.1

The DTS and CS of specimens made from CSA solutions with mass fractions of (15 and 25) % were not significantly different ($p > 0.05$) from those for the control group. However, DTS and CS of specimens made from CSA solutions with mass fractions of (5 and 50) % were significantly lower ($p < 0.05$) than those for the control group (Table 2). These results suggest that CSA may be interacting with the CPC powder to inhibit or prevent optimal formation of HA. However, CSA based CPCs may have biological characteristics that promote enhanced biointegration with mineralized tissues. An optimum concentration of CSA may be needed to achieve the best overall physicochemical, mechanical and biological properties of this mucopolysaccharide-modified CPC.

Table 2 DTS and CS of CPC with several concentrations of CSA.

Concentration of CSA	DTS (MPa)	CS (MPa)
Mass fraction (%)	Mean ± s.d.	Mean ± s.d.
0 (control)	10.6 ± 0.4	64.9 ± 3.2
5	8.4 ± 0.8	59.6 ± 5.8
15	9.5 ± 1.0	71.8 ± 4.3
25	9.3 ± 0.7	66.7 ± 5.6
50	8.5 ± 0.7	54.1 ± 5.3

Materials and equipment do not imply recommendation or endorsement by NIST and Nihon University.

Acknowledgement NIH Grant, Y1-DE-7006-01, DE11789

Biocompatibility of a Resorbable, Composite Bone Graft

Carl G. Simon, Jr. & Francis W. Wang

National Institute of Standards and Technology
Polymers Division, 100 Bureau Drive, Gaithersburg, MD 20899-8545

We plan to evaluate the biocompatibility of a novel composite bone graft using *in-vitro* cell culture assays. The graft consists of calcium phosphate cement (CPC) and poly(lactide-co-glycolide) (PLGA). The CPC itself is known to be biocompatible, but we aim to improve the mechanical properties of the cement by inclusion of PLGA. The morphology, viability, proliferation, and phenotype of osteoblast-like cells (MC3T3-E1 cell line) grown on the surface of the composite graft will be compared to that of cells grown on CPC alone (without PLGA). Cell morphology and viability on the graft will be examined using fluorescence microscopy after staining live and dead cells using calcein-AM and ethidium homodimer-1, respectively. Environmental scanning electron microscopy (ESEM) will also be used to examine cell morphology on the grafts. Proliferation will be assessed with a colorimetric assay (WST-1/1-methoxy-PMS) using a tetrazolium salt that produces a water-soluble formazan dye following dehydrogenase-mediated reductions. Finally, the ability of the cells to express alkaline phosphatase, a marker of the osteoblast phenotype, will be assessed. These studies are designed characterize the biocompatibility of our unique composite bone graft.

Amphiphilic Multiblock Copolymers of PEG and Tyrosine-Derived Diphenols: Self-Assembly in Aqueous Solution and at Hydrophobic Surfaces

Francesca d'Acunzo,[*] Quoc Toan Le,[*] and Joachim Kohn[*]
M. Libera[**] and A. Aitouchen[**]

[*]Department of Chemistry, Rutgers University, Piscataway, NJ 08854, USA
[**]Department of Chemical, Biochemical, and Material Engineering, Stevens Institute of Technology, Hoboken, NJ 07030, USA

Introduction: Polymeric surfactants are important components of pharmaceutical formulations and drug delivery systems. Copolymers based on poly(ethylene glycol) (PEG), such as PLA-PEG, poloxamer and PEG-modified dextrans, are of considerable interest because of their low toxicity, low immunogenicity and low thrombogenicity.[1] Amphiphilic multiblock copolymers of PEG and lysine, with several hydrophobes in a single linear polymer chain, have been synthesized and studied in Kohn's laboratory.[2,3]

Surfactant behavior is generally related to the ability of an amphiphilic molecule to form micellar aggregates in solution and to adsorb at surfaces. A critical issue in the design of surface-active molecules for biomedical applications is to obtain structures that exhibit low critical concentrations for self-assembly in solution and at liquid-solid interfaces. Suitable experimental methods need to be used for the detection of such low concentrations, and for the characterization of the self-assembled structures.

Here we report on the surfactant properties of a new class of multiblock copolymers PEG and the tyrosine-derived diphenol desaminotyrosyl-tyrosine alkyl ester (DTR) (Figure 1). The molecular weight of PEG was varied between 2000 and 8000, and the alkyl pendent chains in the DTR units were C_2 (ethyl), C_6 (hexyl) and C_{12} (dodecyl).

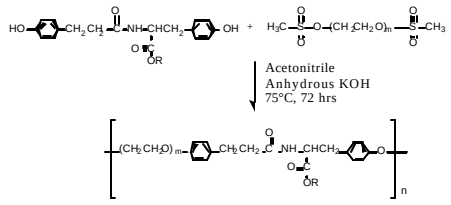

Figure 1. Structure and synthesis of poly(DTR-PEG ether)s. PEGs of molecular weight 2000, 4000, and 8000 were used. The alkyl pendent chains were C_2 (ethyl), C_6 (hexyl), and C_{12} (dodecyl).

Materials and Methods: All polymers were synthesized by direct polymerization of PEG dimethanesulfonate with DTR (Figure 1). Their structure was confirmed by ^{1}H and ^{13}C NMR, and their molecular weights were determined by Gel Permeation Chromatography (GPC) in DMF/LiBr 0.1% relative to PEG standards (Polymer Laboratories Incorporated, MA, USA).

The self-assembly of poly(DTR-PEG ether)s into micellar aggregates in aqueous solution was studied by static light scattering using a miniDawn apparatus (Wyatt Technology Corporation, Santa Barbara, CA – USA) operated in batch mode, with a laser wavelength of 690 nm, and detectors at 41°, 90°, and 139°.

Cryo-transmission electron spectroscopy (TEM) was used for the visualization of the aggregates formed by poly(DTD-PEG4000 ether) in water. A liquid film of 1% (w/w) polymer solution was deposited on a Holey carbon grid, the specimen was frozen by plunging in liquid propane, and a T≤170 °C was maintained throughout the experiment. The sample was transferred into the electron microscope (200 KeV Philips CM20) using a Gatan 626 cryotransfer specimen stage. The phase-contrast image was obtained at 100 KeV, 104 electrons/nm^2 by defocusing.

The adsorption of poly(DTE-PEG8000 ether) and poly(DTE-PEG2000 ether) from aqueous solutions on graphite was studied by X-ray photoelectron spectroscopy (XPS). Graphite discs were soaked for two hours in $4x10^{-4}$ to 0.3% (w/w) polymer solutions, and rinsed four times with water. The samples were dried under high vacuum at room temperature, and surface analysis was carried out using a Kratos XSAM-800 spectrometer equipped with a non-monochromatized Mg Kα X-ray source (1253.6 eV) under a base pressure of $4x10^{-9}$ Torr.

Table 1. Molecular masses and RMS radii og gyration (R_g) of poly(DTR-PEG ether)s by GPC and light scattering.

Polymer	M_w (Da) GPC	M_w (Da) Light Scattering	N_R[(a)]	Rg (nm)[(b)] Light Scattering
DTE-PEG2K	21,000	18,000	7.5	<10
DTH-PEG2K	33,000	69,000	29	60±6
DTD-PEG2K	23,000	242,900	121	55±2
DTD-PEG4K	31,000	215,000	48	45±3
DTD-PEG8K	64,800	427,000	50	58±11
DTE-PEG8K	88,000	87,100	10	21±5

[(a)] N_R= Number of hydrophobes/aggregate. Estimated from the light scattering M_w as in equation (1).
[(b)] Rg= Root mean square radius of gyration.

Static light scattering was used to determine the weight-average molecular weights and root mean square radii of gyration (R_g) of poly(DTR-PEG ether)s in water (Table 1). The light scattering molecular weight reflects interchain aggregation, so that higher values than the ones obtained by GPC indicate the formation of multimolecular aggregates. The average numbers of hydrophobes per aggregate N_R were estimated under the strong assumption that all aggregates contain the same number of hydrophobes. Thus, N_R is given by

$$N_R=M_w(ls)/M_r \qquad (1)$$

where M_w(ls) is the weight-average molecular weight determined by light scattering, and M_r is the molecular weight of one repeat unit. No significant difference was observed between the light scattering and GPC molecular weights of the DTE-containing polymers, indicating that no interchain aggregation occurs in water. Intermolecular association, on the other hand, was observed for all other polymers, with a remarkably large N_R of 121 for poly(DTD-PEG2000 ether).

Cryo-TEM imaging (not shown) shows that the micelles formed by poly(DTD-PEG4000 ether) in water are of spherical shape, and of max. 100 nm in diameter.

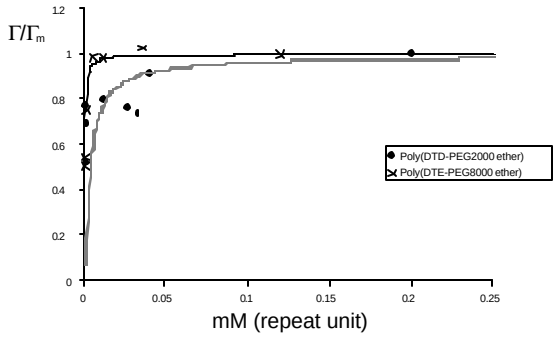

Figure 2. Adsorption isotherms of poly(DTD-PEG2000 ether) and poly(DTE-PEG2000 ether). The lines represent the adsorption isotherms calculated from the Langmuir equation.[4]

The intensity of the O 1s peak determined by X-ray photoelectron spectroscopy (XPS) was used in order to construct the adsorption isotherms of poly(DTE-PEG8000 ether) and poly(DTE-PEG2000 ether) on graphite (Figure 2). Poly(DTE-PEG8000 ether) does not form multichain aggregates in water, and its adsorption isotherm is of the classic Langmuir shape. Poly(DTD-PEG2000 ether) forms multichain aggregates in solution. This behavior gives rise to a first plateau in the adsorption isotherm, as aggregate growth competes with surface adsorption. Coverage increases again upon further increase of solution concentration, until monolayer saturation is reached. The amount of oxygen detected at monolayer saturation is identical for both polymers. This suggests that the limiting surface concentration is determined by PEG packing, rather than by the polymer composition.

Conclusions: Poly(DTR-PEG ether)s are multiblock amphiphilic copolymers exhibiting surface-active behavior, i.e. they form micellar aggregates in aqueous solution and adsorb at hydrophobic surfaces. Their composition can be systematically changed in order to tailor their self-assembling properties. Based on this study of their surfactant behavior, they are potentially useful materials for micellar solubilization of hydrophobic drugs and for surface modification of hydrophobic biomaterials. An example is the stabilization and surface modification of sub-micron particles for intravenous drug delivery.

References:

(1) Rouzes, C.; Gref, R.; Leonard, M.; Delgado, A. D. S.; Dellacherie, E. *Journal of Biomedical Materials Research* **2000**, *50 (4)*, 557-565.
(2) Heitz, C.; Pendharkar, S.; Prud'homme, R. K.; Kohn, J. *Macromolecules* **1999**, *32 (20)*, 6652-6657.
(3) Heitz, C.; Pendharkar, S.; Prud'homme, R. K.; Kohn, J. *Macromolecules* **1999**, *32 (20)*, 6658-6667.
(4) Giles, C. H.; Smith, D.; Huitson, A. *Journal of Colloid ans Interface Science* **1974**, *47 (3)*, 755-765.

Acknowledgements

Support from the New Jersey Center for Biomaterials and from Veritas, Inc. is acknowledged.

Spun Cast Hydrophobic Polymer Films as Biomaterials: In situ AFM Examination of Polystyrene Film Surface Topology Exposed to Aqueous Media

John T. Woodward[1], John T. Elliott[1], Amit Sehgal[2], Jack F. Douglas[2], and Anne L. Plant[1].

[1]Biotechnology Division- Chemical Sciences and Technology Laboratory
[2]Polymers Division- Materials Science and Engineering Laboratory
National Institute of Standards and Technology, 100 Bureau Drive, Gaithersburg, MD

Abstract

Spun cast thin polymer films have a variety of potential biotechnology applications such as fabrication of tissue engineering supports and biomimetic surfaces. The ability to prepare thin coatings with mixed polymers and chemically modify polymers with desirable functional groups allows the creation of unique surfaces that may not be possible on supports prepared from other less flexible materials (e.g. glass). As a biomaterial, the polymer film will be exposed to aqueous environments; thus it is important to characterize the film's behavior under aqueous conditions. We have used in situ atomic-force microscopy to examine a variety of spun cast thin polystyrene films (75 to 200) nm on silicon wafers under aqueous conditions. Before exposure to water, the films are smooth and homogenous over large areas (7 μm x 7 μm). Immediately after submersion in water, the films develop bumps that are (20 to 50) nm in diameter and 5 nm to 20 nm in height. Variations in the polymer molecular weight, film thickness and silicon wafer pretreatment were also examined to determine which parameters influence surface topology. We then determined if the polymer films were capable of supporting phospholipid monolayers. Low-resolution microscopy and fluorescence recovery after photobleaching experiments indicated that continuous phospholipid monolayers formed on some polymer films, but the effective diffusion differed between. The difference in diffusion rate is likely related to the film surface topology that forms under aqueous conditions.

ACKNOWLEDGEMENTS

We wish to acknowledge the following people for their help in developing this workshop. Ms. Cleo Brown, Events Coordinator for The New Jersey Center for Biomaterials for all of her work in preparation of the meeting, and Dr. Richard Parnas of NIST for his help in the early stages of planning the workshop.

Agenda of the Meeting

8:00-9:00 am — Registration and Continental Breakfast

9:00-9:20 — **Welcome and Opening Remarks**
J. Kohn, Director, New Jersey Center for Biomaterials
E. Amis, Chief, Polymers Division, NIST, Gaithersburg, MD

9:20-10:30 — ***Design and Synthesis***
Moderator: A. Karim, Group Leader, Polymers Division, NIST, Gaithersburg, MD

Advances in Materials Design for Biomedical Polymers
J. West, Assistant Professor of Chemistry, Rice University, Houston, Texas

A Combinatorial Approach to Biomaterials Design
J. Kohn, Professor of Chemistry, Rutgers University, New Brunswick, NJ

Novel Polymers for Drug Delivery
K. Uhrich, Assistant Professor of Chemistry, Rutgers University, New Brunswick, NJ

10:30-10:45 — Coffee Break and Poster Session

10:45-12:00 — ***New Imaging Techniques***
Moderator: K. Uhrich, Assistant Professor of Chemistry, Rutgers University, New Brunswick, NJ

Scanning Optical Microscopy for In-situ Characterization of Biomaterials
L. Garfias, Member of Technical Staff, Bell Labs, Lucent Technologies, Murray Hill, NJ

Optical Coherence Tomography (OCT) for Imaging Materials and Tissue Engineering Scaffolds
J. Dunkers, Physical Scientist, Polymers Division, NIST, Gaithersburg, MD

Micro-Thermal Analysis: A Marriage of Atomic Force Microscopy and Thermal Analysis
R. Blaine, Applications Manager, TA Instruments, New Castle, DE

12:00-1:30 — Lunch and Poster Session

1:30-2:00 ***Facilitated Discussion***

Critical Issues in the Characterization of Polymers for Medical Applications
M. Jaffe, Research Professor of Chemical Engineering, Chemistry & Environmental Science, New Jersey Institute of Technology, Newark, NJ

2:00-3:00 ***State-of-the-Art Research in Biomaterials***

Moderator: J. Dunkers, Physical Scientist, Polymers Division, NIST, Gaithersburg, MD

Switching Functional Fates of Cells on Polymer Substrates
P. Moghe, Associate Professor, Chemical and Biochemical Engineering., Rutgers University, New Brunswick, NJ

Biomimetic Membranes as In-Vitro Models to Study Cell-Cell Interactions for Tissue Engineering
H. Elgendy, Research Scientist, Biotechnology Division, NIST, Gaithersburg, MD

3:00-3:20 Break and Poster Session

3:20-3:40 **A Microshear Test to Measure the Bond Between Dental Composites and Dental Substrates**
G. Schumacher, American Dental Association/Paffenbarger Research Center, Gaithersburg, MD

3:40-4:00 **Using Combinatorial Methods for Investigations in Polymer Materials Science**
A. Karim, Group Leader, Polymers Division, NIST, Gaithersburg, MD

4:00-4:15 **Concluding Remarks and Discussion**
J. Kohn, Director, New Jersey Center for Biomaterials
E. Amis, Chief, Polymers Division, NIST

4:15 **Adjournment**

LIST OF ATTENDEES

Advanced Materials Design

David Eisenbud
Vice President, Strategic Planning
Advanced Materials Design
350 5th Avenue, Suite 7412
New York, NY 10118
Tel. (212) 502-5142 Fax: (212) 502-5145

Arvind Viswanathan
Researcher
610 Taylor Road
Piscataway, NJ 08854
Tel: (732) 445-0488 Fax: (732) 445-5006

Anika Therapeutics, Inc.

Stephen J. Kennedy
Senior Product Development Scientist
Anika Therapeutics, Inc.
160 New Boston Street
Woburn, MA 01801
Tel: (718) 932-6616 Fax: (781) 935-7803

AVON Products, Inc.

Derrick McKie
Program Leader
AVON Products, Inc.
Avon Place
Suffern, NY 10901-5605
Tel: (914) 369-2536 Fax (914) 369-2402

CIC y de Yucatan

Juan Cauich-Rodriguez
Research Associate
CIC y de Yucatan
Calle 43, No 130, Col. Chuburna de CP 97200
Merida, Yucatan, MEXICO
Tel 001-52-99-813966 Fax 001-52-99-813900

ElizaNor Biopharmaceuticals, Inc.

John Hartmann
President
ElizaNor Biopharmaceuticals, Inc.,
1 Woodmeadow Lane
Princeton Junction, NJ 08550
Tel: (609) 799-2812 Fax: (609) 897-9660

Evans East

Dave Cole
Manager
Evans East
104 Windsor Center
East Windsor, NJ 08520
Tel: (609) 371-4800 Fax: (609) 371-5666

Fluid Dynamics, Inc.

R.S. Rounds
Director
Fluid Dynamics, Inc.
45 River Road Bldg. 500
Flemington, NJ 08822
Tel: (908) 237-0881 Fax: (908) 237-0884

Integra LifeSciences Corp.

Simon J. Archibald
Senior Director of Neurological Programs
Integra LifeSciences Corp.
PO Box 688
105 Morgan Lane
Plainsboro, NJ 08536
Tel: (609) 936-2343 Fax: (609) 799-3297

Dr Kathy Dejneka
Engineering Manager
Integra LifeSciences Corp.
105 Morgan Lane
Plainsboro, NJ, NJ 08536
Tel: (609) 936-2482 Fax: (609) 799-3297

Life Cell Corporation

Sabena Adhikary
Life Cell Corporation
One Millennium Way
Branchburg, NJ 08876
Tel: 908) 947-1100 Fax: (908) 947-1200

Dr. Rick Owens
Life Cell Corporation
One Millennium Way
Branchburg, NJ 08876
Tel: (908) 947-1100 Fax: (908) 947-1200

Lucent Technologies

Luis Garfias
Technical Staff
Lucent Technologies
600 Mountain Avenue Room 1T-206
Murray Hill, NJ 07974-1542
Tel: (908) 582-1542 Fax: (908) 582-3609

MD3, Inc.

Donald Koenig
Director of Engineering
MD3, Inc.
12335 World Trade Drive. Suite 11A
San Diego, CA 92128
Tel: (858) 451-0736 Fax: (858) 451-8599

Micro-view Consultants, Inc.

Robert Dombrowski
Micro-view Consultants, Inc.
P.O. 6190
East Brunswick, NJ 08816
Tel: (732) 940-8686

National Institute of Standards and Technology

Alamgir Karim
Combinatorials Group
National Institute of Standards and Technology
100 Bureau Drive
Gaithersburg, MD 20899
Tel: (301) 975-6588

Eric J Amis
Chief, Polymers Division
National Institute of Standards & Technology
100 Bureau Drive MS 8540
Gaithersburg, MD 20899
Tel: (301) 975-6762

Hoda Elgendy
Biotechnology Division
National Institute of Standards & Technology
100 Bureau Drive MS 8313
Gaithersburg, MD 20899-8313
Tel: (301) 975-5366

Gary Schumacher
National Institute of Standards & Technology
100 Bureau Drive
Gaithersburg, MD 20899-8546
Tel: (301) 975-6805

Carl Simon
Researcher - Polymers Division
National Institute of Standards & Technology
MS 4730
Gaithersburg, MD 20899
Tel: (301) 975-8574

John A. Tesk
Coordinator, Biomaterials Program
National Institute of Standards & Technology
Room A143, Bldg 224, Polymer Division
Gaithersburg, MD 20899
Tel: (301) 975-6799

Francis Wang
Group Leader, Dental & Medical Materials Group, Polymers Division
National Institute of Standards & Technology
Building 224, Rm A143
Gaithersburg, MD 20899
Tel: (301) 975-6726

Newell Washburn
Researcher - Polymers Division
National Institute of Standards & Technology
MS 4730
Gaithersburg, , MD 20899
Tel: (301) 975-4348

H. Felix Wu
Program Manager
National Institute of Standards & Technology
100 Bureau Drive MS 4730
Gaithersburg, MD 20899
Tel: (301) 975-4685

John Woodward
Researcher
National Institute of Technology and Standard
100 Bureau Drive
Gaithersburg, MD 20899
Tel: (301) 975-5495

Joy P. Dunkers
Physical Scientist, Polymers Division
National Institute of Standards & Technology
US Dept. of Commerce
Building 224, Rm B108
Gaithersburg, MD 20899
Tel: (301) 975-6841

New Jersey Center for Biomaterials

Cleo Brown
Events Coordinator
New Jersey Center for Biomaterials
610 Taylor Road
Piscataway , NJ 08854
Tel: (732) 445-0488 Fax: (732) 445-5006

Sylvia Deloatch
Administrative Assistant
New Jersey Center for Biomaterials
610 Taylor Road
Piscataway , NJ 08854
Tel: (732) 445-0488 Fax: (732) 445-5006

Carolyn Dennis-Phillips
Assistant Director for Outreach
New Jersey Center for Biomaterials
610 Taylor Road-Wright Rieman Labs
Piscataway, NJ 08854
Tel: (732) 445-0488 Fax: (732) 445-5006

Carla N. Epstein
Research Administrator
New Jersey Center for Biomaterials
610 Taylor Road - Wright-Rieman Labs
Piscataway, NJ 08854
Tel: (732) 445-0488 Fax: (732) 445-5006

Carole Kantor
Associate Director
New Jersey Center for Biomaterials
362 North Fourth Avenue
Highland Park, NJ 08904
Tel: (732) 445-0488 Fax: (732) 445-5006

Joachim Kohn
Director
New Jersey Center for Biomaterials
610 Taylor Road
Piscataway, NJ 08854
Tel: (732) 445-0488 Fax: (732) 445-5006

Laura Poole-Warren
New Jersey Center for Biomaterials
610 Taylor Road
Piscataway, NJ 08854
Tel: (732) 445-0488 Fax: (732) 445-5006

Michael Jaffe
Chief Scientist for Industrial Programs, CBMD
New Jersey Center for Biomaterials/NJIT
111 Lock Street
Newark, NJ 07102
Tel: (973) 353-1462 Fax: (973) 353-5336

New Jersey Commission on Science & Technology

Robin-Ann Klotsky
Associate Director
New Jersey Commission on Science & Technology
28 W. State St., CN 832
Trenton, NJ 08625-0832
Tel: (609) 292-6529 Fax: (609) 292-5920

New Jersey Institute of Technology

Michael Huang
Professor
New Jersey Institute of Technology
151 Tiernan Hall
Newark, NJ 07102
Tel: (973) 596-5613 Fax: (973) 596-8436

Rensselaer Polytechnic Institute

Janine Perez
Student
Rensselaer Polytechnic Institute
600 Mountain Avenue Room JT-206
Murray Hill, NJ 07074
Tel: (908) 582-1542 Fax: (908) 582-2226

Rheometric Scientific

Donald Becker
Vice President, Sales & Marketing
Rheometric Scientific
One Possumtown Road
Piscataway, NJ 08854
Tel: (732) 560-8550 Fax: (732) 302-1043

Rice University

Jennifer West
TN Law Assistant Professor - Dept. of Bioengineering
Rice University
6100 Main Street MS 142
Houston, TX 77005
Tel: (713) 348-5955 Fax: (713) 348-5877

Rutgers Univerisity

Sascha D. Abramson
Department of Biomedical Engineering
Rutgers University
617 Bowser Road
Piscataway, NJ 08854-8014
Tel: (732) 445-3996 Fax: (732) 445-5006

Sharon Bourke
Postdoctoral Researcher
Rutgers University
610 Taylor Road
Piscataway, NJ 08854-8087
Tel: (732) 445-3996 Fax: (732) 445-5006

Raman Bahulekar
Research Associate
Rutgers University
610 Taylor Road
Piscataway, NJ 08854-8087
Tel: (732) 445-3996 Fax: (732) 445-5006

Das Bolikal
Center for Biomaterials
Rutgers University
610 Taylor Road
Piscataway, NJ 08854
Tel: (732) 445-3996 Fax: (732) 445-5006

Tomas Brieva
Chemical Engineering
Rutgers University
98 Brett Road
Piscataway, NJ 08854
Tel: (732) 445-5509 Fax: (732) 445-5516

Francesca D'Acunzo
Rutgers University
610 Taylor Road
Piscataway, NJ 08855
Tel: (732) 445-3996 Fax: (732) 445-5006

Elsie Kaufmann
Center for Biomaterials
Rutgers Univerisity
610 Taylor Road
Piscataway, NJ 08854
Tel: (732) 445-3996 Fax: (732) 445-5006

Kristen Sakala Labazzo
Chemistry
Rutgers University
610 Taylor Road
Piscataway, NJ
Tel: (732) 445-3996 Fax: (732) 445-5006

Quoi Toan Le
Research Associate
Rutgers University
610 Taylor Road
Piscataway, NJ 08854
Tel: (732) 445-3996 Fax: (732) 445-5006

Prabhas Moghe
Dept. of Chemical and Biochem. Engineering
Rutgers University
Busch Campus
Piscataway, NJ 08855
Tel: (732) 445-3996 Fax: (732) 445-5006

Arthur L Schwartz
Research Associate
Rutgers University
610 Taylor Road
Piscataway, NJ 08854
Tel: (732) 445-3996 Fax: (732) 445-5006

Samir Shah
Student
Molecular Biology & Biochemistry
Rutgers University
Piscataway, NJ 08854
Tel: (732) 445-3996 Fax: (732) 445-5006

Kathryn Uhrich
Assistant Professor of Chemistry
Rutgers University
610 Taylor Road
Piscataway, NJ 08854
Tel: (732) 445-0361Fax: (732) 445-5312

Xinyun Yu
Research
Rutgers University
136 Frelinghuysen Rd.
Piscataway, NJ 08854
Tel: (732) 445-3996 Fax: (732) 445-5006

Lei Zhang
Physics Department
136 Frelinghuysen Rd.
Piscataway, NJ 08854
Tel: (732) 445-3996 Fax: (732) 445-5006

Stevens Institute of Technology

Ye Hong
Chemical Engineer Dept.
Stevens Institute of Technology
Hoboken, NJ 07030
Tel: (201) 216-8924 Fax: (201) 216-8308

Peter Krisco
Stevens Institute of Technology
Hoboken, NJ 07030
Tel: (201) 216-8924 Fax: (201) 216-8308

Michael McKay
Stevens Institute of Technology
Hoboken, NJ 07030
Tel: (201) 216-8924

Veruna Sundaram
Stevens Institute of Technology
Hoboken, NJ 07030
Tel: (201) 216-8924 Fax: (201) 216-8308

Jennifer Taylor
Stevens Institute of Technology
Hoboken, NJ
Tel: (201) 216-8924 Fax: (201) 216-8308

TA Instruments

Roger Blaine
Applications Manager
TA Instruments
109 Lukens Drive
New Castle, DE 19720
Tel: (302) 427-4017 Fax: (302) 427-4181

UMD-New Jersey Medical School

J. Russell Parsons
Director, Orthopaedic Research
UMD-New Jersey Medical School
185 South Orange Avenue, MSB G574
Newark, NJ 07103
Tel: (973) 972-5293 Fax: (973) 972-5294

UMDNJ - Robert Wood Johnson Medical School

Jeffrey Cartmell
UMDNJ - Robert Wood Johnson Med. School
One Robert Wood Johnson Pl. CN-19
New Brunswick,, NJ 08903
Tel: (732) 235-7972 Fax: (732) 235-6002

Ara Festekjian
UMDNJ - Robert Wood Johnson Med. School
One Robert Wood Johnson Pl. CN-19
New Brunswick,, NJ 08903
Tel: (732) 235-7972 Fax: (732) 235-6002

Jordan Katz
UMDNJ - Robert Wood Johnson Med. School
One Robert Wood Johnson Pl. CN-19
New Brunswick,, NJ 08903
Tel: (732) 235-7972 Fax: (732) 235-6002

Olivia Linton
Student
UMDNJ - Robert Wood Johnson Med. School
One Robert Wood Johnson Pl. CN -19
New Brunswick,, NJ 08903
Tel: (732) 235-7972 Fax: (732) 235-6002

Mark O'Han
UMDNJ - Robert Wood Johnson Medical School
One Robert Wood Johnson Pl. - CN 19
New Brunswick, , NJ 08903
Tel: (732) 235-7972 Fax: (732) 235-6002